ABSTRACT

Title of Thesis: INVESTIGATION OF TWO PERFORMANCE IMPROVEMENT OPTIONS FOR HOUSEHOLD REFRIGERATORS

Ahmet Ors, Master of Science, 2006

Thesis Directed By Professor Reinhard Radermacher, Ph.D.
Department of Mechanical Engineering

Due to environmental concerns, the refrigeration industry is facing the challenge of developing more efficient and environmental friendly refrigerators. Environmentally harmful refrigerants, CFC's and HCFC's, have already been shifted toward environmental friendly refrigerants such as HFC's and hydro carbons. However HFC's have a significant global warming potential. Accordingly, new policies have taken effect which are forcing the refrigerator industry to develop refrigerators that will reduce energy consumption and refrigerant emissions to reduce energy bills and the global warming effects of refrigerators.

This study presents the research conducted on the condenser improvement of one of the commercially available household refrigerators and designing and applying a so-called Alternating evaporator duty cycle (AED) with a two step capacity modulated compressor.

In the condenser improvement study, a household refrigerator's condenser configuration was changed from the cross-flow configuration to the counter-flow configuration without changing other components and cabinet structure. Ten experiments for different refrigerant charges were conducted and it was experimentally proved that the refrigerator with counter flow condenser consumes 1% less energy compared to the one with cross-flow condenser.

To study the potential of the AED cycle, a side-by-side household refrigerator equipped with a conventional cycle was converted into the AED cycle. First of all, the performance of the refrigerator with the new cycle was simulated and then cycle components were designed. Two different kinds of evaporators were used for food (R) cabinet such as forced convection fin-and-tube type evaporator (FCE) and natural convection tube-and-plate type evaporator (NCE), to investigate the humidity control improvement.

Experimental results shows that, average humidity ratios of freezer (F) and R compartments during the cyclic operations are 0.5 gH_2O/(kg of dry air) and 2.5 gH_2O/(kg of dry air), respectively using the FCE and 0.6 gH_2O/(kg of dry air) and 2.4 gH_2O/(kg of dry air), respectively with NCE. Therefore, the humidity ratio of R compartment is maintained at 4-5 times higher level than that of F compartment for the AED cycle, and also 4 – 5 times higher than that R and F compartments for the base cycle. In addition to the better humidity control, AED cycle provides separate and more efficient cabinet temperature control.

INVESTIGATION OF TWO PERFORMANCE IMPROVEMENT OPTIONS FOR HOUSEHOLD REFRIGERATORS

By

Ahmet Ors

Thesis submitted to the Faculty of the Graduate School of the
University of Maryland, College Park, in partial fulfillment
of the requirements for the degree of
Master of Science
2006

Advisory Committee:
Professor Reinhard Radermacher, Chair/Advisor
Assistant Professor Elias Balaras
Assistant Professor Bao Yang

DEDICATION

Dedicated to my parents

ACNOWLEDGEMENTS

I would first like to thank my advisor, Dr. Reinhard Radermacher, for giving me the opportunity to conduct research and gain an advanced education at the University of Maryland, College Park. His continuous support and guidance made this thesis possible. I am also very grateful for the support of Dr. Yunho Hwang. His continuous help and education, limitless patience and encouragement during my life at CEEE were invaluable and unforgettable. A warm thank you also goes to Dr. Nilufer Egrican. Without her support, it would not have been possible to get my degree from the University of Maryland, CEEE.

For their continuous help and friendship, I thank my recent and previous colleagues Jan Muehlbauer, Dae-Hun Jin, XuDong Wang, John Linde, Dr. Rin Yun, Cara Sanderson and all other CEEE members. My special thanks go to Jan Muehlbauer for his help during my experimental setup process and his wonderful friendship, to Dae-Hun Jin for his valuable education and XuDong Wang for his positive energy.

Special thanks are extended to LG Electronics for their continuous support and cooperation during all periods of this project.

Finally, I would like to say that it was not possible to accomplish this thesis without my parents', sister's and girlfriend's invaluable love and support. Although they were far away from me in distance, they were always in my heart during my life in the USA.

TABLE OF CONTENTS

Section **Page**

List of Tables ..... **vii**

List of Figures ..... **xi**

Nomenclature ..... **xv**

1 Introduction **1**

1.1 Conventional Household Refrigerators 2

2 Literature Review **7**

2.1 Single Evaporator Technologies 7

2.2 Two Evaporator Technologies 9

2.3 Advanced Control Technologies 15

3 Motivation and Objectives **19**

3.1 Motivation 19

3.2 Objectives 19

4 Condenser Improvement **20**

4.1 Condenser Improvement Experimental Setup 20

4.1.1 Test Facility 20

4.1.2 Measurement and Data Acquisition 26

4.1.2.1 Measurement 26

4.1.2.2 Data Acquisition 36

4.1.3 Uncertainty Analysis 37

4.2 Condenser Improvement Experimental Method 39

4.2.1 Experimental Procedures 39

4.2.2 Experimental Analysis 39
4.2.2.1 Calculations of the Cycle Properties 40
4.3 Condenser Improvement Experimental Results 43
4.3.1 Counter-flow Condenser Effect on Discharge Pressure 43
4.3.2 Counter-flow Condenser Effect on Suction Pressure 44
4.3.3 Counter-flow Condenser Effect on MFR 45
4.3.4 Counter-flow Condenser Effect on Power Consumption 45
4.3.5 Counter-flow Condenser Effect on Daily Energy Consumption 46
4.3.6 Cycle Comparison 47
4.3.6.1 Comparison of Calculated and Measured Data 47
4.3.6.2 Cycle Graphs 50
4.4 Conclusions 52
5 Alternating Evaporator Duty Cycle with Two Step Capacity Modulated Compressor 53
5.1 AED Cycle Design 53
5.1.1 AED Cycle Simulation 54
5.1.1.1 Assumptions 54
5.1.1.2 Calculation Method 55
5.1.1.3 Simulation Matrix 58
5.1.1.4 Conventional Cycle Simulation 59
5.1.1.5 Theoretical Boundary Conditions 60
5.1.2 AED Cycle Component Design 61
5.1.2.1 Condenser Design 62

5.1.2.2 Forced Convection Evaporators Design 63
5.1.2.3 Suggested Energy Saving Options with FCE for R Cabinet..... 67
5.1.2.4 Natural Convection R Evaporator Design 72
5.1.2.5 Suggested Energy Saving Options with NCE for R Cabinet..... 76
5.1.2.6 Practical Design Recommendations 77
5.2 AED Cycle Experimental Setup 78
5.2.1 FC R Evaporator Test Setup 78
5.2.2 NC R Evaporator Test Setup..... 90
5.2.3 Bi-stable Solenoid Valve 94
5.2.4 Measurement and Data Acquisition..... 96
5.2.4.1 Measurement..... 96
5.2.4.2 Data Acquisition 102
5.3 AED Cycle Control Method and Algorithm..... 103
5.3.1 Experimental Procedures 105
5.3.1.1 Humidity Ratio Measurement Experimental Procedure 106
5.3.2 Experimental Data Analysis 107
5.3.2.1 Calculations of the Cycle Properties..... 108
5.4 AED Cycle Experimental Results..... 108
5.4.1 FC R Evaporator Experimental Results..... 108
5.4.2 FC R Evaporator Humidity Ratio Measurement Test Results..... 112
5.4.3 NC R Evaporator Experimental Results 116
5.4.4 NC R Evaporator Humidity Ratio Measurement Test Results 122
5.4.5 AED Cycle Defrost Energy Consumption Calculations..... 126

5.5 Conclusions 128

6 Recommendations and Future Work 130

7 References 131

List of Tables

Table 1 Refrigerator specifications 21

Table 2 Compressor specifications 23

Table 3 Pressure transducer specifications 29

Table 4 T-Type thermocouple specifications 31

Table 5 Watt meter specifications 36

Table 6 Averaged F+R operation properties 38

Table 7 Error analysis 38

Table 8 Condenser Improvement test matrix 39

Table 9 Calculated cycle properties 48

Table 10 Measured cycle properties 49

Table 11 Cabinet temperatures 50

Table 12 Variables in simulation matrix 59

Table 13 TEvapR values in simulation matrix 59

Table 14 Conventional cycle simulation summary 60

Table 15 Theoretical boundary conditions 60

Table 16 The least energy savings options 61

Table 17 The best energy saving options 61

Table 18 Condenser specifications 62

Table 19 Designed FC R evaporators I 64

Table 20 Designed FC R evaporators II 65

Table 21 Designed FC F evaporators 66

Table 22 Energy saving option 1 67

Table 23 Energy saving option 1 68
Table 24 Energy saving option 2 68
Table 25 Energy saving option 2 68
Table 26 Energy saving option 3 69
Table 27 Energy saving option 3 69
Table 28 Energy saving option 4 69
Table 29 Energy saving option 4 70
Table 30 Energy saving option 5 70
Table 31 Energy saving option 5 70
Table 32 Energy saving option 6 71
Table 33 Energy saving option 6 71
Table 34 NCE design conditions 76
Table 35 Designed NCE 76
Table 36 R Cycle with NCEs 77
Table 37 Specifications of Capillary tube 83
Table 38 Lengths of Cap, SL and SLHX 85
Table 39 Specifications of the bypass expansion valve 86
Table 40 Specifications of the Solenoid valve 86
Table 41 Specifications of the bi-stable solenoid valve 95
Table 42 Watt meter for Solenoid valves 101
Table 43 Watt meter for fans 101
Table 44 Specifications of humidity sensors 102
Table 45 Specifications of compared tests 109

Table 46 Comparison of cycle properties 110

Table 47 Comparison of cabinet heat loads 110

Table 48 Summary of FCE AED cycle test results 111

Table 49 Cycle properties for a HR experiment with FCE 116

Table 50 Optimum AED cycle with NCE 117

Table 51 NCE AED cycle properties 121

Table 52 NCE AED cycle cabinet heat loads 121

Table 53 Summary of NCE AED cycle test results 122

Table 54 One cycle properties of HR experiment with NCE 126

List of Figures

Figure 1 Schematic diagram of a conventional refrigeration cycle 2

Figure 2 Conventional refrigerator/freezer air distributions 4

Figure 3 Single evaporator two fans refrigerator 8

Figure 4 SEDS cycle R/F unit 9

Figure 5 SEDS cycle 9

Figure 6 Two series evaporators cycle 10

Figure 7 Two parallel evaporators cycle 11

Figure 8 Alternatively parallel evaporators (AED) cycle 12

Figure 9 Lorenz and Meutzner two series evaporator cycle 13

Figure 10 AED Cycle with bi-stable solenoid valve 14

Figure 11 AED cycle cabinet temperatures 15

Figure 12 AED cycle power consumption 15

Figure 13 Performance map of the household refrigerator 16

Figure 14 Cycle pressures with different compressor speeds in on/off control 16

Figure 15 Energy consumption in the whole capacity range 17

Figure 16 AED cycle with variable speed compressor 18

Figure 17 Side-by-side refrigerator 21

Figure 18 Refrigerator's cabinet inside 21

Figure 19 Counter cross-flow evaporator 22

Figure 20 Cross-flow condenser 22

Figure 21 Counter-flow condenser 23

Figure 22 Compressor cabinet 24

Figure 23 Schematic diagram of refrigerator's original refrigeration cycle 25
Figure 24 Pressure transducer locations 27
Figure 25 Pressure transducers' installation 28
Figure 26 Evaporator inlet pressure transducer connection 28
Figure 27 Pressure transducer 29
Figure 28 Refrigeration cycle temperature measurement 30
Figure 29 T-Type thermocouple 31
Figure 30 Cycle TCs locations 32
Figure 31 Evaporator air side temperature measurement 33
Figure 32 Cabinets' temperature measurement 35
Figure 33 Watt Meter 35
Figure 34 Cycles used in random error analysis 37
Figure 35 Base unit cycle pressures and power 40
Figure 36 Charge vs. discharge pressure 44
Figure 37 Charge vs. suction pressure 44
Figure 38 Charge vs. MFR 45
Figure 39 Charge vs. power consumption 46
Figure 40 Daily energy consumption vs. charge 47
Figure 41 Cycles' pressures and powers 51
Figure 42 Cycle temperatures 51
Figure 43 Schematic diagram of natural convection evaporator 72
Figure 44 Heat transfer to the NC evaporator 73
Figure 45 Modified R cabinet 79

Figure 46 F evaporator and fan 80
Figure 47 FC R evaporator and its connection 81
Figure 48 FC R evaporator and air guide 82
Figure 49 Evaporator tubing 83
Figure 50 SLHX prototype 84
Figure 51 AED cycle compressor and bypass line 85
Figure 52 Solenoid valves and filter-dryers 87
Figure 53 AED cycle tubing and insulation 88
Figure 54 AED cycle counter-flow condenser 89
Figure 55 Compressor compartment 89
Figure 56 AED refrigerator cabinet inside with FC R evaporator 90
Figure 57 NC R evaporator 91
Figure 58 R Cabinet with NC evaporator 92
Figure 59 Capillary tube connection in NCE experiments 93
Figure 60 AED Cycle experimental setup 94
Figure 61 Bi-stable solenoid valve 95
Figure 62 AED cycle experiments with pressure transducer locations 97
Figure 63 AED cycle experiments TCs locations 98
Figure 64 AED experiments cabinets' temperature measurement 100
Figure 65 Humidity sensors position 102
Figure 66 AED cycle control box 104
Figure 67 AED cycle pressures and power consumption 107
Figure 68 Humidity ratios during pull down operation 112

Figure 69 Humidity ratios during cyclic operation 113

Figure 70 Humidity ratios during defrost cycles 114

Figure 71 R evaporator condition during off-cycle 115

Figure 72 AED cycle pressures and W_{Comp} with the NC R evaporator 118

Figure 73 NCE surface temperatures 119

Figure 74 Humidity ratios during pull down with NCE for R cabinet 123

Figure 75 Humidity ratios during cyclic operation with NCE 124

Figure 76 Defrost cycles with NCE 125

Nomenclature

AED	Alternating Evaporator Duty
Calc	Calculated
Cap	Capillary Tube
C_{Comp}	Compressor Efficiency Coefficient
CFC	Chlorofluorocarbon
CHL	Cabinet Heat Load
C_{Vol}	Volumetric Efficiency Coefficient
DEC	Daily Energy Consumption
Disp	Displacement
EC	Energy Consumption
EES	Engineering Equation Solver
Eff	Efficiency
F	Freezer
FC	Forced Convection
FCE	Forced Convection Evaporator
h	Enthalpy
H	Height
HCFC	Hydrochlorofluorocarbon
HFC	Hydrofluorocarbon
HL	Heat Load
HTC	Heat Transfer Coefficient
HX	Heat Exchanger

ID	Inside Diameter
Meas	Measured
MEC	Monthly Energy Consumption
MFR	Mass Flow Rate
NC	Natural Convection
NCE	Natural Convection Evaporator
OCEC	One Cycle Energy Consumption
OD	Outside Diameter
OTR	On Time Ratio
Q	Capacity
P	Pressure
PR	Pressure ratio
R	Refrigerator
RPM	Revolution Per Minute
R/F	Refrigerator/Freezer
s	Entropy
SEDS	Single Evaporator Dual Source
SL	Suction Line
SLHX	Suction Line Heat Exchanger
T	Temperature
TC	Thermocouple
t	Time
V	Voltage

W	Power Consumption
X	Refrigerant Quality

Greek Symbols

ρ	Density	[kg/m^3]
η	Efficiency	

Subscripts

Cap	Capillary
Comp	Compressor
Cond	Condenser
Cyc	Cycle
Suc	Suction
Dis	Discharge
Diss	Isentropic Discharge
Evap	Evaporator
F	Freezer
i	Inlet
Isen	Isentropic
Mot	Motor
o	Outlet
off	Off Cycle
PT	Pressure Transducer
R	Refrigerator

Sub	Subcooling
Sup	Superheat
T	Total
Vol	Volumetric

1 Introduction

Due to environmental concerns, the refrigerator industry is facing the challenge of developing more efficient and environmentally friendly refrigerators. Through extensive study, refrigerants, CFC's and HCFC's, which have environmentally harmful effects on the environment, have been shifted to new generation environmentally friendly refrigerants, HFC's. Recent investigations show, however, that HFC's contribute to global warming. Accordingly, new policies have taken affect that force the refrigerator industries to develop refrigerators that reduce energy consumption and refrigerant emissions in order to ultimately reduce energy bills and global warming effects.

A conventional refrigerator's system efficiency can be improved by the following options:

- Developing more efficient refrigeration cycles
- Developing more efficient control algorithms
- Reducing on/off cycle losses
- Improving insulation effects and decreasing air infiltration to reduce cabinet heat load
- Reducing electrical load coming from electrical components such as fans, defrost heaters, and control electronics.

One of the most promising options to improve a refrigerator's system efficiency is to develop a more efficient refrigeration cycle. Current studies include improving cycle component efficiency, minimizing cycle losses and building alternative refrigeration cycles that are more efficient than conventional ones.

In order to successfully design an energy efficient alternative for refrigeration cycles used for household refrigerators, the conventional cycle should be well understood.

1.1 Conventional Household Refrigerators

The conventional refrigeration cycle used in household refrigerators is comprised of one fixed capacity compressor, one condenser, one evaporator and one suction line heat exchanger, as shown in Figure 1.

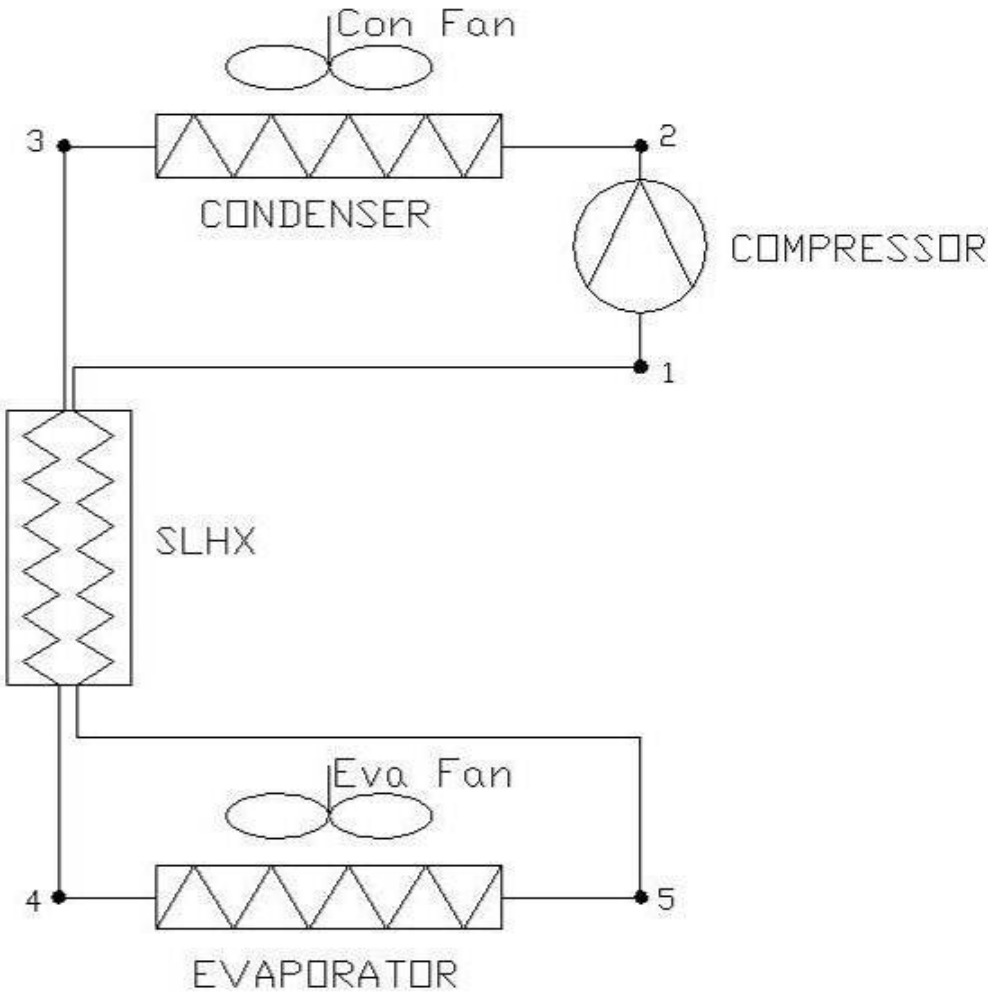

Figure 1 Schematic diagram of a conventional refrigeration cycle

In the conventional cycle, the compressor sucks refrigerant at the superheated low pressure condition, state point 1, and discharges it as superheated high pressure refrigerant, state point 2. Then refrigerant enters the condenser. In the condenser, the refrigerant's condition is changed from high pressure superheated vapor, state point 2, to high pressure subcooled liquid, state point 3. From the condenser, refrigerant enters a capillary tube at state point 3 and travels up to the evaporator entrance. During this process the refrigerant pressure is decreased to the desired evaporating pressure. This process is called an adiabatic expansion process. Following the capillary tube, the low pressure refrigerant enters the evaporator. During the evaporation process, cooling is supplied to the cabinets and the refrigerant's state is changed from a low pressure two-phase state, state point 4, to a low pressure superheated state, state point 5. As shown in Figure 1, refrigerant enters the capillary tube and the refrigerant from the evaporator enters the SLHX. In the SLHX, the subcooled hot refrigerant looses heat and the superheated cold refrigerant gains heat. As a result, cycle efficiency is increased.

Generally, household refrigerators contain two different temperature level cabinets. One of them is the food or refrigeration cabinet (R) in which the temperature is kept around 3^{o}C, and the other one is the freezer cabinet (F) in which the temperature is kept around -18^{o}C. In conventional refrigerators the cabinet temperatures are kept at desired levels with a single evaporator as shown in Figure 2.

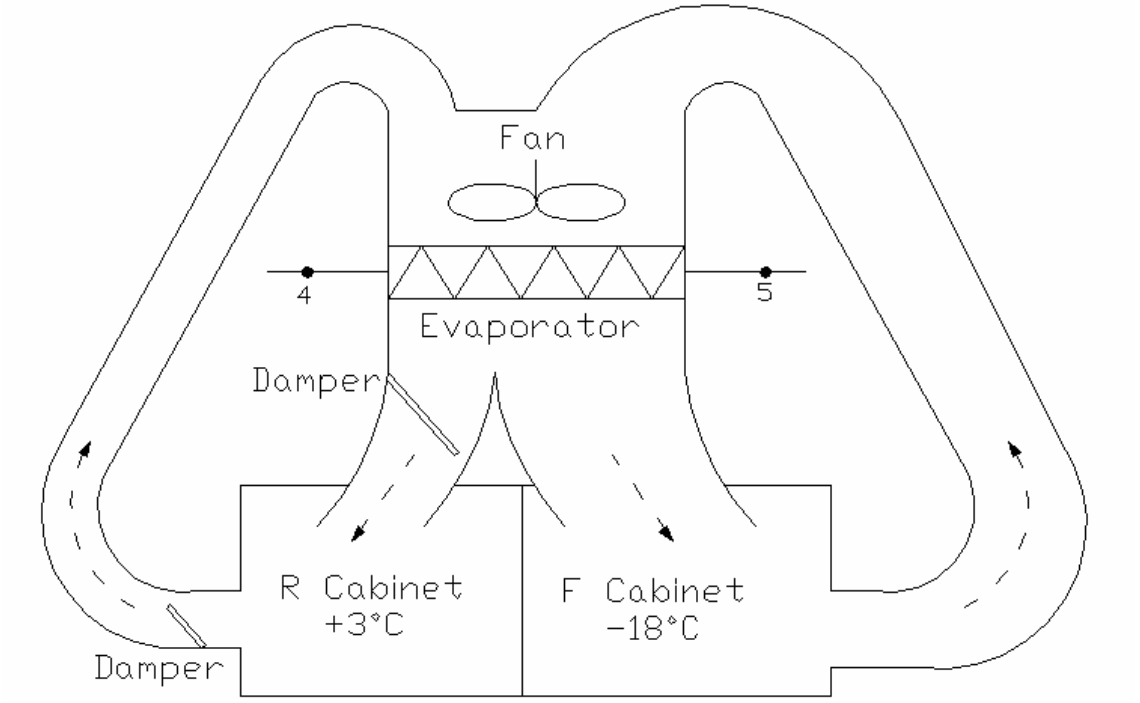

Figure 2 Conventional refrigerator/freezer air distributions

While refrigerant is evaporating inside the evaporator, heat is transferred from the air to the refrigerant and necessary cold air is supplied to the cabinets. When the F cabinet temperature reaches its upper limit of the F thermostat band, the refrigeration cycle starts running and the air is cooled below F cabinet air temperature. Then the F cabinet temperature starts to decrease to its lower limit value of the F thermostat band. While the F cabinet is cooled, the R cabinet temperature is controlled by dampers. If the R cabinet temperature reaches its upper limit, the air inlet damper is opened a specified amount and cold air is allowed to flow into the R cabinet. After the R cabinet temperature reaches its lower limit, the damper is closed and air flow to the R cabinet is stopped. As a result, the R cabinet temperature is kept at its pre-set temperature.

Although conventional single evaporator refrigerators are reliable, there are some drawbacks that force engineers to find better technologies.

The first drawback is that a conventional cycle cannot supply individual cabinet temperature control. As explained in the previous chapter, conventional household refrigerators/freezers have a single evaporator, even though they have two different temperature level cabinets. In a conventional system R cabinet temperature depends on the F cabinet temperature because system runs based on the F cabinet thermostat settings. R cabinet cannot be individually cooled and its temperature cannot be separately controlled.

Secondly, although it is possible to use a higher pressure level evaporation for the R cabinet compared to that of the F cabinet, conventional cycles cannot achieve this benefit because they only have a single evaporator. As can be seen in Eq. 1, thermodynamic rules state that a refrigeration cycle that has a higher cabinet temperature consumes less energy than one with a lower cabinet temperature [1].

$$P = \dot{Q}_0 \cdot \frac{T_a - T_0}{T_0} \tag{1}$$

where $\dot{Q}_0$ is required cooling capacity, T_a is ambient temperature, T_0 is desired cabinet temperature and P is thermodynamic energy. Conventional refrigerators/freezers consume more energy since they only have one temperature level evaporator and they cannot get benefit from a higher temperature level R cabinet.

Another important drawback of conventional units is insufficient humidity ratio control for the R cabinet. Humidity ratio level is an important factor for food freshness and food life. Dry air in the R cabinet decreases the quality of effective food storage. Therefore, the R cabinet humidity level should be kept at higher humidity ratio levels to supply better food storage. However, in conventional units it is impossible to maintain

high humidity level in the R cabinet, because the R cabinet air is mixed with F cabinet air and then flows through a low temperature evaporator. Because of the low surface temperature of the evaporator, typically below -25^0C, moisture from the R cabinet air condenses on the evaporator surface and air humidity ratio entering the R cabinet decreases. As a result, the R cabinet food storage quality decreases.

2 Literature Review

Many studies have been conducted in attempts to get rid of conventional refrigerator/freezer (R/F) drawbacks and develop R/Fs that are more efficient and have better storage quality. Studies in this area can be classified into two main parts: single evaporator technologies and two evaporator technologies. Two evaporator technology studies can be divided into three main subparts: two series evaporator technologies, two parallel evaporator technologies, and alternatively parallel evaporator (AED) technologies.

In addition to studies about new cycle options, studies are also being conducted in order to find new compressor control methods, such as variable speed compressor control or two fixed speed compressor control.

2.1 Single Evaporator Technologies

Single evaporator technologies are similar to conventional R/F units. Their main similarity is that they both have one evaporator, one compressor, and one condenser. However additional developments such as two separate air passages and two individual capillary tubes one for both the R and F cabinets, can improve conventional R/F units' cycle efficiency and food storage quality.

Lee et al. (1994, Daewoo) designed a new R/F which has one evaporator but two separated cooling fans and air passages, one for both the F and R cabinet as seen in Figure3. Their main purpose was to control the refrigerator cabinet temperature individually. Indeed, results showed that they supplied better R cabinet temperature control as compared to conventional refrigerators. Consequently, they also achieved

longer fresh food life. In addition to improved R cabinet temperature control, Daewoo's new invention decreased total defrost energy consumption by approximately 25%. This energy saving was achieved by circulating warm R cabinet air through the evaporator in the defrost cycle, which accounts for 2% of the overall energy consumption.

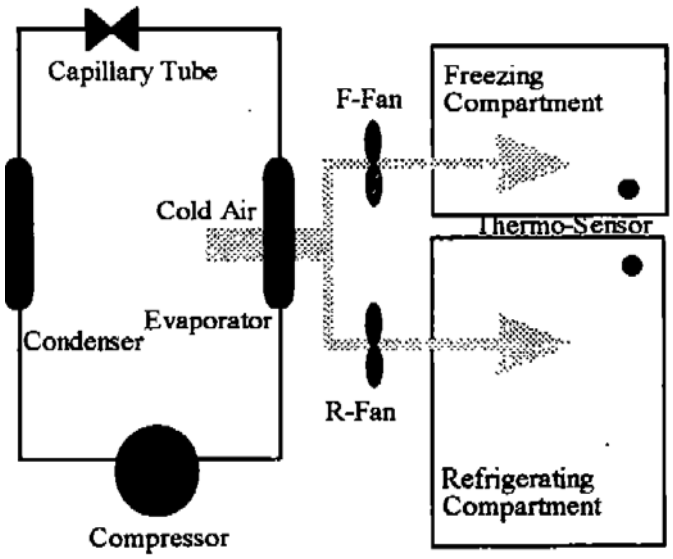

Figure 3 Single evaporator two fans refrigerator

Park et al. (1998, LGE) invented a R/F, Single Evaporator Dual Source (SEDS) cycle, which has an air flow switching system that uses two dampers, two fans and two solenoid valves, which control the refrigerant flow path either through a R compartment capillary tube or through a F compartment capillary tube. As seen in Figures 4 and 5, F cabinet air and R cabinet air are totally separated from one to another. In this invention when the R cabinet needs cooling, solenoid valves direct refrigerant to the R capillary tube and close the F capillary tube. At the same time dampers close the F air passage and open the R air passage then the food compartment fan is turned on. Accordingly, the

system cools the R cabinet down. Similarly, when the F cabinet needs cooling, components belonging to the F cabinet are activated and the system cools the F cabinet.

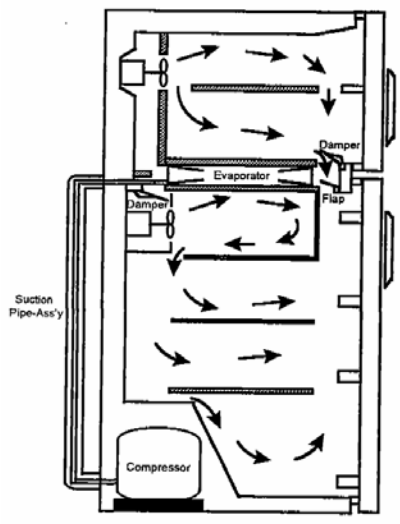

Figure 4 SEDS cycle R/F unit

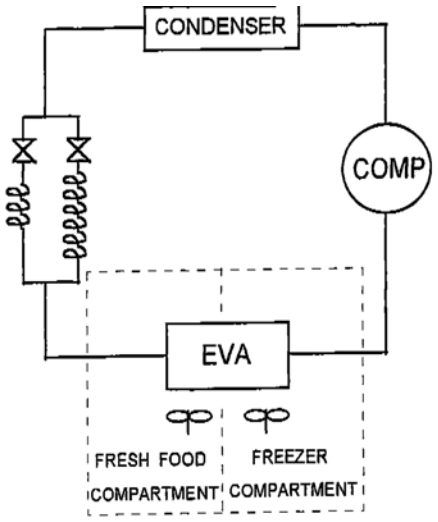

Figure 5 SEDS cycle

The main purpose pf the Park et al. project was to consume less energy by using a higher evaporating temperature in the food compartment cycle. Park reported that their refrigerator saved 17.3% of the total energy: 8.5% from compressor energy efficiency improvements, 5.2% from improved cycle operation conditions, and 3.6% from the solenoid valves, which shut off during off-cycle and prevent warm refrigerant migration to the evaporator.

2.2 Two Evaporator Technologies

In two evaporator technology, R/F units include two separate evaporators, one for the R cabinet and one for the F cabinet. If the evaporators are connected in series, as in Figure 6, then the cycle is called a two series evaporators cycle.

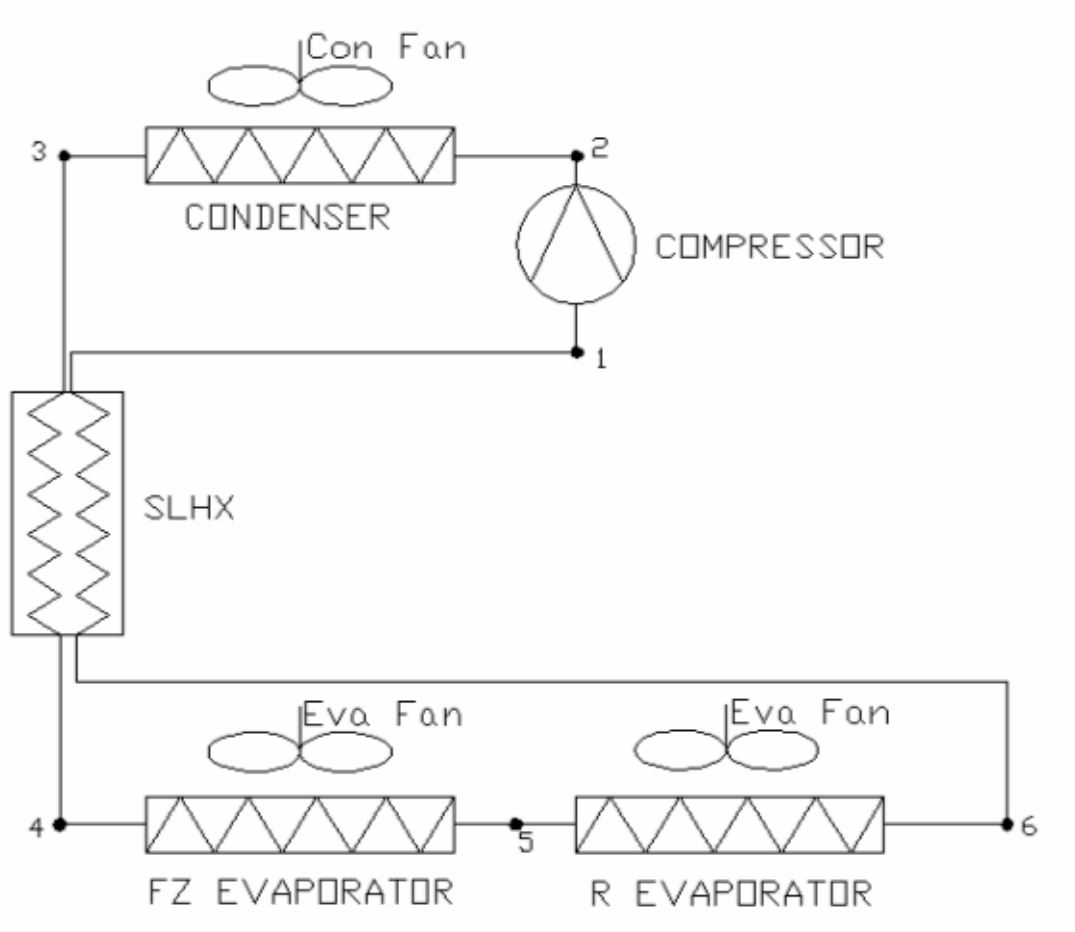

Figure 6 Two series evaporators cycle

If the evaporators are connected in parallel, as in Figure 7, then the cycle is called a two parallel evaporators cycle.

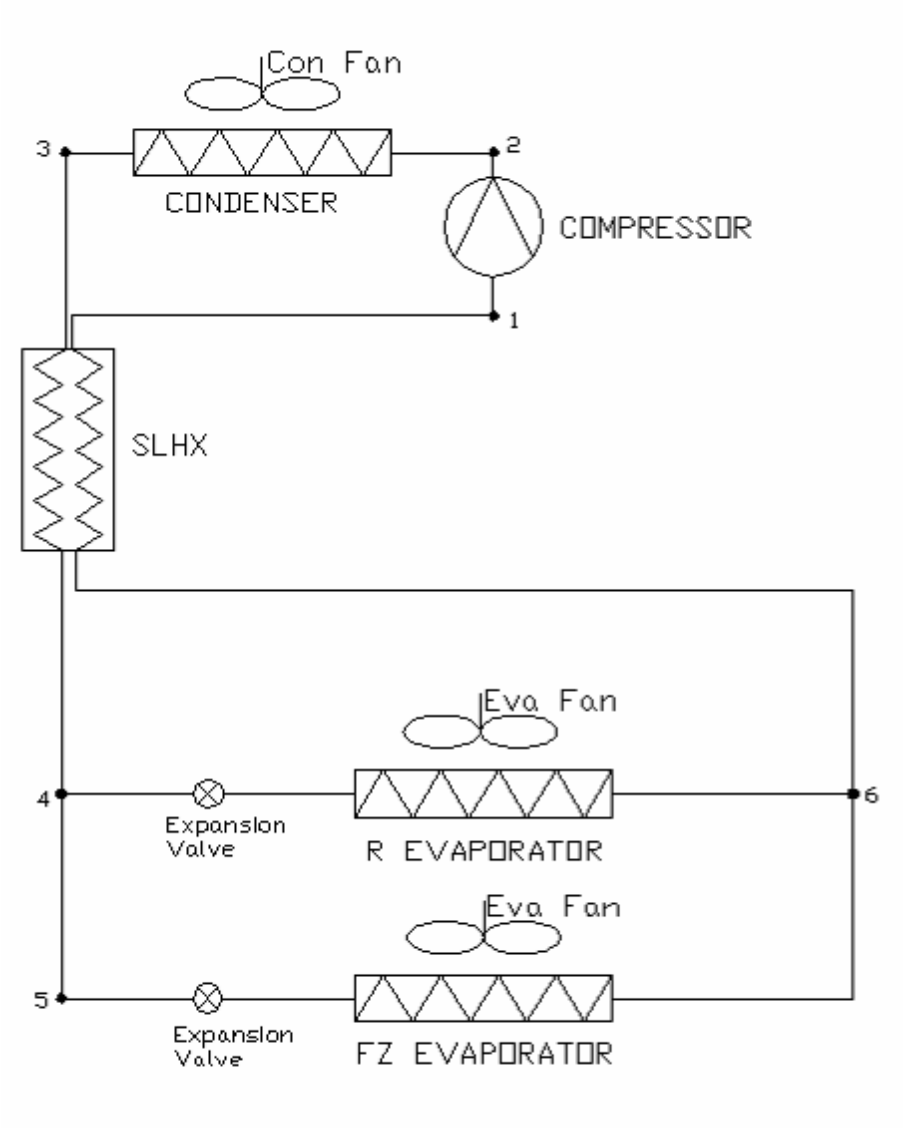

Figure 7 Two parallel evaporators cycle

If evaporators are connected in parallel and if the flow path is controlled by a bi-stable solenoid valve, as in Figure 8, then the cycle is called an alternatively parallel evaporators (AED) cycle.

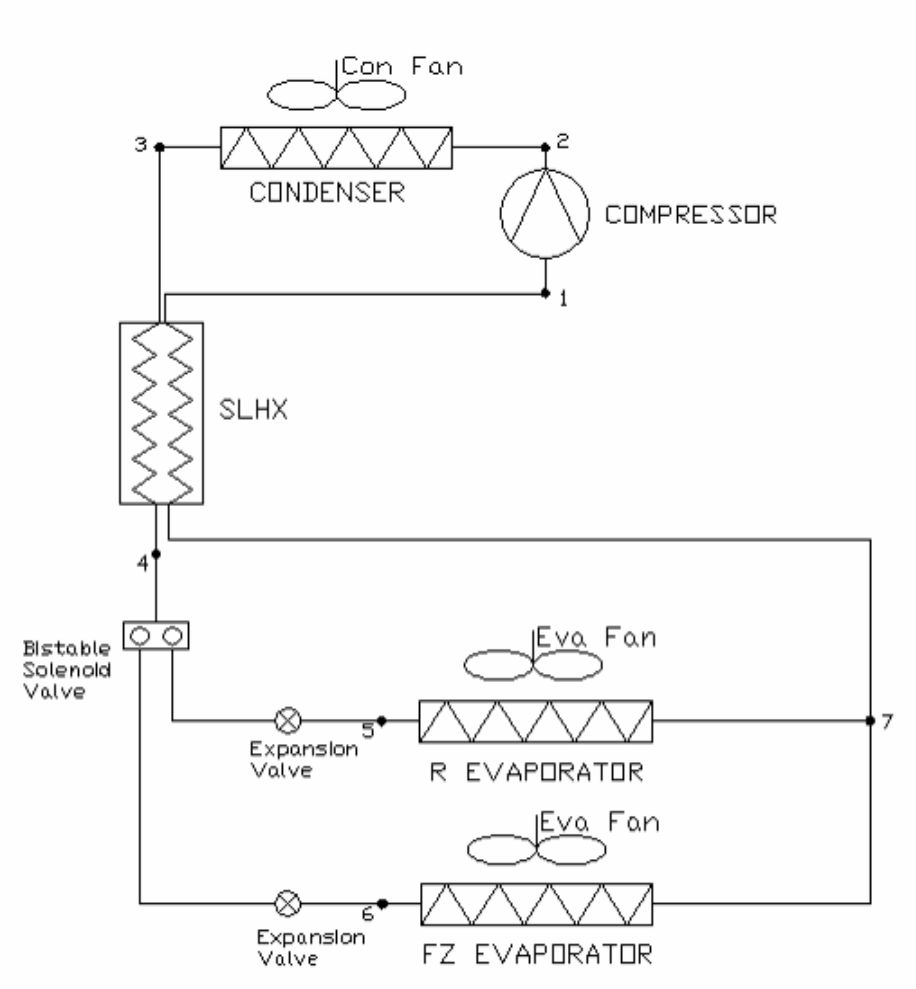

Figure 8 Alternatively parallel evaporators (AED) cycle

Lorenz and Meutzner (1975) invented a two series evaporator refrigeration cycle with two intercoolers using zeotropic refrigerant mixtures as shown in Figure 9. The refrigerant leaving the condenser enters the SLHX where it exchanges heat with the suction line. After the SLHX, liquid refrigerant enters the internal heat exchanger. Liquid refrigerant is cooled and two-phase refrigerant coming from the F evaporator is evaporated in the internal heat exchanger. More subcooled refrigerant enters the expansion device after leaving the internal heat exchanger and its pressure is decreased to the desired level for F cabinet cooling. The low pressure two-phase refrigerant enters the

F evaporator and then passes through the internal heat exchanger, the R evaporator and the SLHX, respectively. In this cycle, the internal heat exchanger and the SLHX supply more subcooling at the condenser outlet and proper temperature levels for both evaporators.

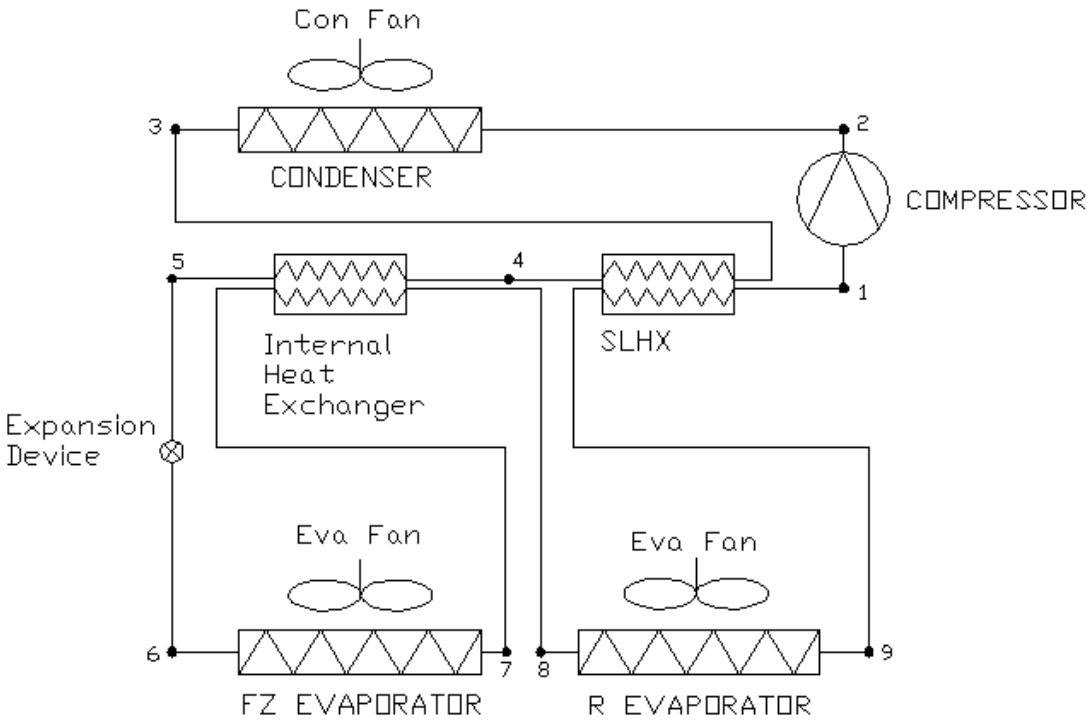

Figure 9 Lorenz and Meutzner two series evaporator cycle

Lorenz and Meutzner (1975) reported 20% energy savings for a Lorenz – Meutzner cycle using a mixture of R22/R11 compared to a conventional refrigerator utilizing R12.

Radermacher et al. (1998, University of Maryland, CEEE) invented and patented an AED cycle that includes two natural convection type evaporators, one for the R cabinet and one for the F cabinet; one tube in tube style SLHX, two throttle valves, one for the R compartment and one for the F compartment; one bi-stable solenoid valve used to direct refrigerant flow path either to the food compartment evaporator or to the F

compartment evaporator; and one intercooler between the bi-stable solenoid valve F side outlet and the F evaporator outlet to improve cycle efficiency, as seen in Figure 10.

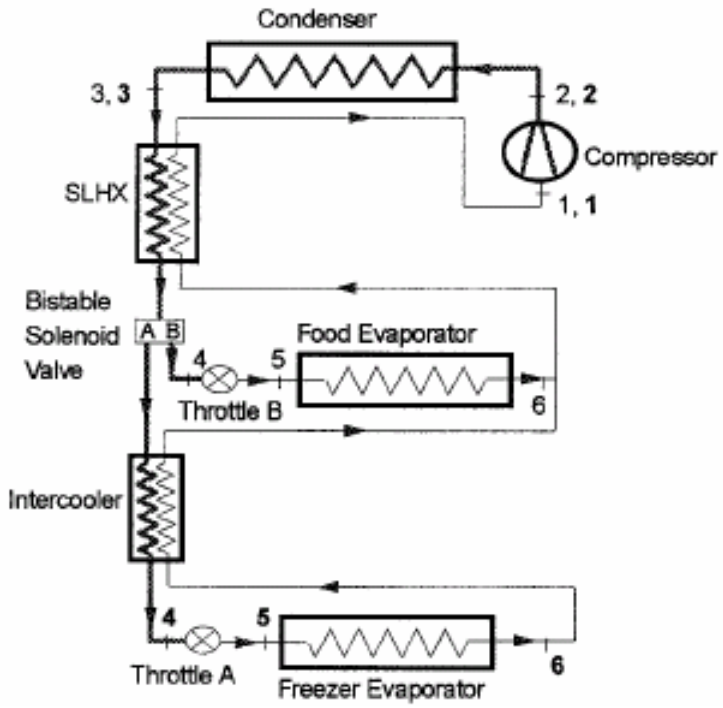

Figure 10 AED Cycle with bi-stable solenoid valve

Radermacher et al. experimented with the new AED cycle and conventional two series evaporator cycle using isobutene as refrigerant. For both experiments same cabinet structures were used. Results proved that their new AED cycle design consumes 9% less energy compared to a conventional two series evaporator cycle. Results also showed that even though the system is in the off-cycle, cabinet temperatures keep decreasing. This phenomenon is typical for natural convection type evaporators. Figure 11 shows results of this phenomenon.

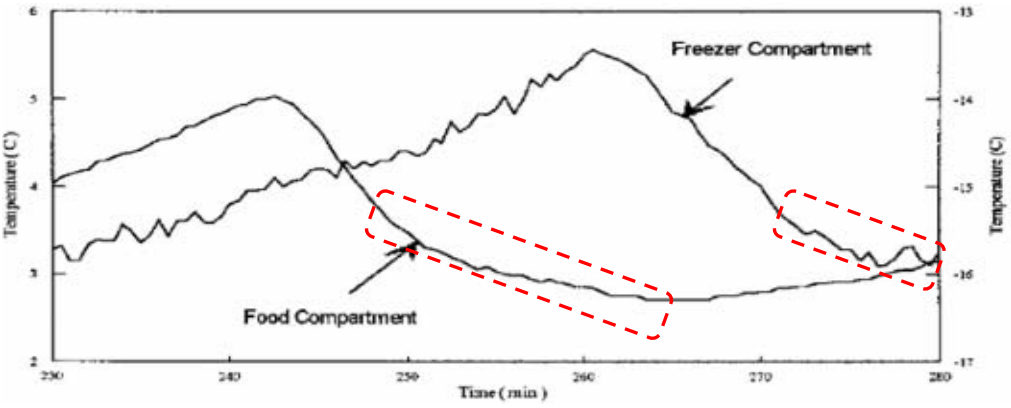

Figure 11 AED cycle cabinet temperatures

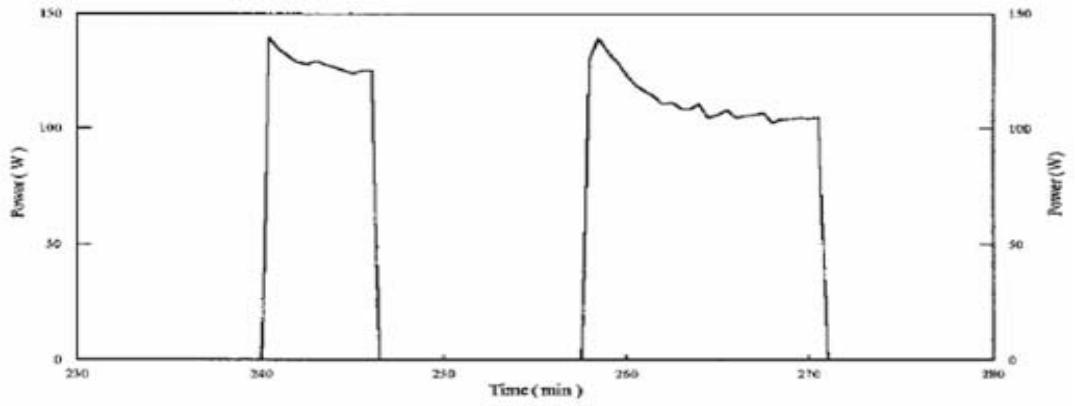

Figure 12 AED cycle power consumption

2.3 Advanced Control Technologies

Binneberg et al. (2002, Dresden University) investigated three different control methods for household refrigerator compressors such as on/off control, continuous operation with variable speed control, and continuous operation with two fixed speed control. They mentioned Figure 13, performance map of the refrigerator, and concluded that since the required cooling capacity and even the ambient temperature vary with time,

the required operating range of the refrigeration cycle of a household refrigerator is quite large, so an adequate capacity control is required.

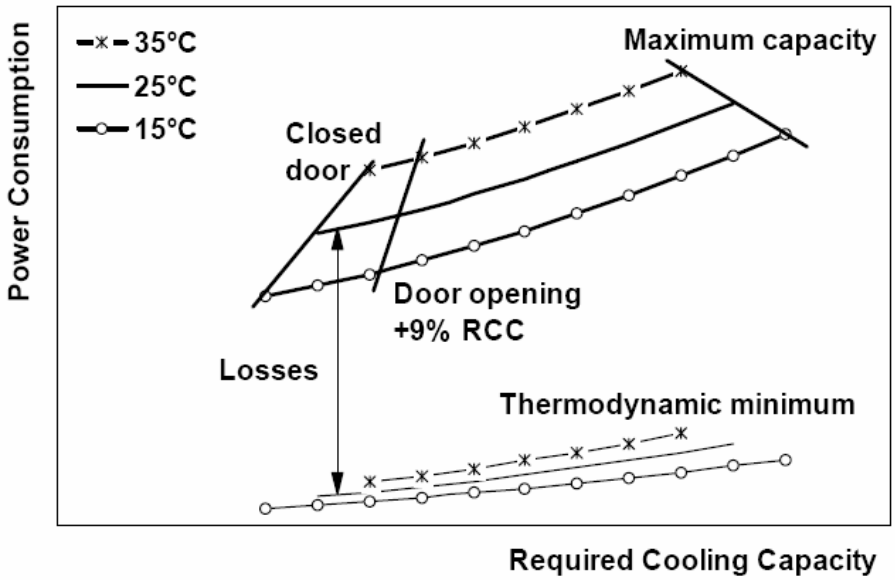

Figure 13 Performance map of the household refrigerator

They measured energy consumption for different speed compressors under on/off control method. As shown in Figure 14, 1800rpm compressor speed cycles have lower condensing and higher evaporating pressure. Even though this operation has longer on time, it has a smaller amount of on/off operation. Binneberg et al. measured that the resultant energy consumption at 1800rpm is about 21% lower than that at 3000rpm.

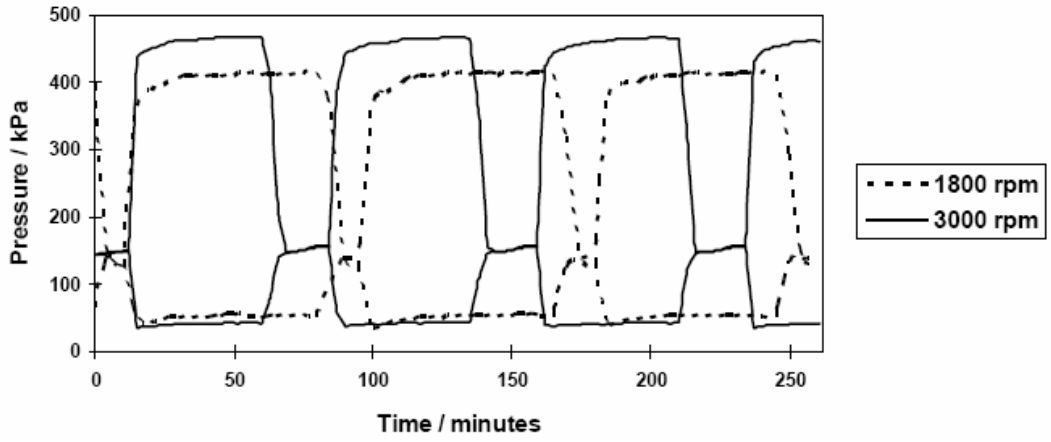

Figure 14 Cycle pressures with different compressor speeds in on/off control

Binneberg et al. did further studies about variable speed compressor control and they suggested that if they run the compressor at a lower speed where it doesn't need to be stopped, then they can save 30% of the total energy. Their measurements proved that continuous operation with a variable speed compressor saves 21% energy compared to household refrigerators equipped with 3000rpm fixed compressor speed that has on/off control . Additionally, they compared the continuous operation variable speed control with the continuous operation two fixed speed control. The results showed that two fixed speed control operation only consumes 3% more energy than continuous speed control operation, as shown in Figure 15. Finally, they concluded that because of the higher cost of a variable speed compressor control, continuous two fixed speed control is much more beneficial for household refrigerators.

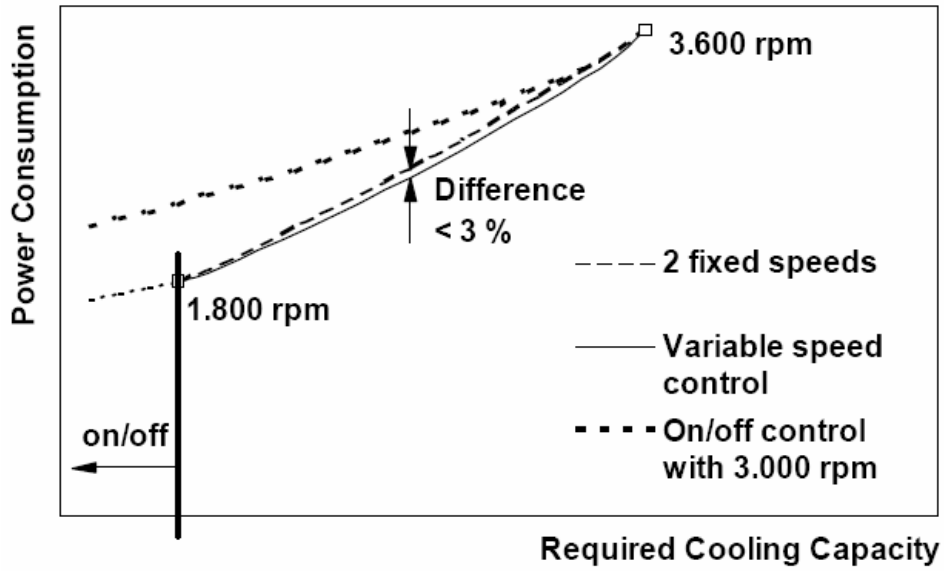

Figure 15 Energy consumption in the whole capacity range

Sakuma et al. (2002, Toshiba) patented a R/F unit including an AED cycle integrated with a variable speed compressor. In their design they used a variable speed compressor to modulate cooling capacity of the R/F unit with respect to cooling needs of

the cabinets. In Toshiba's AED cycle, the compressor runs continuously at different speeds. It is turned off only when its lower capacity is higher than cooling demand or during the defrost cycle. Therefore, losses due to compressor on and off switching can be eliminated. Toshiba suggested using 3-way solenoid valve to control the refrigerant flow path either to the R evaporator or to the F evaporator, as seen in Figure 16. Toshiba's patent specifies that the temperature control of the cabinets would be improved and a more efficient cycle was expected with the new design. However, their patent does not indicate exactly how much energy can be saved with the new design.

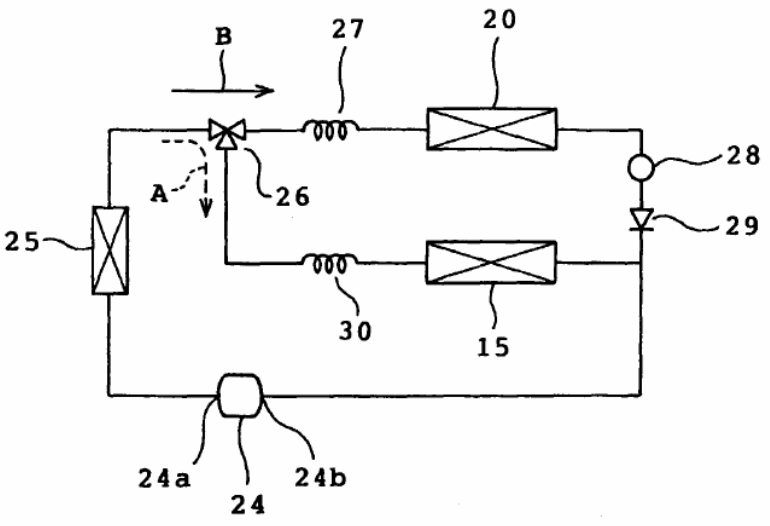

Figure 16 AED cycle with variable speed compressor

In conclusion, many studies have already been conducted in order to improve conventional household refrigerators efficiency. It can be easily said that there is not much more room for improvement using single evaporator technologies except for improving individual cycle components such as the compressor, condenser, evaporator or SLHX. On the other hand, two evaporators technologies are much more promising for reducing energy consumption by household refrigerators. Refrigerators with an AED cycle were proven to consume around 10% less energy than that consumed by two series

evaporator refrigerators and even less for conventional single evaporator refrigerators. The most recent approach in refrigeration research/practice is to use a modulated speed compressor with an AED cycle for household refrigerators.

3 Motivation and Objectives

3.1 Motivation

According to the literature review, there is not much research available in household refrigerators that combines AED cycles with two step capacity modulated compressors. There is also not much experimentation or simulation conducted to validate the feasibility of this promising technology. Therefore, the cycle component Improvement, AED cycle design and its experimental validation can justify the potential of the AED cycle toward the new energy efficient household refrigerators.

3.2 Objectives

The objectives of this study are to:

- Improve the base unit's condenser by improving its heat transfer configuration.
- Simulate the performance potential of the AED cycle under theoretical conditions.
- Design cycle components and validate the feasibility of the new AED cycle with experimental study.

4 Condenser Improvement

One of the options to improve household refrigerators' efficiency is to optimize cycle components individually and apply them back to the original cycle. In this process, an individual component's efficiency may be improved, but if it does not perform better with the combination of the other cycle components, then the individual component improvement cannot be validated in the system. Therefore, it should be verified that the cycle that includes the improved component works more efficiently than the cycle without it.

In the condenser Improvement study, a household refrigerator's condenser configuration was changed from the cross-flow configuration to the counter-flow configuration without changing any other components or the cabinet model. The aim of the study was to improve cycle efficiency within the same capital cost of the current condenser.

4.1 Condenser Improvement Experimental Setup

4.1.1 Test Facility

Household Refrigerator Unit

For this study, a commercially available side-by-side household refrigerator, as shown in Figures 17 and 18, was used. The refrigerator was equipped with the conventional single evaporator refrigeration cycle. The refrigerator's specifications are shown in Table 1.

.

Figure 17 Side-by-side refrigerator

Figure 18 Refrigerator's cabinet inside

Table 1 Refrigerator specifications

Model number	R-S686DMS
Total volume	676L
Freezer compartment volume	250L
Food compartment volume	426L
Width	890mm
Depth	826mm
Height	1750mm
Electric box	AC 220V 60Hz
Weight	114kg
Compressor model	LD72LADM
Manufacturer	LG Electronics

This unit has one fin-and-tube type counter cross flow forced convection type evaporator and one tube-and-wire type cross-flow forced convection type condenser, as shown in Figures 19 and 20.

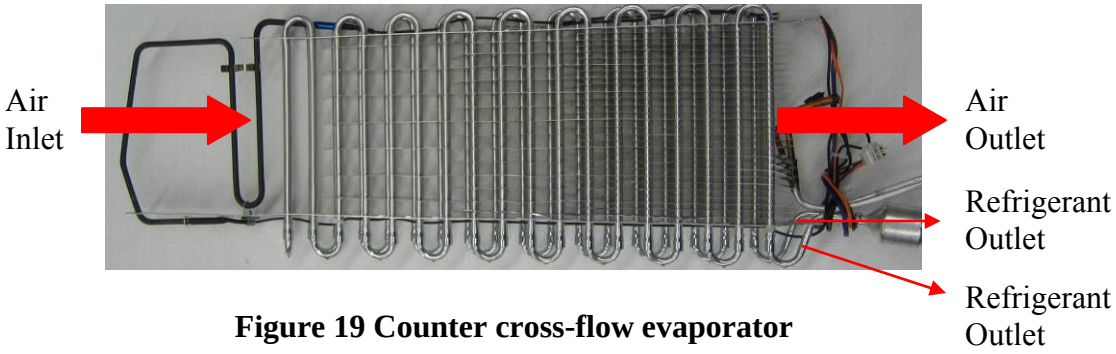

Figure 19 Counter cross-flow evaporator

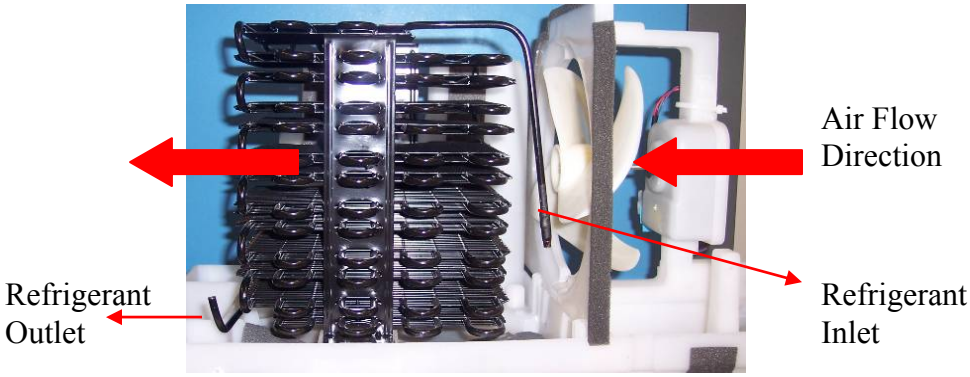

Figure 20 Cross-flow condenser

To build a counter flow condenser, a prototype of the cross-flow condenser was modified, as shown in Figure 21. Two straight tube fittings were used to install the counter-flow condenser to the cycle so it would be easy to change from one condenser to the other. A carrier part, as shown in the figure, was used to mount the counter-flow condenser to the refrigerator.

.

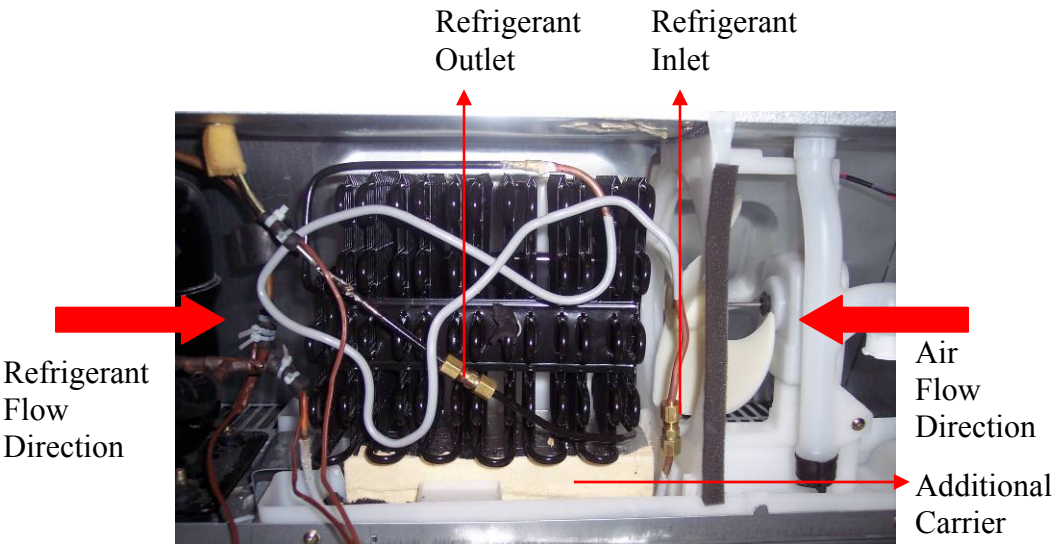

Figure 21 Counter-flow condenser

As a compressor one reciprocating compressor was used. Compressor specifications are shown in Table 2.

Table 2 Compressor specifications

Model number	LD72LADM
Type	Reciprocating
Refrigerant	R134a
Displacement Volume	7.2cc
Compressor Speed	3550RPM
Compressor Efficiency	0.9
Voltage & Frequency	220V & 60Hz
Manufacturer	LG Electronics

The Refrigerator's compressor compartment is shown in Figure 22. It can be seen that air is sucked from ambient conditions, flows through the condenser, then passes around the compressor and decreases the compressor's shell temperature.

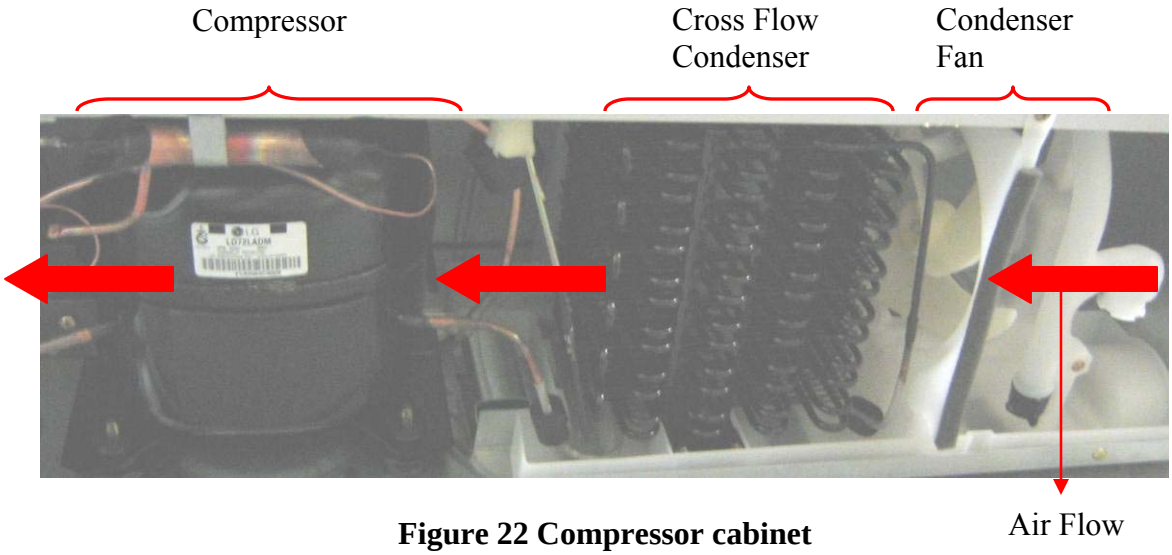

Figure 22 Compressor cabinet

In addition to the aforementioned components, the refrigerator has a capillary tube as an expansion device and a SLHX to improve cycle efficiency. A schematic diagram of the original refrigerator's refrigeration cycle is shown in Figure 23.

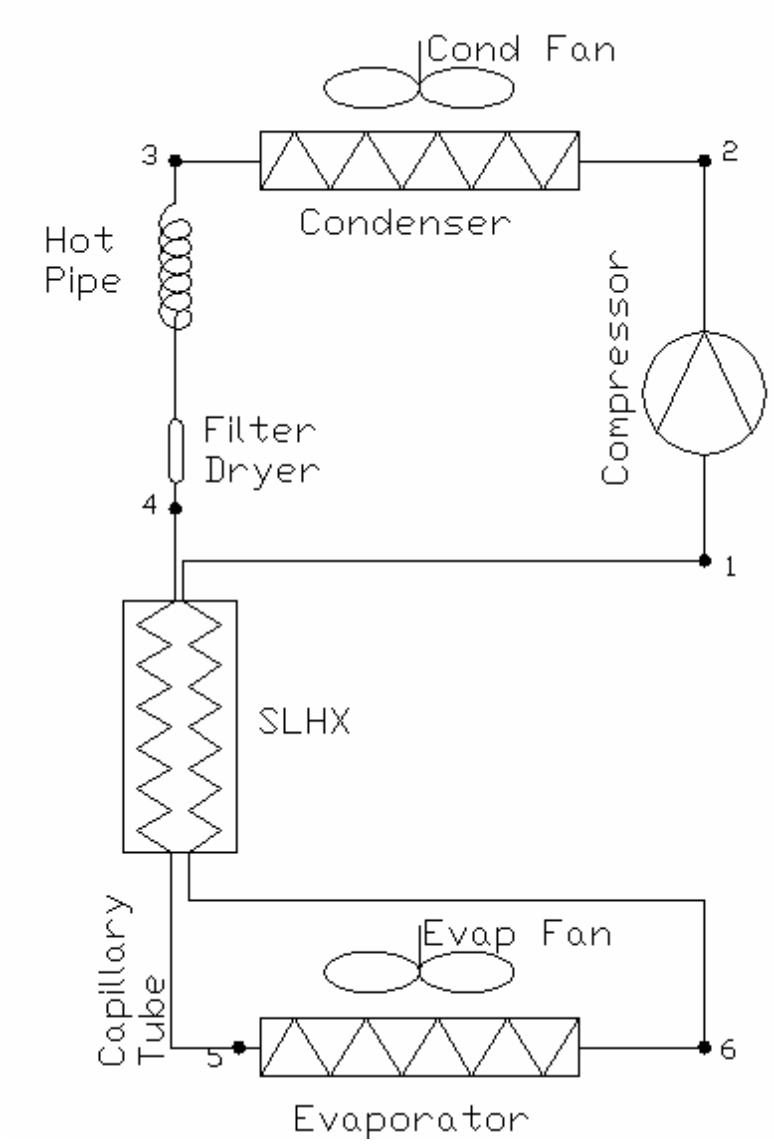

Figure 23 Schematic diagram of refrigerator's original refrigeration cycle

The path between point four and five represents the capillary tube which works as an expansion device in the cycle and whose length is 2.5m and inside diameter is 0.83mm.

Environmental Chamber

Ambient temperature around the test unit was controlled within 30°C ± 0.1 °C by an environmental control chamber. In addition to the chamber control, ambient temperature was monitored by a data acquisition system (DAS) and two copper cylinder masses hanging within the chamber. Thermocouples recording the temperatures of the

copper masses were connected to the DAS as another control for measuring the ambient air temperature.

4.1.2 Measurement and Data Acquisition

4.1.2.1 Measurement

In the condenser Improvement test, cycle pressures, cycle temperatures, the heat exchanger's air side temperatures, the cabinet's air temperatures, and the overall refrigerator power were measured.

Refrigeration Cycle Pressure Measurement

As shown in Figure 24, pressures, important for calculations and analyzing of the cycle properties, were measured at four different locations during the experiments. These locations include the compressor inlet (evaporator outlet), compressor outlet (condenser inlet), hot pipe outlet (capillary tube inlet) and evaporator inlet (capillary outlet).

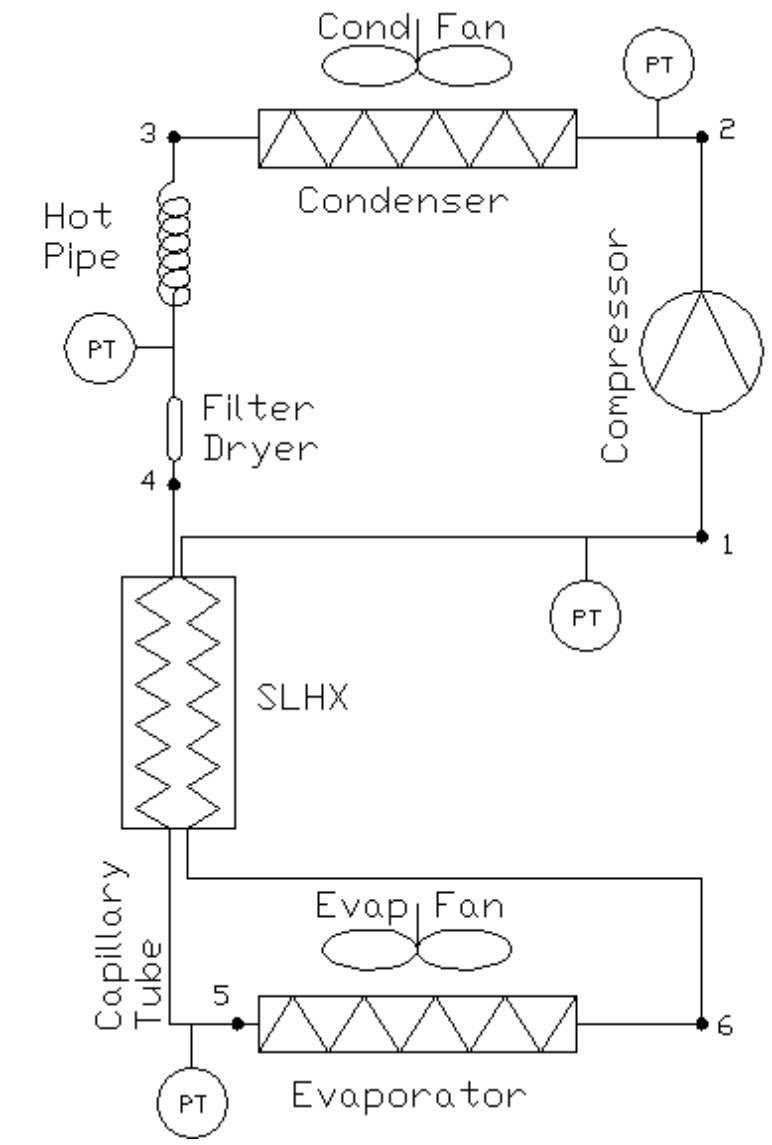

Figure 24 Pressure transducer locations

Figure 25 shows how suction, discharge and capillary inlet pressure transducers were installed to the system.

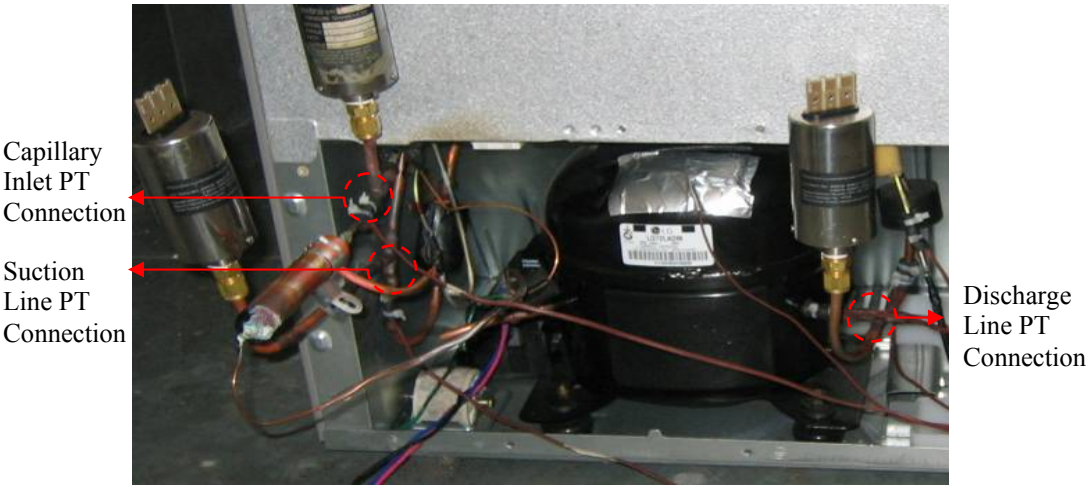

Figure 25 Pressure transducers' installation

To measure evaporator inlet pressure, a long capillary tube was brazed to the evaporator inlet with a T copper connection as shown in Figure 26. Then the capillary tube outlet was carried out of the F and the pressure transducer was installed. To prevent heat loss from the capillary tube, it was insulated with 9.5mm (0.375") thick insulation material.

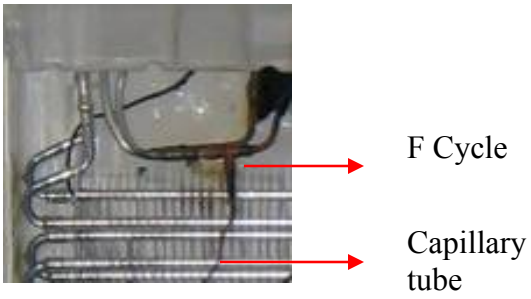

Figure 26 Evaporator inlet pressure transducer connection

Absolute pressure transducers, shown in Figure 27, were used for pressure measurement. For better measurement accuracy, small pressure range and high accurate pressure transducers were chosen. Model specifications are shown in Table 3.

Figure 27 Pressure transducer

Table 3 Pressure transducer specifications

Model	280E
Full Scale Pressure Output	5.03 VDC
Zero Pressure Output	0.03 VDC
Accuracy (RSS Method)	+ - 0.11%
Pressure Type	Absolute
Pressure Range	0 – 250 psia
Manufacturer	Setra

Refrigeration Cycle Temperature Measurement

As shown in Figure 28, temperatures, which are important for calculations and analysis of cycle properties, were measured at ten different locations during the experiments. These locations are compressor inlet, compressor dome, compressor outlet (condenser inlet), middle of the condenser, condenser outlet, hot pipe outlet (capillary tube inlet), evaporator inlet (capillary outlet), the middle of the evaporator, evaporator outlet and the suction side SLHX outlet.

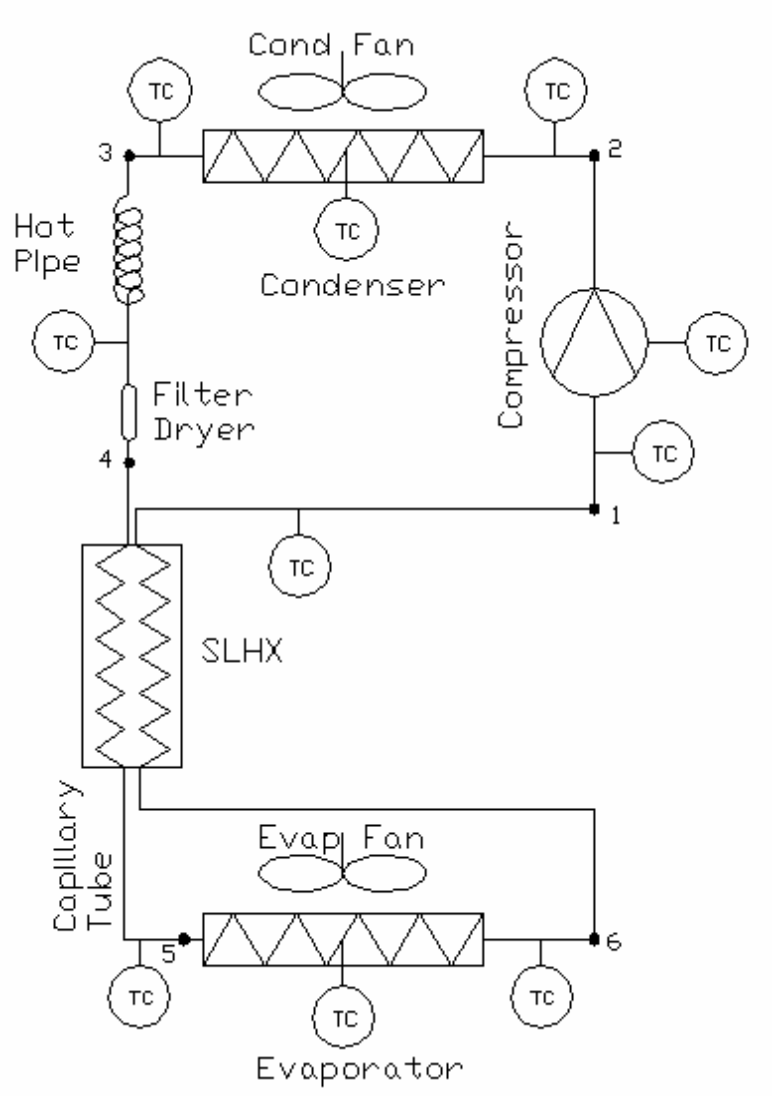

Figure 28 Refrigeration cycle temperature measurement

To measure temperature, T type thermocouples (TC) were used. A picture of T type TC is shown in Figure 29 and specifications are shown in Table 4. All temperatures were measured from the copper tube surface.

Figure 29 T-Type thermocouple

Table 4 T-Type thermocouple specifications

Model Number	FF-T-24
Temperature Range	-200°C to +350°C
Tolerance (@ 0 to -200°C)	0.75%
Tolerance (@ 0 to 350°C)	1.50%
Manufacturer	Omega Engineering Inc.

To prevent atmosphere temperature effects, TC were covered with insulation and cable ties were used to ensure contact between the tube surface and the TC, as shown in Figure 30.

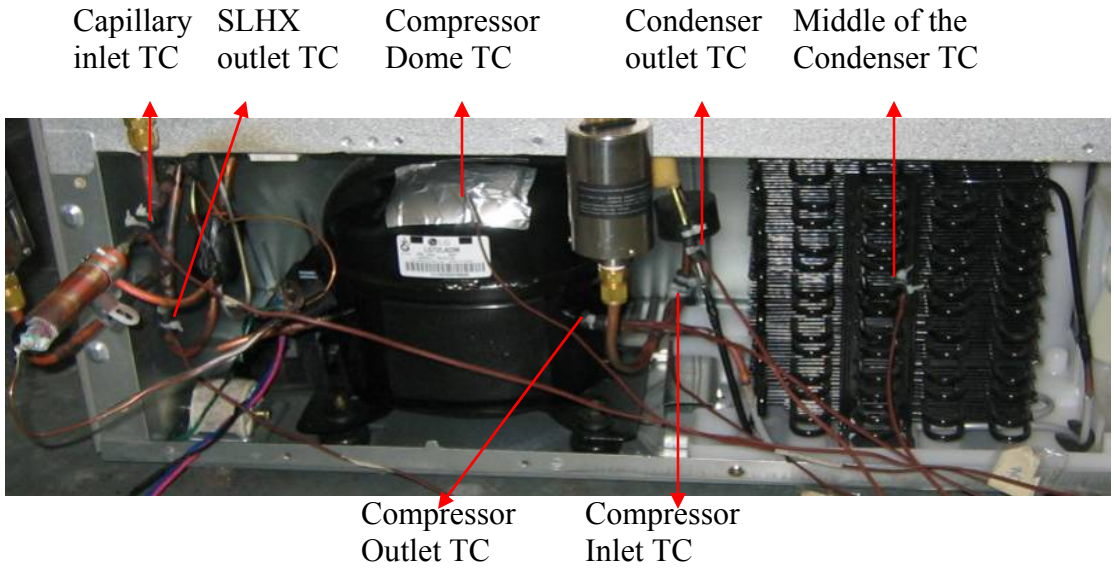

Figure 30 Cycle TCs locations

Evaporator and Condenser Air Side Temperature Measurement

To measure evaporator and condenser air side temperatures, many TC were installed to the heat exchangers (HX) air inlet and outlet.

Figure 31 shows the installation of the evaporator air inlet and outlet TCs. Three TCs were used to measure air inlet temperatures and three of them were attached at the air outlet. Each point's temperatures were measured. After getting data from the DAS, averaged evaporator inlet and outlet values were calculated.

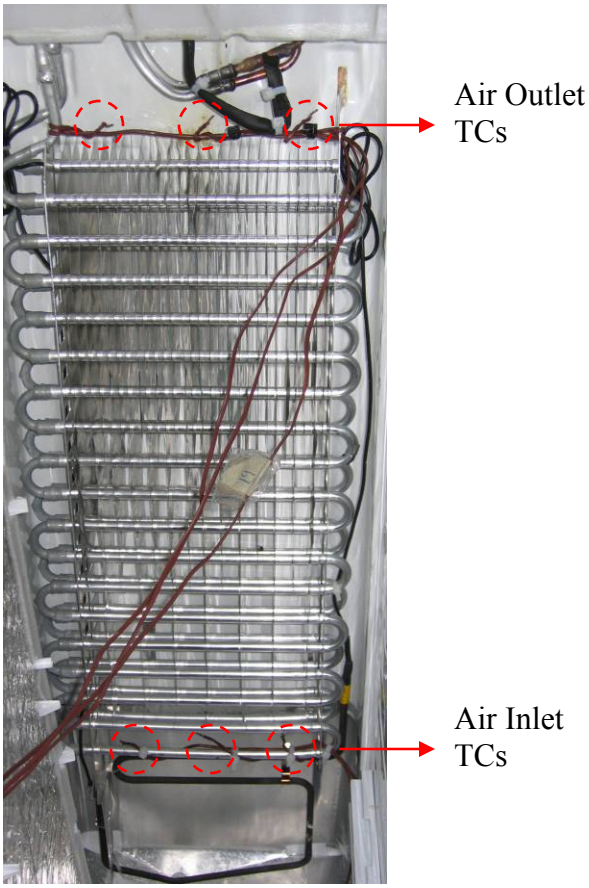

Figure 31 Evaporator air side temperature measurement

Similar to the evaporator air side temperature measurement, nine TC were used at the condenser air inlet and nine of them at the condenser air outlet. Air inlet TC constantans and coppers were individually twisted together and only one TC was connected to the DAS. The same procedure was also done for the air outlet. Then averaged condenser air inlet and outlet values were measured.

Condenser air outlet temperature measurements were not accurate because the condenser air outlet is close to the compressor, so the temperature measurement was affected by the radiation from the compressor shell.

Cabinet Air Temperature Measurement

To measure cabinet temperatures, cylindrical copper masses 2.54cm (1”) in diameter and height, which were soldered to the TC, were attached within the compartments as illustrated in Figure 32. Four copper cylinders were installed to the R compartment and three of them were installed to the F compartment. In the R and F compartments, copper cylinders were placed at the middle of the horizontal section at “h/4” distance between them where h is the compartments height.

In addition to the copper cylinders, normal TC were installed at the various compartment air inlet and outlet gaps as shown in the Figure 32. R and F sensor temperatures were also measured with TC that were positioned on top of the cabinet sensors.

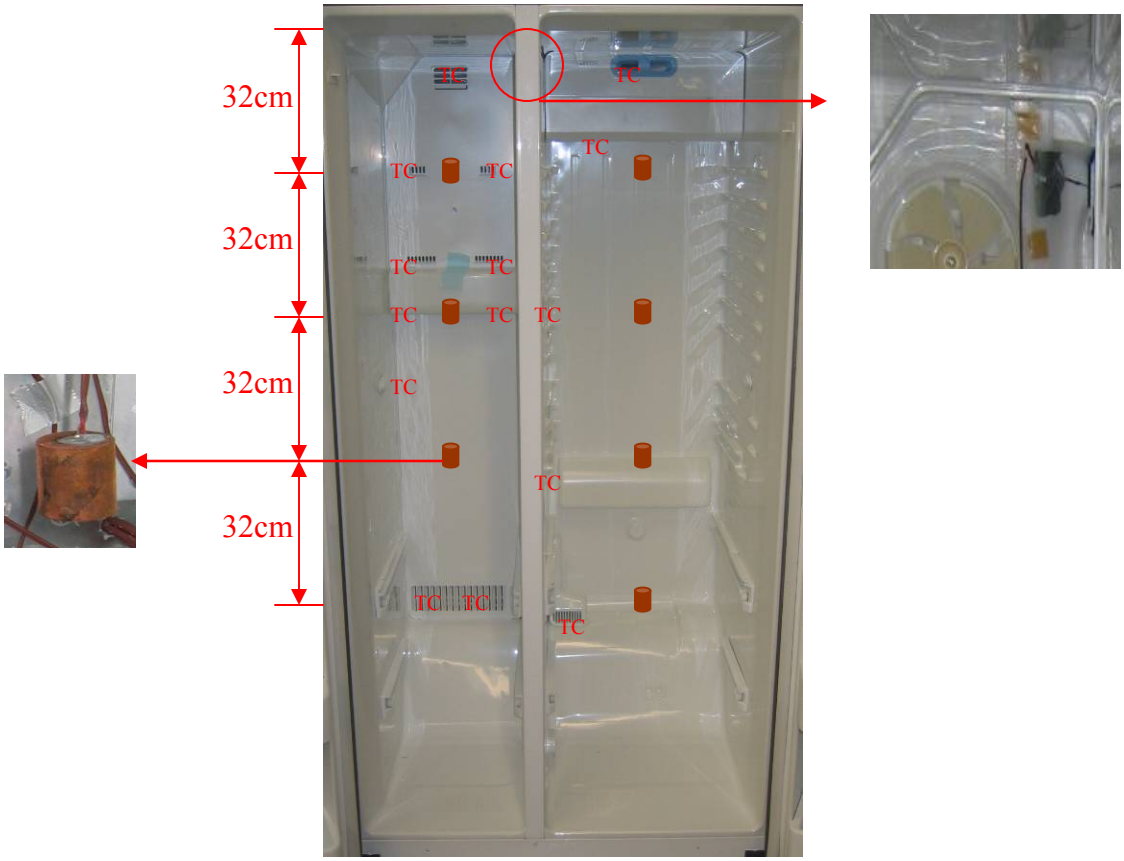

Figure 32 Cabinets' temperature measurement

Power Measurement

To measure power, a very accurate watt meter, as shown in Figure 33, was used. Table 5 shows the watt meter's specifications.

Figure 33 Watt Meter

Table 5 Watt meter specifications

Model Number	PC5 – 002X5	
Input	Volts AC	0 to 300 VAC
	Amps AC	0 to 5 amps
	Frequency Range	48 to 70 Hz
Output	Watts F.S.	1000 W
	Response time	250 msec
	Voltage DC	0 to 5 VDC
	Accuracy (Manufacturer)	0.5% F.S.
	Accuracy (Measured)	± 0.7 W
Manufacturer	Ohio Semitronics	

4.1.2.2 Data Acquisition

System measurement devices such as the TC, pressure transducers and watt meter, send signals to the DAS, which has hardware and software components. A Hewlett Packard Data Acquisition Unit (HP 3497A) to collect and channel the data and a personal computer to display and store the data were used. Two DAS cards were used to accomplish different functions. The T-Couple Acquisition Card was used to measure input signals from T-type thermocouples, and the Guarded Acquisition Card was used to measure voltage output coming from the pressure transducers and watt meter.

All signals coming from the thermocouples, pressure transducers and watt meter were displayed with Q-Basic software. The Q-Basic program converts the voltage readings into physical information such as temperature, pressure and power. While the experiments were running, data was displayed and stored in 10 second intervals.

4.1.3 Uncertainty Analysis

Uncertainty analysis was done for the151g charged counter-flow condenser experiment. Random and systematic errors of the important measured values such as power consumption, P_{Dis}, P_{Suc}, F and R cabinet temperatures, and important derived values such as daily energy consumption were calculated. For random error calculations, only F+R operations were used from 6 cycles in row, as shown in Figure 34.

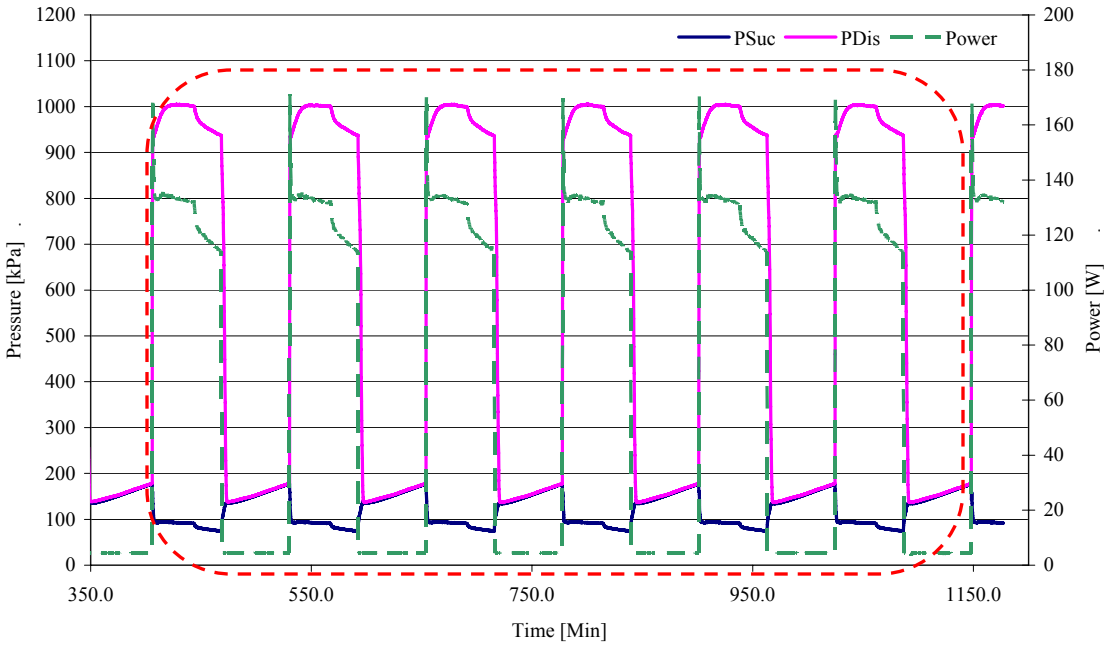

Figure 34 Cycles used in random error analysis

Averaged F+R cycle properties and the error analysis results are shown in Tables 6 and 7.

Table 6 Averaged F+R operation properties

Cycle	Time [Min]	Power [W]	P_{Dis} [kPa]	P_{Suc} [kPa]	$T_{RSensor}$ [^oC]	$T_{FSensor}$ [^oC]
Cycle1	38.0	132.5	995.8	92.0	1.2	-16.7
Cycle2	37.3	132.4	994.6	91.9	1.2	-16.6
Cycle3	33.8	133.2	995.2	92.8	1.4	-16.3
Cycle4	35.3	133.0	994.5	92.6	1.3	-16.4
Cycle5	37.2	132.7	993.6	92.4	1.3	-16.4
Cycle6	37.3	132.8	993.3	92.4	1.4	-16.4

Table 7 Error analysis

	Time	Power [W]	P_{Dis} [kPa]	P_{Suc} [kPa]	$T_{RSensor}$ [^oC]	$T_{FSensor}$ [^oC]
All Cycle Averages	36.5	132.8	994.5	92.4	1.31	-16.5
Random Error (Standard Deviation)		0.3	0.9	0.4	0.08	0.1
Systematic Error		0.7	2.0	2.0	0.02	0.2
% Random Error of Mean		0.2	0.1	0.4	5.77	0.9
% Systematic Error of Mean		0.5	0.2	2.2	1.50	1.5
% Total Error		0.8	0.3	2.6	7.27	2.4

As shown in Table 7, power consumption measurement error is quite small. Pressure measurements are also very accurate. Although temperature measurement errors are large, they are reasonable for this type of temperature measurement.

Daily energy consumption is calculated with Eq 2.

$$DEC = \frac{Power \cdot On\ Time * 24}{Total\ Time} \tag{2}$$

The error of the DEC (w_R) is calculated with Eq 3 [8].

$$w_{DEC} = \left(\frac{\partial DEC}{\partial Power} \cdot w_{Power} \right) \tag{3}$$

The % error of the DEC was calculated to be ± 0.8%.

4.2 Condenser Improvement Experimental Method

4.2.1 Experimental Procedures

To verify the effect of the condenser configuration on the refrigeration cycle, many experiments were performed. The test unit was first tested with the original condenser at different refrigerant charges. Then the cross-flow condenser was changed with a counter cross-flow one and the same experiments were conducted. The experimental matrix is shown in Table 8.

Table 8 Condenser Improvement test matrix

Condenser Type	Charge [g]				
Cross Flow	120	130.5	142	151	172
Counter Cross Flow	120	130.5	142	151	172

4.2.2 Experimental Analysis

After finishing the above experiments, data stored by the DAS computer was converted into an excel file. The excel data were copied to a template excel file, which was prepared beforehand and includes important cycle graphs such as cabinet temperatures, cycle pressures and power consumption.

The basic household refrigerator has three cycles: the F+R cycle, F cycle and off cycle. In normal running operation, it completes cycles as shown in Figure 35.

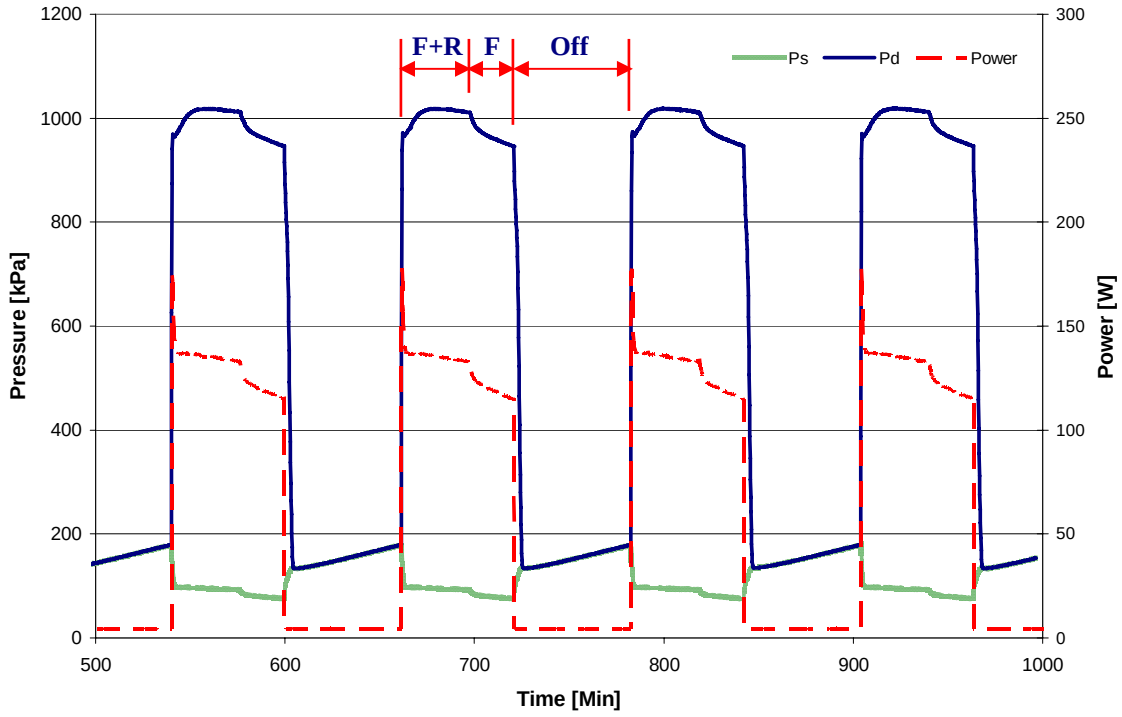

Figure 35 Base unit cycle pressures and power

When the cycle repeats the previous cycle more than 3 times, that cycle is selected and analyzed. In one cycle sheet, the measured data are averaged for different cycle periods of the one cycle such as F+R, F and off cycle. All cycle calculations are performed using averaged values.

4.2.2.1 Calculations of the Cycle Properties

All calculations were done using the Engineering Equation Solver (EES) program. EES provides a useful equation solving platform as well as many refrigerant properties needed for calculation.

Averaging the power consumption of the unit

The cycle power consumption was measured as explained in the measurement chapter. After obtaining raw data as outlined in the previous section, the power of each cycle period was found by averaging measured values for one cycle.

Mass Flow Rate (MFR) Calculation

The mass flow rate of the refrigeration cycle was found by using the compressor map data that was supplied by the compressor manufacturer. The map, which includes MFR changes depending on the evaporating temperature (T_{Evap}) and condensing temperature (T_{Cond}), was integrated into the regression equation by using a curve-fitting software (Table Curve 3). Compressor and volumetric efficiencies were also fitted with compressor map data.

$$MFR = \left(C_1 + C_2 \cdot T_{Evap} + C_3 \cdot T_{Cond} + C_4 \cdot T_{Evap}^2 + C_5 \cdot T_{Cond}^2 + C_6 \cdot T_{Evap} \cdot T_{Cond}\right) \Big/ 3.6 \quad (4)$$

Where;

C_1=6.8260705; C_2=0.20065924; C_3=0.15814114; C_4=0.0018097331;

C_5= -0.00088811357; and C_6=0.0029643735.

The calculated MFR found using Eq.4 is in grams per second.

Efficiency equations are shown in Eq.5 and Eq.6.

$$Eff_{Vol} = (1.0006325 - 0.0327 \cdot PR) \quad (5)$$

$$Eff_{Comp} = (0.628 - 0.00044 \cdot PR) \quad (6)$$

$$PR = \frac{P_{Dis}}{P_{Suc}} \quad (7)$$

T_{Evap} is the saturation temperature of R134a at suction pressure and T_{Cond} is the saturation temperature of R134a at discharge pressure.

After calculating evaporating and condensing temperatures, MFR was calculated using Eq.4

Evaporator capacity calculation

To find evaporator capacity, Eq.8 was used:

$$Q_{Ev} = MFR \cdot \left(h_{Evapo} - h_{Evapi} \right) \tag{8}$$

h_{Evapo} was easily calculated using T_{Evapo} and P_{Suc} in EES as the experimental results showed that the evaporator outlet condition was always a superheated vapor phase. As a control, however, the superheated value was checked during each test. If there was no superheat, it was assumed that the evaporator outlet condition was a saturated vapor phase. On the other hand, h_{Evapi} was calculated from the energy balance of the SLHX using Eq. 9:

$$h_{Suc} - h_{Evapo} = h_{Capi} - h_{Evapi} \tag{9}$$

h_{Suc} was calculated using suction temperature (T_{Suc}) and pressure (P_{Suc}). h_{Capi} was calculated using capillary tube inlet temperature (T_{Capi}) and pressure (P_{Capi})

After calculating $h_{Evapi,}$ the evaporator capacity was calculated with Eq.8. In addition, the evaporator inlet quality (X_{Evapi}) was calculated using h_{Evapi} and P_{Evapi}.

Condenser capacity calculation

Condenser capacity was calculated using Eq.10:

$$Q_{Cond} = MFR \cdot \left(h_{Condi} - h_{Capi} \right) \tag{10}$$

Thermodynamically Q_{Cond} is expected to equal the sum of Q_{Evapa}, Q_{Comp} and Q_{SLHX}.

Daily energy consumption (DEC) calculation

One time step's energy consumption (EC) was first calculated using Eq.11:

$$EC = Q_{Comp} \cdot \frac{Time\ Step\ (10\,\text{sec})}{3600} \quad [\text{Wh}] \tag{11}$$

Then all time steps ECs were calculated and added. Accordingly, individual cycle periods' (F+R, F and Off) EC value was defined. Finally, all ECs were added and one cycle's energy consumption (OCEC) was calculated.

After calculating OCEC, daily energy consumption (DEC) was calculated with the Eq.12:

$$DEC = \frac{OCEC \cdot 24}{Total\ Cycle\ Time\ (hours)} \quad [\text{Wh/Day}] \tag{12}$$

Additionally, monthly energy consumption (MEC) was calculated using Eq.13:

$$MEC = \frac{DEC \cdot 30}{1000} \quad [\text{kWh/Month}] \tag{13}$$

4.3 Condenser Improvement Experimental Results

4.3.1 Counter-flow Condenser Effect on Discharge Pressure

Experimental results show that using a counter-flow condenser decreases discharge pressure by 2%. Figure 36 shows that a 2% decrease is valid for every different refrigerant amount.

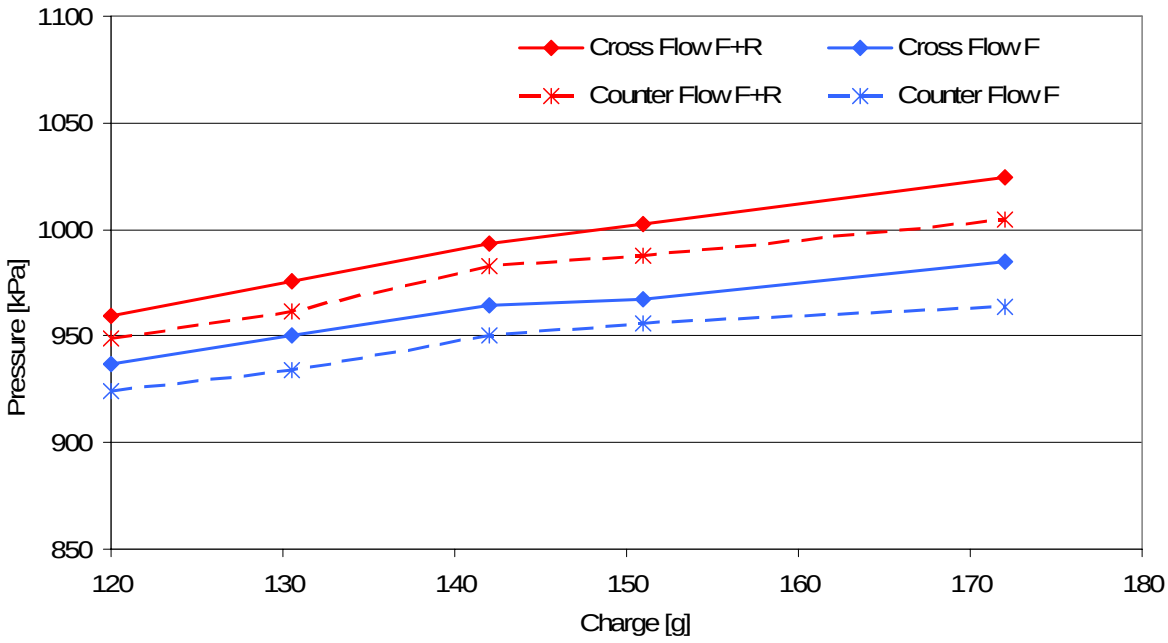

Figure 36 Charge vs. discharge pressure

4.3.2 Counter-flow Condenser Effect on Suction Pressure

There is no measurable effect of using a counter-flow condenser on suction pressure, as shown in Figure 37.

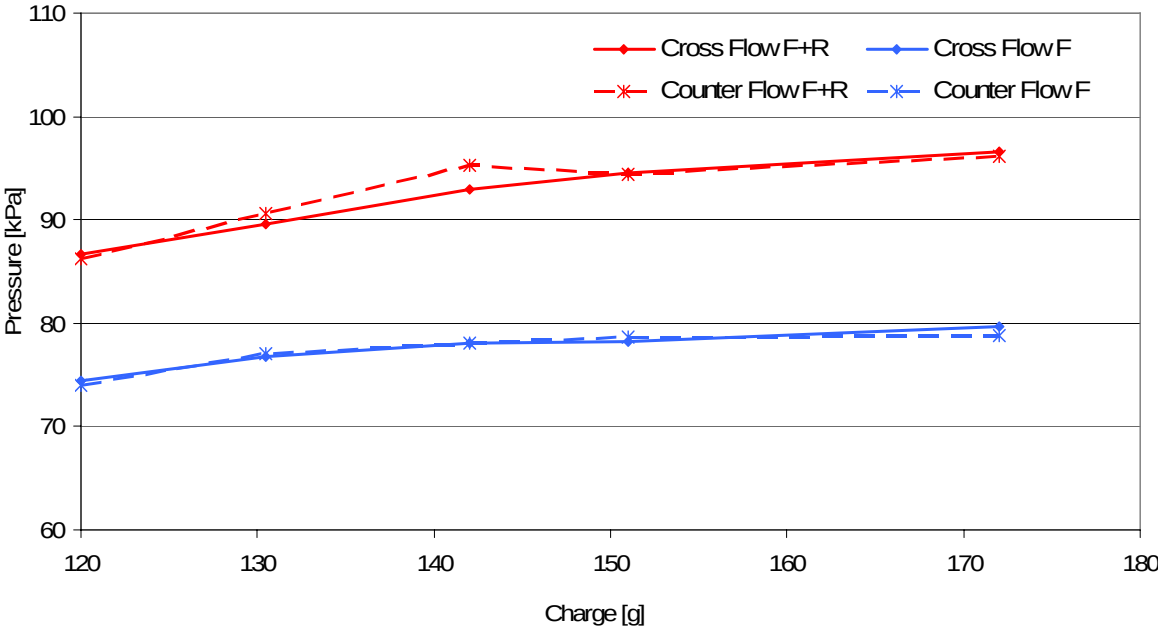

Figure 37 Charge vs. suction pressure

4.3.3 Counter-flow Condenser Effect on MFR

Experimental results showed that using a counter-flow condenser decreased the MFR within 1%.

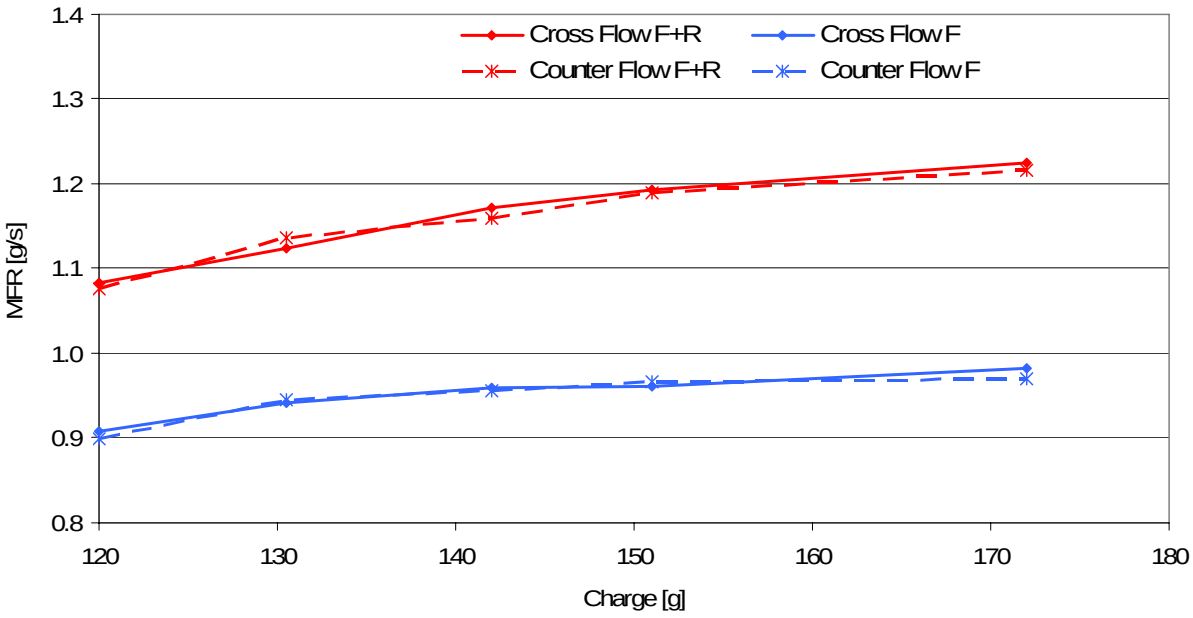

Figure 38 Charge vs. MFR

4.3.4 Counter-flow Condenser Effect on Power Consumption

Experimental results show that using a counter-flow condenser decreased power consumption within 1%, as shown in Figure 39. It should be noted that the compressor's individual power consumption was not measured. Since the all energy saving is coming from refrigeration cycle, the refrigeration cycle's power consumption was decreased more than 1%. Additionally, the trend of the graph verifies that a counter-flow condenser has more effect with an increased amount of refrigerant.

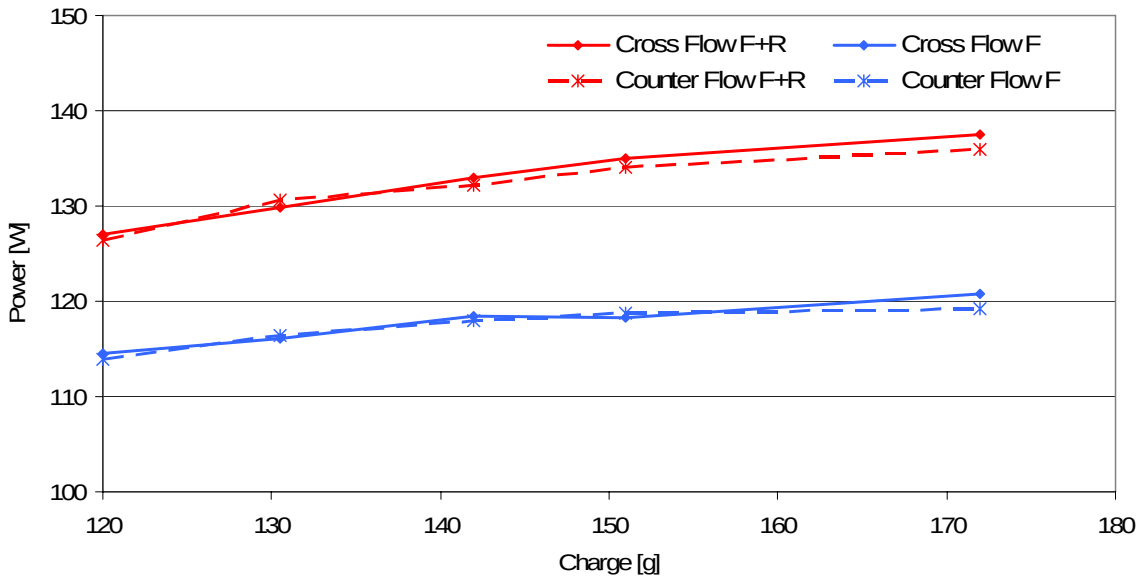

Figure 39 Charge vs. power consumption

4.3.5 Counter-flow Condenser Effect on Daily Energy Consumption

Experimental results proved that using a counter-flow condenser instead of a cross-flow condenser can save at least 1% energy per day. At the low pressure side of the cycle there was not a considerable difference, but at the high pressure side, condensing pressure was decreased within 2% and condenser capacity was increased within 1%. As a result, the basic household refrigerator's daily energy consumption was decreased within 1%. Moreover, this saving is valid for every charge amount, as shown in Figure 40, so there is at least 1% energy saving with a counter-flow condenser for every case tested.

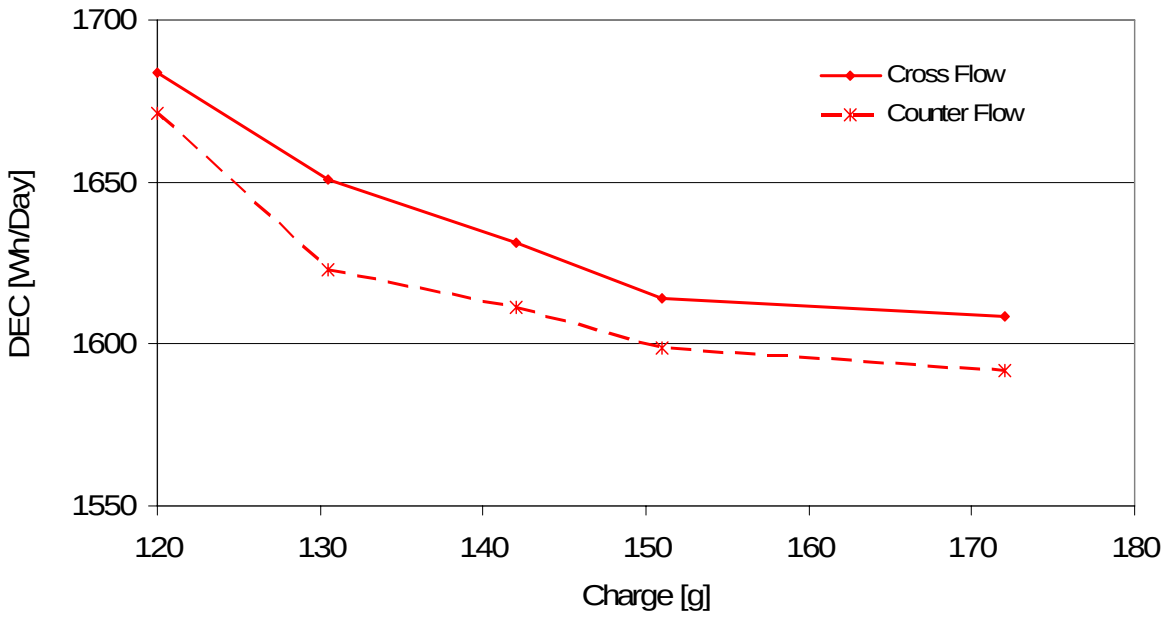

Figure 40 Daily energy consumption vs. charge

4.3.6 Cycle Comparison

In addition to the comparison of all cycles, one cycle of the cross-flow condenser and counter-flow condenser was compared.

4.3.6.1 Comparison of Calculated and Measured Data

In this section only 172g charged tests results are compared, because 172g is the original charge of the test refrigerator and experimental results show that the minimum energy consumption occurred at this charge.

Table 9 shows that the condensing capacity of the cycle with the counter-flow condenser is 1.5% higher than the capacity for the cross-flow condenser. When power consumptions are compared, it can bee seen that the refrigerator with the counter-flow condenser saves 1% energy.

.

Table 9 Calculated cycle properties

Condenser Type		Cross-Flow	Counter-Flow
Charge [g]		**172**	**172**
Duration [Min.]	**F+R**	36.3	37.2
	F	23.2	22.2
	Off	61.5	61.5
	Total	121.0	120.8
MFR [g/s]	**F+R**	1.224	1.216
	F	0.982	0.970
Q_{Evap} [W]	**F+R**	227.8	227.9
	F	184.1	183.2
Q_{Cond} [W]	**F+R**	224.8	227.5
	F	182.0	183.4
Power [W]	**F+R**	137.4	136.0
	F	120.7	119.3
	Off	4.5	4.5
COP	**F+R**	1.7	1.7
	F	1.5	1.5
OCEC [Wh/Cyle]	**F+R**	83.6	84.6
	F	46.9	44.4
	Off	4.6	4.6
	Total	135.2	133.6
DEC [Wh/Day]	**Daily**	1608.4	1592.0
MEC [KWh/Month]	**Monthly**	48.3	47.8

Table 10 includes measured cycle properties. It can easily be seen that the counter-flow condenser does not have any effect on the low pressure side but it increases the temperature difference between the inlet and outlet of the air side and refrigerant side.

.

Table 10 Measured cycle properties

Condenser Type		**Cross-Flow**	**Counter-Flow**
Charge [g]		**172**	**172**
P_{Dis} [kPa]	**F+R**	1024.3	1004.9
	F	985.2	963.9
P_{Suc} [kPa]	**F+R**	96.6	96.2
	F	79.7	78.9
T_{Cond} [^oC]	**F+R**	40.3	39.6
	F	38.8	38.0
T_{Evap} [^oC]	**F+R**	-27.1	-27.2
	F	-31.2	-31.4
$T_{CondRefi}$ [^oC]	**F+R**	47.4	50.2
	F	48.8	51.6
$T_{CondRefo}$ [^oC]	**F+R**	36.9	36.3
	F	35.9	35.3
$T_{CondAiri}$ [^oC]	**F+R**	30.8	30.7
	F	30.8	30.6
$T_{CondAiro}$ [^oC]	**F+R**	37.1	38.6
	F	36.3	37.7
$T_{EvapRefi}$ [^oC]	**F+R**	-24.3	-24.2
	F	-29.0	-28.9
$T_{EvapRefo}$ [^oC]	**F+R**	-25.0	-25.1
	F	-29.8	-29.9
$T_{EvapAiri}$ [^oC]	**F+R**	-14.7	-14.8
	F	-20.4	-20.5
$T_{EvapAiro}$ [^oC]	**F+R**	-22.3	-22.3
	F	-27.7	-27.8

It can be seen from Table 11 that there is no significant difference in cabinet temperatures for each condenser. Therefore, obviously we can conclude that the counter-

flow condenser is more efficient than the cross-flow condenser while providing the same cabinet conditions.

Table 11 Cabinet temperatures

Condenser Type		Cross-Flow	Counter-Flow
Charge [g]		172	172
T_R [^{o}C] (Average of four copper blocks)	F+R	3.6	3.5
	F	1.4	1.4
	Off	3.5	3.4
R Sensor2 [^{o}C]	F+R	1.6	1.6
	F	1.7	1.8
	Off	5.0	5.0
T_F [^{o}C] (Average of three copper blocks)	F+R	-15.2	-15.3
	F	-19.4	-19.5
	Off	-18.9	-18.9
F Sensor [^{o}C]	F+R	-16.2	-16.3
	F	-21.7	-21.8
	Off	-16.5	-16.5

4.3.6.2 Cycle Graphs

Although averaged values can be used to calculate cycle properties, complete cycle data should be shown to prove that a counter-flow condenser has positive effects on every minute of the refrigeration on-cycle.

Figure 41 shows pressures and power values of the counter-flow and cross-flow condensers. In the figure, it is easy to see that counter-flow discharge pressure and power consumption are lower than cross-flow discharge pressure and power consumption during on time.

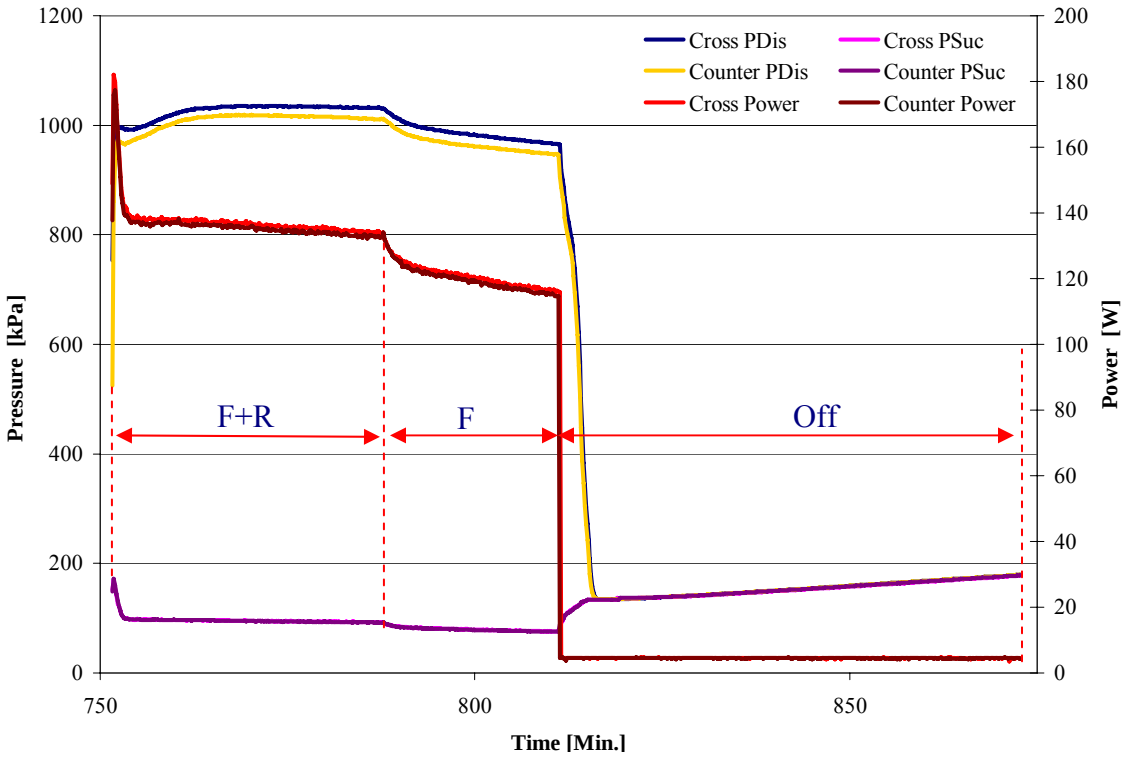

Figure 41 Cycles' pressures and powers

Cycle temperatures can be seen in Figure 42.

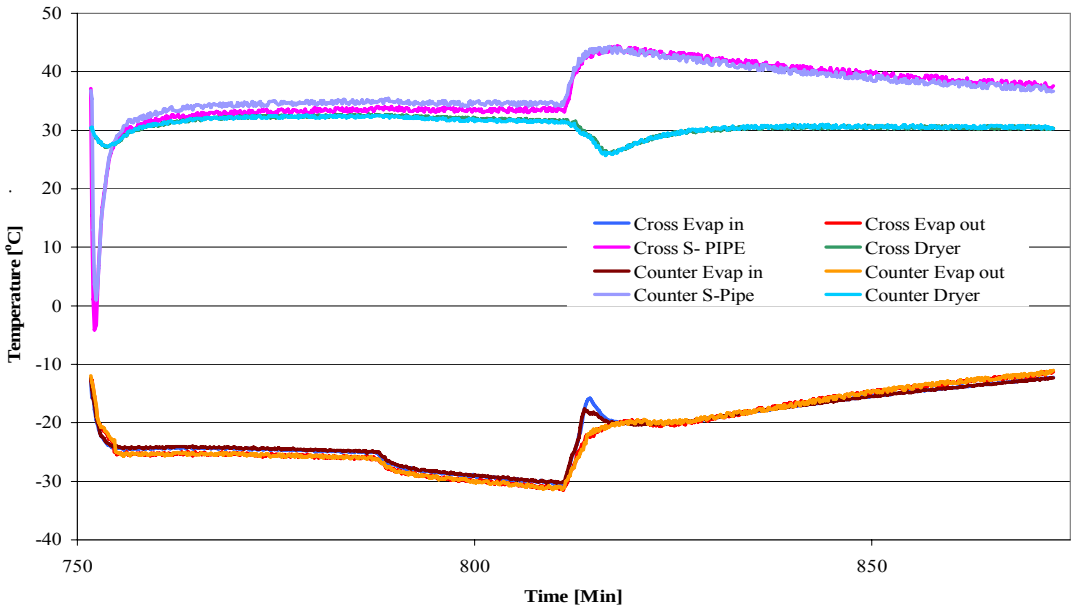

Figure 42 Cycle temperatures

4.4 Conclusions

A refrigerator with a counter-flow condenser consumes 1% less energy compared to one with a cross-flow condenser.

Energy consumption of the refrigerator with the counter-flow condenser can be decreased with further improvements such as an additional air guide to the top of the counter flow condenser and a higher air flow rate If an air guide is installed at the top of the counter-flow condenser and air is forced to flow through the condenser, condenser efficiency increases and energy consumption decreases. In addition, increasing the condenser air flow rate with a counter-flow condenser decreases the condensing temperature a reasonable amount. Moreover, a higher air flow rate also decreases the compressor shell temperature and lower condenser and compressor surface temperatures means lower heat load to the cabinets from the compressor compartment. Details are explained in chapter 5.

.

5 Alternating Evaporator Duty (AED) Cycle with Two Step Capacity Modulated Compressor

As explained in the previous chapters, an AED cycle with a capacity modulated compressor is the most promising technology to date for decreasing energy consumption of household refrigerators.

To study the potential of the AED cycle, a conventional cycle in a side-by-side household refrigerator was converted into an AED cycle. Before testing, the performance of the refrigerator with the new cycle was simulated and then cycle components were adequately designed.

To modulate the capacity of the compressor, a bypass line and an expansion device were installed to adjust the refrigerant bypass ratio. The new cycle was designed to run at a lower capacity while cooling the R cabinet. However, in F cabinet operation the full capacity of the compressor was used.

A forced convection fin-and-tube type evaporator and a natural convection tube-and-plate type evaporator were used for the R cabinet in order to investigate the energy saving potentials and the humidity control improvement. Energy consumption and humidity ratio experiments were conducted for both evaporator types.

5.1 AED Cycle Design

Although the AED cycle is known as a refrigeration cycle that has energy saving potential, if it is not designed properly it cannot demonstrate its full capability. Therefore, a comprehensive design study should be conducted in order to utilize the benefit of an AED cycle.

For the AED cycle with a modulated capacity compressor study, a cycle simulation program was written in EES to simulate an AED cycle. Then proper assumptions, which were decided based on the conventional unit's experimental results, were made. After getting reasonable results for the conventional cycle from the EES code, the simulation matrix including variables for the AED cycle was determined. After running the code for all different possibilities, results were compared and the theoretical boundary conditions were estimated for the AED with a modulated capacity compressor.

After estimating theoretical boundary conditions, the cycle components such as the R evaporator, F evaporator and condenser were designed for different energy saving options.

Finally the applicability of the components and energy saving potentials were considered together, and practical component designs were chosen for the new cycle.

5.1.1 AED Cycle Simulation

An EES code was written to simulate the AED cycle with capacity modulated compressor. The code included theoretical thermodynamic rules and assumptions that were chosen based on the conventional cycle experimental results.

5.1.1.1 Assumptions

In order to get reasonable results from a simulation, it is very important to make accurate assumptions. In the AED cycle simulation, assumptions for the subcooling (T_{Sub}), superheating (T_{Sup}) and suction ($T_{Suc)}$ temperatures were made based on conventional cycle experimental results. The assumed values are as follows:

$T_{Sub} = 2K$,

T_{Sup} = 0K,

T_{Suc} = 32°C.

In addition to the above assumptions, it was assumed that there was no pressure change across the heat exchangers except in the capillary tube and compressor. This means that in all calculations, only the evaporating and condensing pressures were used. Also, cabinet heat loads (CHL) were assumed to be the same as those for the conventional cycle. Furthermore, the off time of one cycle was assumed to be the same as that of the conventional cycle.

CHL_R = 26W

CHL_F = 70W

Off time = 61 minutes

The last assumption was for power consumption by components other than the compressor. W_{Other} was estimated with the data from the conventional cycle.

W_{Other} = 18W

5.1.1.2 Calculation Method

Calculations of the cycle properties

Evaporator inlet and outlet temperatures were calculated using Eqs. 14 and 15:

$$T_{Evapo} = T_{Evap} + T_{Sup} \tag{14}$$

$$T_{Condo} = T_{Cond} - T_{Sub} \tag{15}$$

Evaporating and condensing pressures are saturation pressures of R134a at T_{Evap} and T_{Cond}, respectively. The pressure ratio (PR) of the refrigeration cycle was calculated using Eq.16:

$$PR = \frac{P_{Cond}}{P_{Evap}} \tag{16}$$

Cycle enthalpies, suction entropy and density were defined using following functions:

$$h_{Evapo} = f\left(T_{Evapo}, P_{Evap}\right)$$
$$h_{Condo} = f\left(T_{Condo}, P_{Cond}\right)$$
$$h_{Suc} = f\left(T_{Suc}, P_{Evap}\right)$$
$$s_{Suc} = f\left(T_{Suc}, P_{Evap}\right)$$
$$h_{Diss} = f\left(s_{Suc}, P_{Cond}\right)$$
$$\rho_{Suc} = f\left(T_{Suc,}P_{Evap}\right)$$

h_{Evapi} was calculated using SLHX energy balance Eq.17:

$$h_{Evapi} - h_{Condo} = h_{Suc} - h_{Evapo} \tag{17}$$

Correlated Efficiency Equations

Compressor and volumetric efficiencies for the conventional unit compressor were used. However, it was expected that efficiencies would change when the compressor capacity was modulated. Therefore correlated efficiency equations were multiplied with adjusting coefficients (C_{Vol} and C_{Comp}), as seen in Eqs. 18 and 19.

$$Eff_{Vol} = (1.0006325 - 0.0327 \cdot PR) \cdot C_{Vol} \tag{18}$$

$$Eff_{Comp} = (0.628 - 0.00044 \cdot PR) \cdot C_{Comp} \tag{19}$$

Derived Efficiency Equation

In addition to the correlated efficiency equations, there is a derived isentropic efficiency (Eff_{Isen}), as shown in Eq. 20:

$$Eff_{Isen} = \frac{Eff_{Comp}}{Eff_{Mot}} \tag{20}$$

Cycle Calculations

MFR, Q_{Evapa}, Q_{Comp} and COP were calculated using Eqs. 21 – 24.

$$Mfr = EFF_{Vol} \cdot (\rho_{Suc} \cdot Disp \cdot RPM / 60) \cdot 1000 \quad [g/s] \quad (21)$$

$$Q_{Evap} = Mfr \cdot (h_{Evapo} - h_{Evapi}) \quad [W] \quad (22)$$

$$Q_{Comp} = Mfr \cdot (h_{Diss} - h_{Suc}) / EFF_{Comp} \quad [W] \quad (23)$$

$$COP = \frac{Q_{Eva}}{Q_{Comp}} \quad (24)$$

Calculation of cycle time

Cycle time was calculated using energy balance of the R/F cabinets. From the cabinet energy balance, heat load to the cabinet in one cycle is equal to the provided cooling (PC) in the same cycle period. PC is the cooling that was supplied by the evaporator during on time. Therefore, the energy balance equation for each cabinet was written as:

$$CHL_R \cdot t_{Cyc} = Q_{EvapR} \cdot t_R \quad (25)$$

$$CHL_F \cdot t_{Cyc} = Q_{EvapF} \cdot t_F \quad (26)$$

In addition to the previous equations, total cycle time was calculated using Eq.27:

$$t_{Cyc} = t_R + t_F + t_{Off} \quad (27)$$

As a result, three unknowns were defined from three equations.

Energy consumption calculations

After calculating on times and W_{Comp}, energy consumption of the AED cycle was calculated using the following:

$$W_{RTotal} = W_{CompR} + W_{Other} \quad (28)$$

$$W_{FTotal} = W_{CompF} + W_{Other} \tag{29}$$

$$OCEC = W_{RTotal} \cdot t_R + W_{FTotal} \cdot t_F \tag{30}$$

$$DEC = OCEC \cdot 24 / t_{Cyc} \tag{31}$$

5.1.1.3 Simulation Matrix

Evaporating and condensing temperatures of the cycle can be varied in a wide range. Theoretically, an evaporator can supply cooling to a cabinet as long as the evaporating temperature is lower than the cabinet air temperature. Therefore, a refrigeration cycle should be designed in a wide operation range.

Experimental results from the conventional refrigerator were used to define boundary conditions for condensing temperatures and the F evaporating temperature. However, since the R evaporating temperature of an AED cycle with a capacity modulated compressor was not available, its range was chosen wider than the other variables.

In a simulation for an AED cycle with a modulated compressor, capacity modulation of the compressor is a critical point. In order to modulate compressor capacity, different displacement volume values were used starting from full volume, which represents the full capacity of the compressor, to half volume. Tables 12 and 13 show the simulation matrices.

Table 12 Variables in simulation matrix

	T_{EvapF} [^oC]	T_{CondF} [^oC]	T_{CondR} [^oC]	$Disp_R$ [cm^3]	C_{CompR}	C_{VolR}
1	-28	35	35	7.2	1.00	1.00
2	-29	36	36	6.3	1.05	1.03
3	-30	37	37	5.4	1.10	1.06
4	-31	38	38	4.5	1.15	--
5	-32	39	39	3.6	1.20	--

Although 5 different values were set for previous variables, 25 different values were set for the R evaporating temperature in order to observe all possibilities..

Table 13 TEvapR values in simulation matrix

No	**1**	**2**	**20**	**21**
T_{EvapaR} [^oC]	-5	-6	-24	-25

7.2cm^3 was used for the F operation displacement volume of the compressor because the compressor is running at its full capacity during F operation. Therefore, C_{CompF} and C_{VolR} were set to 1.

As shown in the tables, 262,500 different variations were simulated.

5.1.1.4 Conventional Cycle Simulation

The same code that was written to simulate an AED cycle was modified for a conventional cycle so the conventional cycle could also be simulated using experimental results as inputs. A summary of simulation results can be found in Table 14.

.

Table 14 Conventional cycle simulation summary

T_{EvapF}	[^oC]	-31
T_{CondF}	[^oC]	38
T_{EvapFR}	[^oC]	-27
T_{CondFR}	[^oC]	39
Eff_{VolF}		0.68
Eff_{CompF}		0.62
Eff_{VolFR}		0.73
Eff_{CompFR}		0.62
Displacement	[cm^3]	7.2
DEC	[Wh/Day]	1514

5.1.1.5 Theoretical Boundary Conditions

Total simulation results were sorted depending on energy consumption. Results that had a higher energy consumption than the simulated conventional cycle's value were skipped and the condition that had the minimum energy savings was defined. The best option that had the most energy savings was also defined, and theoretical boundary conditions for the AED cycle with a capacity modulated compressor were established.

Conditions that had efficiency coefficients (C_{Vol} and C_{Comp}) greater than 1 weren't considered, because if the cycle consumes less energy with recent compressor efficiencies, then it can save more energy if the real compressor efficiencies are higher.

The theoretical boundary conditions are shown in Table 15.

Table 15 Theoretical boundary conditions

	T_{EvapR}	T_{CondR}	T_{EvapF}	T_{CondF}	Eff_{CompR}	Eff_{VolR}
	[^oC]	[^oC]	[^oC]	[^oC]		
The Least	-20	37	-31	38	0.62	0.82
The Best	-5	35	-28	35	0.63	0.91

These conditions can be used for different compressor displacement volumes which are shown in Tables 16 and 17.

Table 16 The least energy savings options

Displacement Volume	Eff_{CompR}	Eff_{VolR}	Energy Saving
[cm^3]			%
7.2	0.62	0.82	1.5
6.3	0.62	0.82	1
5.4	0.62	0.82	1
4.5	0.62	0.82	0
3.6	0.62	0.82	0

Table 17 The best energy saving options

Displacement Volume	Eff_{CompR}	Eff_{VolR}	Energy Saving
[cm^3]			%
7.2	0.63	0.91	20
6.3	0.63	0.91	20
5.4	0.63	0.91	20
4.5	0.63	0.91	19
3.6	0.63	0.91	19

5.1.2 AED Cycle Component Design

Although there are energy saving potentials for all displacement volumes, there are many limitations that make it hard to use them in practice. Consequently, cycle components were designed for different specified conditions.

5.1.2.1 Condenser Design

In addition to the basic LGE condenser, two wider condensers were designed by adding new rows.

These three condensers were used with different air velocities to match calculated condensing capacity demands at different evaporating temperatures.

Table 18 shows condensers' specifications.

Table 18 Condenser specifications

Cond Model	Unit	Base Cond #1	Cond #2	Cond #3
Number of Rows	ea	9	9	9
Number of Columns	ea	13	15	18
Tube Length	m	0.13	0.13	0.13
Tube OD	mm	4.7	4.7	4.7
Tube ID	mm	3.3	3.3	3.3
Wire Spacing	mm	8.125	8.125	8.125
Wire Diameter	mm	1.4	1.4	1.4
Wire Length	m	0.18	0.18	0.18
Total Heat Transfer Area	m^2	0.55	0.64	0.77
Coil Face Area	m^2	0.023	0.023	0.023
Volume	m^3	0.0048	0.0056	0.0068

All condensers were used in the counter-flow configuration and the third condenser option is the largest condenser that can fit into the base refrigerator without changing any other components in the cabinet.

Designing condensers are directly related to the evaporating conditions because in the refrigeration cycle evaporating condition is the dominant factor on the MFR.

5.1.2.2 Forced Convection Evaporators Design

Four different R cabinet evaporators were designed for different evaporating temperature levels starting from -5^{o}C to -15^{o}C. CEEE's CoilDesigner software, whose accuracy has already been verified, was used to design these evaporators.

Some assumptions were made to design the new evaporators. First of all, it was assumed that the evaporator outlet superheated vapor was 0K, which was the same assumption for the cycle simulation. Then it was assumed that the evaporating capacity did not change depending on the different condensing temperature, which means the same evaporator could be used for different condensing temperatures. Additionally, evaporator inlet pressure was assumed to be the same as the evaporating pressure and the inlet condition was assumed to be in a two-phase state.

Cooling needs and MFRs were calculated by the EES cycle simulation code for various evaporating temperatures. Then evaporator dimensions were designed to provide the same cooling need as the simulated one with same MFR.

Tables 19 and 20 show the design results for the FC R evaporators.

Table 19 Designed FC R evaporators I

Evap Model	Unit	Base Evap	R Evap #1	R Evap #2
T_{Evap}	^oC		-5	-8
Designed Q_{Evap}	W		363.0	318.0
Calculated Cooling Need	W		360.0	316.0
Number of Rows	ea	2	2	2
Number of Columns	es	18	18	18
Tube Length	m	0.20	0.30	0.27
Tube ID	mm	6.7	5.4	5.4
Tube OD	mm	8.3	6.6	6.6
Fin Spacing	mm	14	5	5
Fin Thickness	mm	0.2	0.2	0.2
Air Velocity	m/s	1.57	2.50	1.57
Ref. Inlet Pressure	kPa		243.5	217.5
Ref. Inlet Temperature	^oC		-5.0	-8.0
MFR	g/s		1.98	1.73
Total Heat Transfer Area	m^2	1.04	3.77	3.37
Coil Face Area	m^2	0.012	0.018	0.016
Volume	m^3	0.0066	0.01	0.009
Avg. Air Side HTC	W/m²-K		48.2	35.9
Avg. Ref. Side HTC	W/m²-K		1438.6	1452.1

Table 20 Designed FC R evaporators II

Evap Model	Unit	Base Evap	R Evap #3	R Evap #4
T_{Evap}	^oC		-12	-15
Designed Q_{Evap}	W		264.6	228.0
Calculated Cooling Need	W		263.5	228.4
Number of Rows		2	2	2
Number of Columns		18	18	9
Tube Length	m	0.20	0.20	0.20
Tube ID	mm	6.7	6.7	6.7
Tube OD	mm	8.3	8.3	8.3
Fin Spacing	mm	14	8	7
Fin Thickness	mm	0.2	0.2	0.2
Air Velocity	m/s	1.57	1.57	1.57
Ref. Inlet Pressure	kPa		185.4	164.0
Ref. Inlet Temperature	^oC		-12.0	-15.0
MFR	g/s		1.44	1.25
Total Heat Transfer Area	m^2	1.04	1.64	0.91
Coil Face Area	m^2	0.012	0.012	0.012
Volume	m^3	0.0066	0.0066	0.0033
Avg. Air Side HTC	W/m²-K		33.4	33.4
Avg. Ref. Side HTC	W/m²-K		932.5	1024.3

The base evaporator is the evaporator which was used in the conventional single evaporator baseline refrigerator and evaporator options 1, 2, 3 and 4 were designed to use for an AED cycle R cabinet.

The results show that, as the evaporating temperature decreases, evaporator size increases. If -5^{o}C is used for R evaporating temperature, the evaporator size and air velocity should be increased by 50% and 60%, respectively. However, if -15^{o}C is used

for R evaporating temperature, then a 50% smaller evaporator can be used with the same air flow rate.

In addition to the R evaporator design, four different F evaporators were designed similar to the R evaporators. Specifications of newly designed F evaporators are shown in Table 21.

Table 21 Designed FC F evaporators

Evap Model	Unit	Base Evap	F Evap #1	F Evap #2	F Evap #3	F Evap #4
T_{Evap}	^{o}C	-31.5	-28	-29	-30	-31
Designed Q_{Evap}	W	195.0	226.5	209.9	193.7	185.2
Calculated Cooling Need	W	183.0	224.0	210.3	197.0	184.3
Number of Rows	ea	2	2	2	2	2
Number of Columns	ea	18	22	22	19	16
Tube Length	m	0.20	0.22	0.20	0.20	0.20
Tube ID	mm	6.7	5.4	5.4	6.7	6.7
Tube OD	mm	8.3	6.6	6.6	8.3	8.3
Fin Spacing	mm	14	5	14	14	14
Fin Thickness	mm	0.2	0.2	0.2	0.2	0.2
Air Velocity	m/s	1.57	1.80	1.57	1.57	1.57
Ref. Inlet Pressure	kPa	79.0	92.7	88.5	84.5	80.5
Ref. Inlet Temperature	^{o}C	-31.5	-28.0	-29.0	-30.0	-31.0
MFR	g/s	1.22	1.21	1.14	1.10	1.00
Total Heat Transfer Area	m^2	1.04	1.34	1.25	1.10	0.92
Coil Face Area	m^2	0.012	0.013	0.012	0.012	0.012
Volume	m^3	0.007	0.009	0.008	0.007	0.007
Avg. Air Side HTC	W/m²-K	34.2	39.9	36.6	34.1	34.1
Avg. Ref. Side HTC	W/m²-K	1093.8	1412.5	1481.4	1014.1	960.2

5.1.2.3 Suggested Energy Saving Options with FCE for R Cabinet

The following approach was used to evaluate the energy saving potential of the AED cycle with FCE for the R cabinet for different evaporating and condensing temperature conditions.

From the experimental results, it was found that the condensing inlet temperature is approximately 9°C higher than T_{Cond}. Therefore, (T_{Cond} + 9°C) was used as the condenser inlet temperature. The subcooling was assumed to be 2°C and the condenser air velocity was adjusted to obtain the desired degree of subcooling.

Evaporating and condensing temperatures were varied. Then, condenser inlet conditions were defined and condensing capacities for different condenser options were calculated using CEEE's CoilDesigner software. The energy saving potential of the AED cycle with the designed cycle components was then calculated.

Tables 22-33 show the energy saving potentials of the AED cycle with FCE for the R cabinet under different conditions.

Table 22 Energy saving option 1

Option#	Energy Saving	Cond#	Operation Mode	Evap#	T_{Evap}	T_{Cond}	MFR	$V_{CondAir}$
	%				°C	°C	g/s	m/s
1	10.0	3	F	1	-28	38	1.179	1.25
			R	3	-12	39	1.417	1.40
		2	F	1	-28	38	1.179	1.40
			R	3	-12	39	1.417	1.60
		1	F	1	-28	38	1.179	1.65
			R	3	-12	39	1.417	1.75

Table 23 Energy saving option 1

Option#	Energy Saving	Cond#	Operation Mode	Evap#	$T_{CondAiri}$	$T_{CondAiro}$	Q_{Cond} Demand	Q_{Cond} Design
	%				°C	°C	W	W
1	10.0	3	F	1	30.0	35.3	209.8	211.6
			R	3	30.0	35.8	250.7	255.5
		2	F	1	30.0	35.0	209.8	206.2
			R	3	30.0	35.4	250.7	254.3
		1	F	1	30.0	34.5	209.8	213.3
			R	3	30.0	35.3	250.7	253.7

Table 24 Energy saving option 2

Option#	Energy Saving	Cond#	Operation Mode	Evap#	T_{Evap}	T_{Cond}	MFR	$V_{CondAir}$
	%				°C	°C	g/s	m/s
2	8.7	3	F	1	-28	38	1.179	1.25
			R	4	-15	38	1.228	1.35
		2	F	1	-28	38	1.179	1.45
			R	4	-15	38	1.228	1.55
		1	F	1	-28	38	1.179	1.65
			R	4	-15	38	1.228	1.75

Table 25 Energy saving option 2

Option#	Energy Saving	Cond#	Operation Mode	Evap#	$T_{CondAiri}$	$T_{CondAiro}$	Q_{Cond} Demand	Q_{Cond} Design
	%				°C	°C	W	W
2	8.7	3	F	1	30.0	35.3	209.8	211.6
			R	4	30.0	35.2	218.5	221.8
		2	F	1	30.0	34.9	209.8	213.0
			R	4	30.0	34.8	218.5	221.3
		1	F	1	30.0	34.5	209.8	213.3
			R	4	30.0	34.4	218.5	220.9

Table 26 Energy saving option 3

Option#	Energy Saving	Cond#	Operation Mode	Evap#	T_{Evap}	T_{Cond}	MFR	$V_{CondAir}$
	%				°C	°C	g/s	m/s
3	7.3	3	F	3	-30	37	1.044	1.30
			R	3	-12	39	1.417	1.40
		2	F	3	-30	37	1.044	1.50
			R	3	-12	39	1.417	1.60
		1	F	3	-30	37	1.044	1.70
			R	3	-12	39	1.417	1.75

Table 27 Energy saving option 3

Option#	Energy Saving	Cond#	Operation Mode	Evap#	$T_{CondAiri}$	$T_{CondAiro}$	Q_{Cond} Demand	Q_{Cond} Design
	%				°C	°C	W	W
3	7.3	3	F	3	30.0	34.6	186.7	188.8
			R	3	30.0	35.8	250.7	255.5
		2	F	3	30.0	34.2	186.7	188.8
			R	3	30.0	35.4	250.7	254.3
		1	F	3	30.0	33.8	186.7	188.6
			R	3	30.0	35.3	250.7	253.7

Table 28 Energy saving option 4

Option#	Energy Saving	Cond#	Operation Mode	Evap#	T_{Evap}	T_{Cond}	MFR	$V_{CondAir}$
	%				°C	°C	g/s	m/s
4	6.0	3	F	3	-30	37	1.044	1.30
			R	4	-15	38	1.228	1.35
		2	F	3	-30	37	1.044	1.50
			R	4	-15	38	1.228	1.55
		1	F	3	-30	37	1.044	1.70
			R	4	-15	38	1.228	1.75

Table 29 Energy saving option 4

Option#	Energy Saving	Cond#	Operation Mode	Evap#	$T_{CondAiri}$	$T_{CondAiro}$	Q_{Cond} Demand	Q_{Cond} Design
	%				°C	°C	W	W
4	6.0	3	F	3	30.0	34.6	186.7	188.8
			R	4	30.0	35.2	218.5	221.8
		2	F	3	30.0	34.2	186.7	188.8
			R	4	30.0	34.8	218.5	221.3
		1	F	3	30.0	33.8	186.7	188.6
			R	4	30.0	34.4	218.5	220.9

Table 30 Energy saving option 5

Option#	Energy Saving	Cond#	Operation Mode	Evap#	T_{Evap}	T_{Cond}	MFR	$V_{CondAir}$
	%				°C	°C	g/s	m/s
5	5.8	3	F	3	-30	38	1.032	1.00
			R	3	-12	39	1.417	1.40
		2	F	3	-30	38	1.032	1.15
			R	3	-12	39	1.417	1.60
		1	F	3	-30	38	1.032	1.30
			R	3	-12	39	1.417	1.75

Table 31 Energy saving option 5

Option#	Energy Saving	Cond#	Operation	Evap#	$T_{CondAiri}$	$T_{CondAiro}$	Q_{Cond} Demand	Q_{Cond} Design
	%				°C	°C	W	W
5	5.8	3	F	3	30.0	35.7	183.6	185.3
			R	3	30.0	35.8	250.7	255.5
		2	F	3	30.0	35.3	183.6	185.6
			R	3	30.0	35.4	250.7	254.3
		1	F	3	30.0	34.9	183.6	185.8
			R	3	30.0	35.0	250.7	248.7

Table 32 Energy saving option 6

Option#	Energy Saving	Cond#	Operation Mode	Evap#	T_{Evap}	T_{Cond}	MFR	$V_{CondAir}$
	%				^oC	^oC	g/s	m/s
6	4.0	3	F	3	-30	38	1.032	1.00
			R	4	-15	39	1.222	1.10
		2	F	3	-30	38	1.032	1.15
			R	4	-15	39	1.222	1.25
		1	F	3	-30	38	1.032	1.30
			R	4	-15	39	1.222	1.40

Table 33 Energy saving option 6

Option#	Energy Saving	Cond#	Operation Mode	Evap#	$T_{CondAiri}$	$T_{CondAiro}$	Q_{Cond} Demand	Q_{Cond} Design
	%				^oC	^oC	W	W
6	4.0	3	F	3	30.0	35.7	183.6	185.3
			R	4	30.0	36.3	216.3	222.4
		2	F	3	30.0	35.3	183.6	185.6
			R	4	30.0	35.9	216.3	220.7
		1	F	3	30.0	34.9	183.6	185.8
			R	4	30.0	35.4	216.3	219.7

As shown in the above tables, 10% energy savings can be achieved with an AED cycle with the appropriate components as compared to a conventional single evaporator cycle.

Although R evaporators were designed for -5^{o}C and -8^{o}C evaporating temperatures, they could not be used in energy savings options because the R evaporating temperature smaller than -12^{o}C resulted in too high MFR which made impossible to reach desired condensing capacity with the biggest possible condenser.

5.1.2.4 Natural Convection R Evaporator Design

Three different NC evaporators were designed for the R cabinet using the following schematic diagram shown in Figure 43. The number of rows was determined through calculation depending on the desired evaporating capacity.

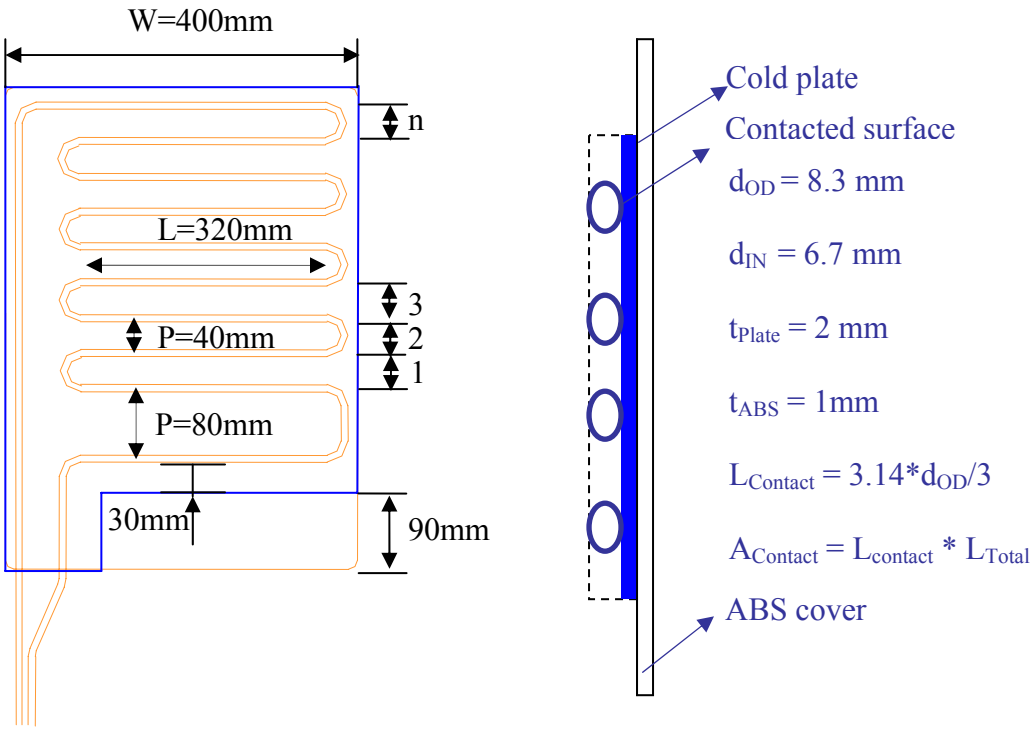

Figure 43 Schematic diagram of natural convection evaporator

Designing a R cabinet NC evaporator consists of four steps:

1. Calculation of food compartment-side natural convection heat transfer coefficient
2. Calculation of refrigerant-side forced convection heat transfer coefficient
3. Calculation of $U_{in}A$ and $U_{out}A$ values
4. Calculation of evaporator capacity

The heat transfer to the NC evaporator is shown in Figure 44.

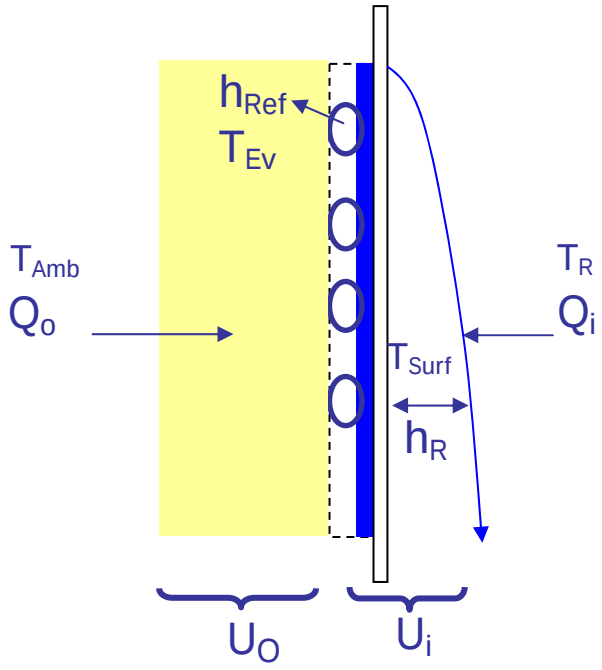

Figure 44 Heat transfer to the NC evaporator

Energy balance equations for NC evaporators can be written as follows:

$$Q_I = U_I \cdot A_{plate} \cdot \left(T_R - T_{Evap}\right) \tag{32}$$

$$Q_O = U_O \cdot A_{plate} \cdot \left(T_{Amb} - T_{Evap}\right) \tag{33}$$

$$Q_{Evap} = Q_I + Q_O \tag{34}$$

$U_I \cdot A_{plate}$ can be calculated with Eq. 35.

$$\frac{1}{U_I \times A_{plate}} = \frac{1}{h_{Ref} \times A_{Contact}} + \frac{l_{Plate}}{k_{Plate} \times A_{plate}} + \frac{l_{ABS}}{k_{ABS} \times A_{plate}} + \frac{1}{h_R \times A_{plate}} \tag{35}$$

U_O can be calculated with Eq. 36.

$$\frac{1}{U_O \cdot A_{Plate}} = \frac{1}{h_O \cdot A_{Plate}} + \frac{l_{Ins}}{k_{Ins} \cdot A_{Plate}} \tag{36}$$

Equations used for NC evaporator design calculations were taken from the ASHREA Handbook (1997).

The R cabinet natural heat transfer coefficient was calculated using Eq.37:

$$h_R = \frac{Nu \cdot k}{L} \tag{37}$$

The Nusselt number (Nu) was calculated using Eq.38.

$$Nu = 0.13 \times \left(Gr \times \mathrm{Pr}\right)^{0.33} \tag{38}$$

Grasshoff and Prandtl numbers were calculated using Eqs. 39 and 40.

$$Gr = \frac{L^3 \cdot \rho^2 \cdot \beta \cdot g \cdot \Delta T}{\mu^2} \tag{39}$$

$$\mathrm{Pr} = \frac{\mu \times C_p}{k} \tag{40}$$

The two-phase forced convection heat transfer coefficient was calculated with Kandlikar's Correlation:

$$h_{NBD} = h_l \times \left[0.6683 \times Co^{-0.2} + 1058 \times Bo^{0.7} \times F_{fl}\right] \tag{41}$$

$$h_{CBD} = h_l \times \left[1.1360 \times Co^{-0.9} + 667.2 \times Bo^{0.7} \times F_{fl}\right] \tag{42}$$

After comparing h_{NBD} and h_{CBD} the larger h value was used as a forced convection heat transfer coefficient.

In the Kandlikar equation, Co and Bo are convection and boiling numbers, respectively. Additionally, F_{fl} is the fluid dependent number and it is 1.63 for R134a.

$$Co = \left[\frac{(1-X)}{X}\right]^{0.8} \times \left(\frac{\rho_g}{\rho_l}\right)^{0.5} \tag{43}$$

where X is refrigerant vapor quality. For these calculations, it was assumed that X was 0.5 and remained constant.

$$Bo = \left[\frac{\dot{q}}{G \times h_{fg}} \right] \tag{44}$$

where G, h_{fg} and $\dot{q}$ are mass flux, fluid gas specific enthalpy and heat flux, respectively. The heat flux from the cabinet to the evaporator surface was calculated using Eq. 45:

$$\dot{q} = \frac{Q_I}{A_{Contact}} \tag{45}$$

Kandliker's Correlation includes the liquid phase heat transfer coefficient, h_l, which was calculated using the Dittus – Boetler Correlation for single phase flow:

$$h_l = \frac{Nu \times k}{D} \tag{46}$$

$$Nu = 0.023 \times \mathrm{Re}^{0.8} \times \mathrm{Pr}^{0.3} \tag{47}$$

where D is the inside diameter of the tube and k is the heat conduction coefficient of the refrigerant.

The Reynolds and Prandtl numbers were calculated as following using Eqs. 48 and 49:

$$\mathrm{Re} = \frac{\rho \times V \times D}{\mu} \tag{48}$$

$$\mathrm{Pr} = \frac{\mu \times C_P}{k} \tag{49}$$

In the previous equations, Q_I was calculated using various number of NCE row amounts and it was compared with the demanded evaporating capacity (Q_{Dem}) at the

design condition. The number of NCE row was increased step by step until Q_l becomes greater than the Q_{Dem}.

Three different NCE were designed for three different conditions as shown in Table 34.

Table 34 NCE design conditions

Condition	Cond#	Operation Mode	T_{Evap}	T_{Cond}	MFR
			°C	°C	g/s
1	1	F	-30	38	1.032
		R	-18	38	1.05
2	1	F	-30	37	1.032
		R	-21	38	0.90
3	1	F	-30	37	1.032
		R	-23	37	0.80

It should be mentioned that design conditions for NCE are different than design conditions for FCE. This is because NCE surface temperatures should be low enough to supply the desired amount of cooling needed for the R cabinet. Consequently, NCE evaporating temperatures should be lower than FCE temperatures.

5.1.2.5 Suggested Energy Saving Options with NCE for R Cabinet

Three different energy saving options can be suggested with different size NCE, as shown in Table 35.

Table 35 Designed NCE

Option	Numbers of Row	Width	Height	HTC_{Ref}	HTC_{Ri}	En. Sav.
#	#	m	m	W/m^2K	W/m^2K	%
1	34	0.4	1.56	1514	15.6	3
2	25	0.4	1.20	1424	15.7	2
3	20	0.4	1.00	1335	15.7	1.5

The R cycle with three above NCEs are shown in Table 36.

Table 36 R Cycle with NCEs

Option	T_{Evap}	MFR	Superheat	Q_{Dem}	Q_{Evap}
#	[^oC]	[g/s]	[^oK]	[W]	[W]
1	-18	1.05	0	188.8	194.4
2	-21	0.90	4	160.8	173.5
3	-23	0.80	5	146	154.5

5.1.2.6 Practical Design Recommendations

A practical design option for FCEs is minimizing the design change by using the current heat exchangers and using a smaller size R evaporator than that for the F. Based on this fact and results from experimentation, the following factors are recommended

- Use FCE option number #6 with condenser#1 (base condenser), $V_{CondAirF}$ =1.3 m/s, $V_{CondairR}$=1.4 m/s, R_{Evapa}#4 (half of the length of the base evaporator), and F_{Evapa}#3 (it has 19 columns instead of 18 columns)
- With this design option, an energy savings of 4% is expected.

Practical design options for the NCE also include minimizing the design change by using the current condenser and the NC R evaporator, which can make reasonable energy savings. The following combination for NCEs is recommended:

- Use NCE option number #1 with condenser#1 (base condenser), $V_{CondAirF}$ =1.3 m/s, $V_{CondairR}$=1.4 m/s, and F_{Evapa}#3 (it has 19 columns instead of 18 columns)
- With this design option, an energy savings of 3% is expected.

5.2 AED Cycle Experimental Setup

5.2.1 FC R Evaporator Test Setup

Household Refrigerator Unit

In the AED cycle study, the base unit, whose specifications were outlined in chapter 4.1.1, was used as a cabinet model. However, some modifications were made to convert the conventional refrigerator into the AED refrigerator. The main difference between a conventional refrigerator and an AED refrigerator is that there is no opening between the R and F cabinets in an AED test setup. A conventional unit is comprised of air inlets from the F to the R and air outlets from the R to the F. In addition, tubing of the AED cycle is very different from that of the base unit. Only hot pipe tubing between the condenser outlet and capillary inlet was used for the AED cycle tubing.

To modify the base unit into the AED refrigerator, the damper and R air inlet section were first removed from the base unit. All air gaps were then filled with polyurethane foam. The foam surfaces were cleaned and covered with aluminum tape. Additionally, 2.4 cm thick insulation pieces were added to the air inlet and outlet of the R cabinet to prevent heat transfer from the R cabinet to the F cabinet. A picture of the AED R cabinet is shown in Figure 45.

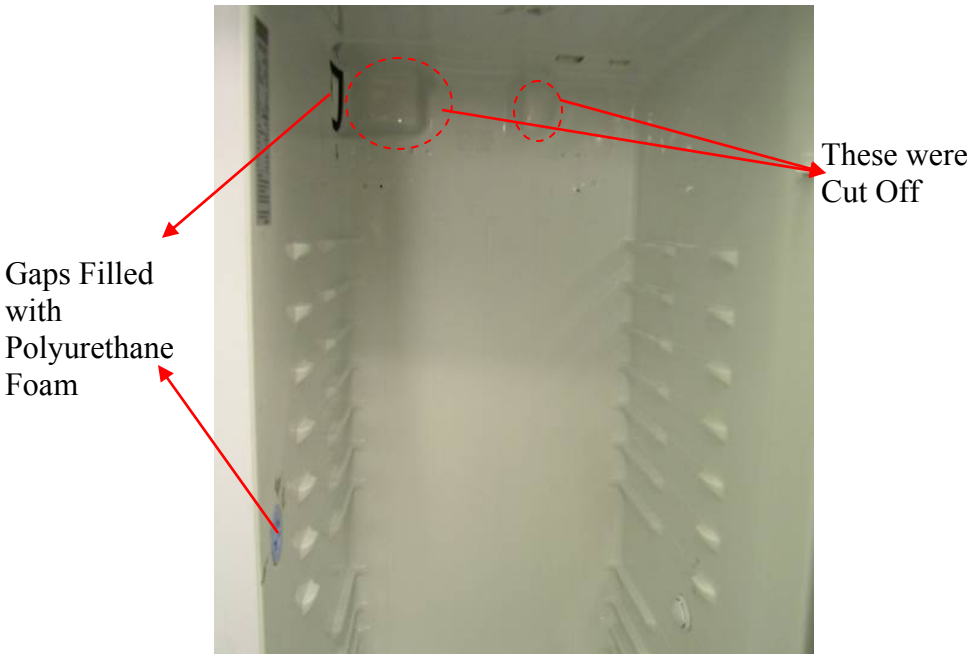

Figure 45 Modified R cabinet

The base conventional refrigerator's evaporator was used as a F evaporator. Even though it was suggested to use an evaporator with an additional row for the F cabinet, it was quick and easy to use the base evaporator for the F cabinet. The F evaporator and fan that were used are shown in Figure 46.

Figure 46 F evaporator and fan

The base conventional refrigerator's evaporator was used to build the FC R evaporator. Since it was suggested to use an evaporator half of the size of the base evaporator for the R cabinet, the base evaporator were shortened to half of its size. The 10^{th} row tubing was cut, and straight tube fittings were used to close open ends. The FCE and its connections are shown in Figure 47.

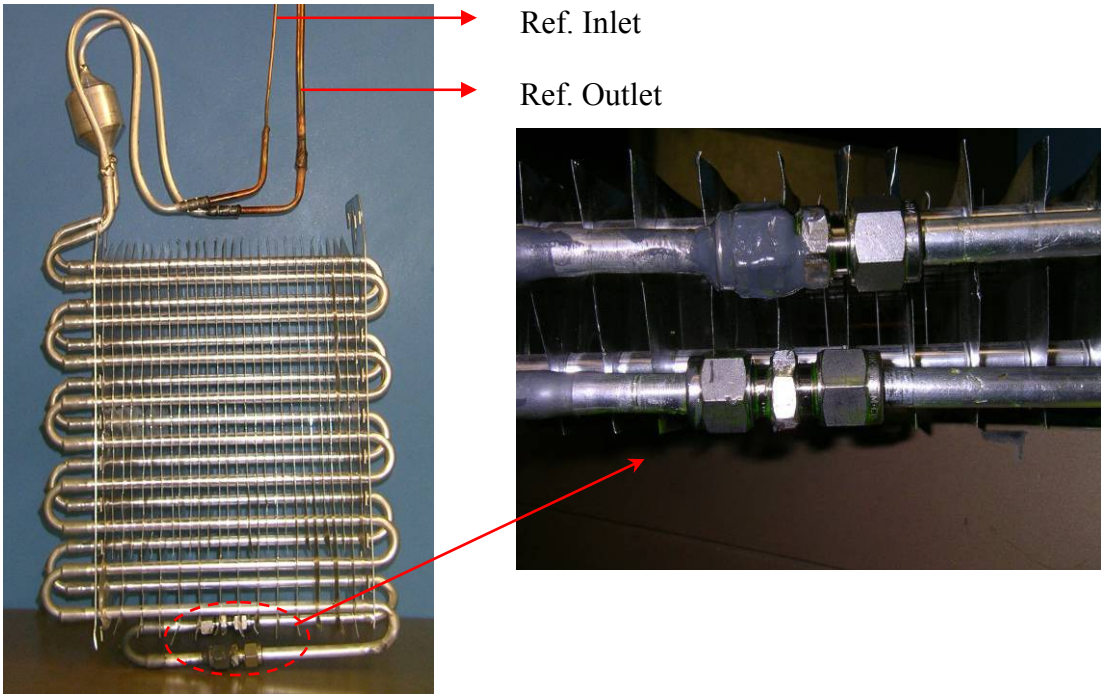

Figure 47 FC R evaporator and its connection

An air guide was built to help air flow only through the evaporator. It was built similar to the F evaporator air guide and as small as possible so as not to take up too much space. In addition to guiding the air, the air guide acted as a support for the evaporator inside the cabinet. The evaporator was fixed to the air guide and then the guide was fixed to the R cabinet. The FC R evaporator, fan and air guide are shown in Figure 48.

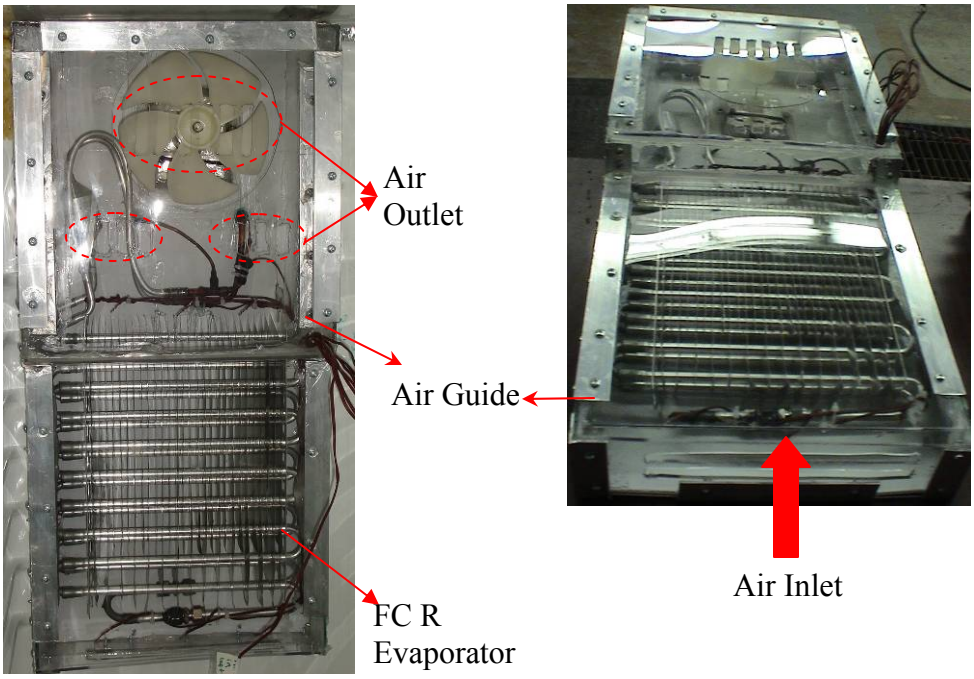

Figure 48 FC R evaporator and air guide

A brushless DC motor fan that is same as the conventional unit's evaporator fan was used for the FC R evaporator fan.

All air guide connections were sealed with clear silicon to prevent air leak.

The air inlet and outlet gaps in the base unit were originally maintained for the F side. Later on, after trial tests, additional air outlet holes were made to increase the air flow rate to the R cabinet.

The evaporator's inlet and outlet connections were separated from the conventional cycle and new connections were made for the AED cycle. New holes were drilled on the back wall of the cabinets and the evaporator's inlet, outlet and pressure measurement tubing were carried out from these holes. Figure 49 shows the back wall of the refrigerator with the new holes and tubing arrangement.

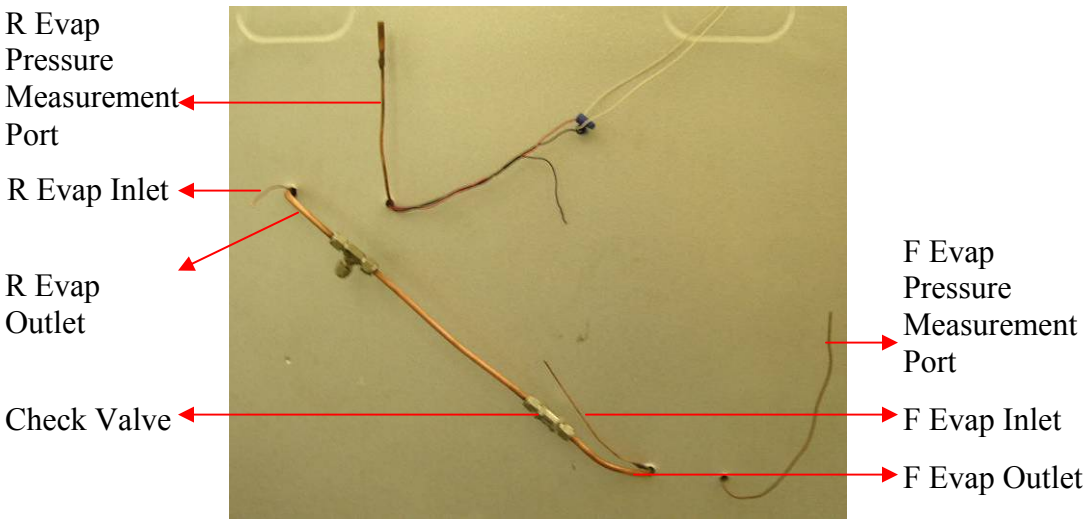

Figure 49 Evaporator tubing

A check valve was used at the outlet of the F evaporator to prevent the back flow of the higher pressure refrigerant from the R evaporator into the lower pressure level F evaporator. This is also shown in Figure 49.

In the AED cycle, new capillary tubes were used. The specifications of the capillary tube are shown in Table 37.

Table 37 Specifications of Capillary tube

Model	7190K71
Material	Alloy 122 Copper
Outside Diameter	1.59 mm (0.0625”)
Inside Diameter	0.876 mm (0.0345”)
Supplier	McMaster

For all tubing except the capillary tube, 6.35mm (0.25”) outside diameter (OD) and 3.86mm (0.152”) inside diameter ID copper tubes were used.

Since the AED cycle includes two evaporators, it also includes two capillary tubes and accordingly needs two SLHXs, one for R operation and the other one for F operation.

In this design, instead of using two separate SLHXs, only one integrated SLHX was used. A 1.9 m copper tube were used as a suction line and the F capillary tube, which was 2.5 m long and the R capillary tube, which was 1.65 m long, were soldered together to the suction line. The SLHX was insulated with 9.5 mm (0.375”) thick insulation tubing. Black electrical tape was used to cover and secure the outside of the insulation. The SLHX prototype is shown in Figure 50.

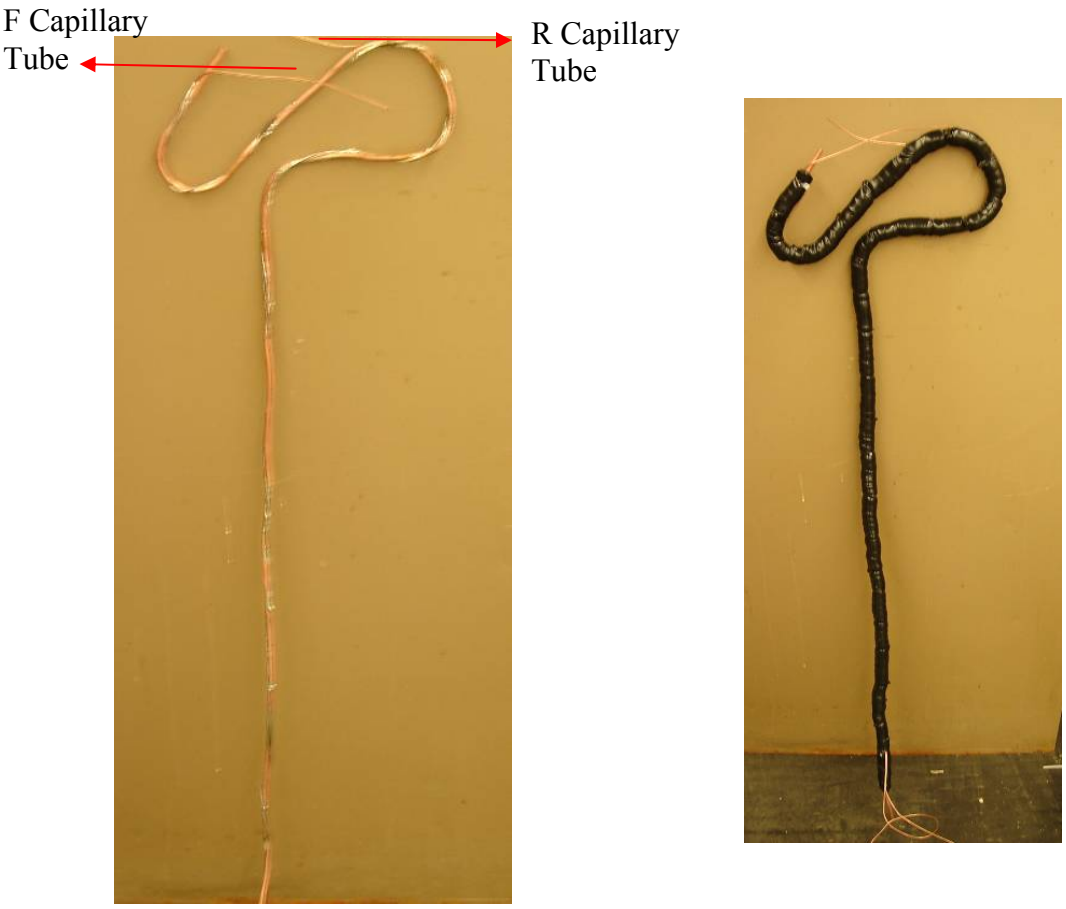

Figure 50 SLHX prototype

Capillary tubes (Cap), suction lines (SL) and SLHXs lengths are shown in Table38.

Table 38 Lengths of Cap, SL and SLHX

Length		F	R
L_{Cap}	[m]	2.50	1.65
L_{SL}	[m]	2.40	2.20
L_{SLHX}	[m]	1.60	1.30

The base compressor, whose specifications are listed in Table 2, was equipped with a bypass line in order to bypass refrigerant in R operation and to modulate the compressor capacity. The bypass line was equipped with one normally closed solenoid valve and one expansion valve. The solenoid valve was used to prevent refrigerant back flow in the F cycle and the expansion valve was used to adjust the refrigerant bypass ratio. A charging valve was also installed to the compressor. The compressor equipped with the bypass line is shown in Figure 51.

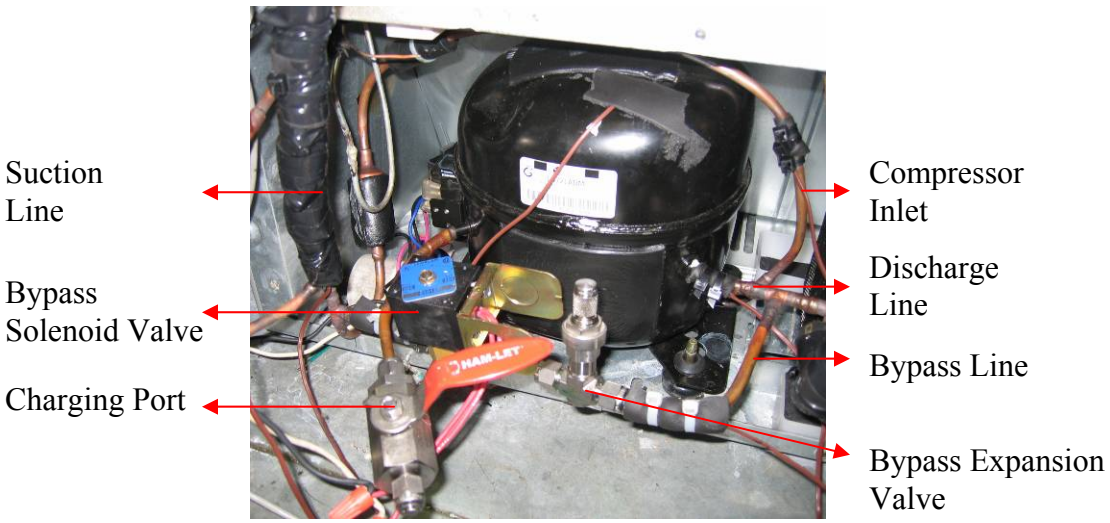

Figure 51 AED cycle compressor and bypass line

Tables 39 and 40 show specifications of the solenoid and expansion valves.

Table 39 Specifications of the bypass expansion valve

Model number	SS-SS4
Body material	Stainless Steel
Connection size	6.35 mm (0.25")
Manufacturer	Swagelok

Table 40 Specifications of the Solenoid valve

Model number	E3S120
Body material	Brass
Connection size	6.35 mm (0.25")
In rest position	Closed
Refrigerant	R134a
Volts/Cycle	208-240/50-60
Manufacturer	Sporlan

Two solenoid valves were used to control the refrigerant flow direction to either the F capillary tube or the R capillary tube. To do so, the hot pipe outlet was separated into two tubes. Each tube was equipped with a solenoid valve and filter-dryer. The filter-dryer outlets were connected to the capillary tubes as shown in Figure 52.

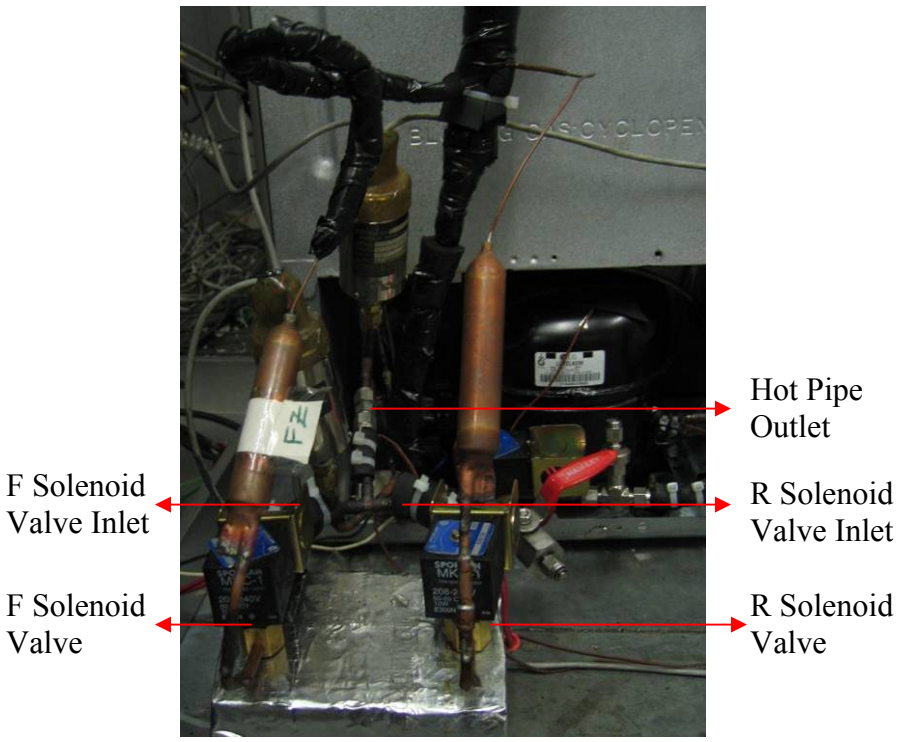

Figure 52 Solenoid valves and filter-dryers

All additional holes were filled with polyurethane foam after the final assembly in order to prevent air leakage, and the SLHX was insulated with 25.4mm (1") thick insulation material to minimize heat gain to the refrigerant from the ambient air. In the base unit, most of the tubing was positioned inside the wall insulation. To provide the same insulation effect as that for the base unit, insulating the tubing located outside of the wall was important for the AED cycle. In addition to the tubing insulation, 25.4 mm thick insulation materials were applied to the back wall of the cabinet where the temperature was lower than the averaged back wall temperature. These positions are around the holes which were drilled for tubing. The closed cycle ready to test is shown in Figure 53.

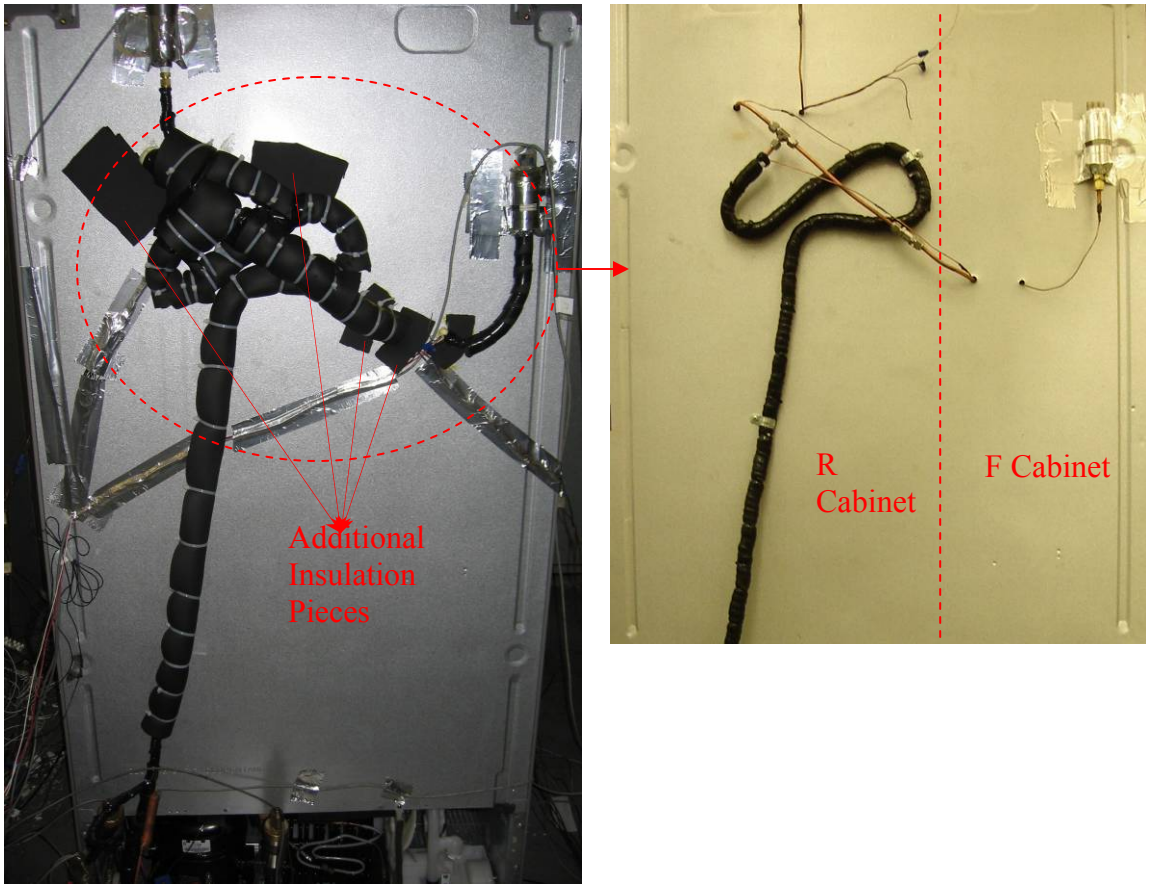

Figure 53 AED cycle tubing and insulation

The AED cycle condenser is shown in Figure 54. A base condenser with a counter-flow configuration was used as an AED cycle condenser. After some experimentation, it was concluded that an air guide should be added above the condenser to force the air to flow through the condenser.

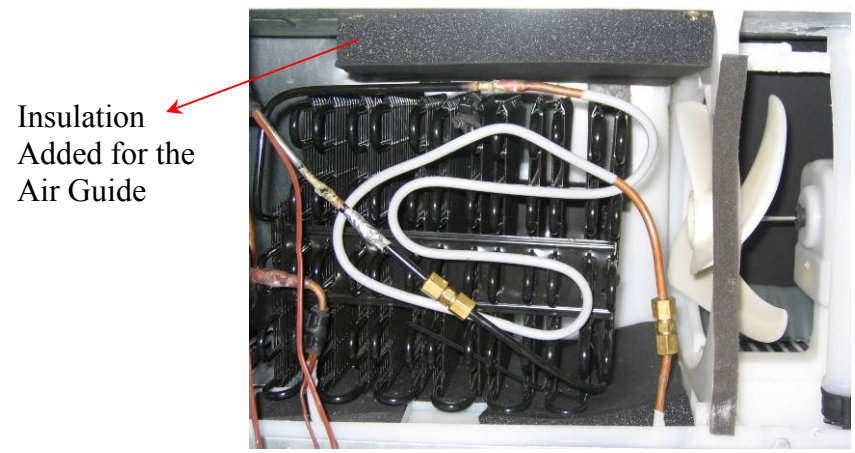

Figure 54 AED cycle counter-flow condenser

The compressor compartment was closed, as shown in Figure 55 and experiments were conducted in this configuration.

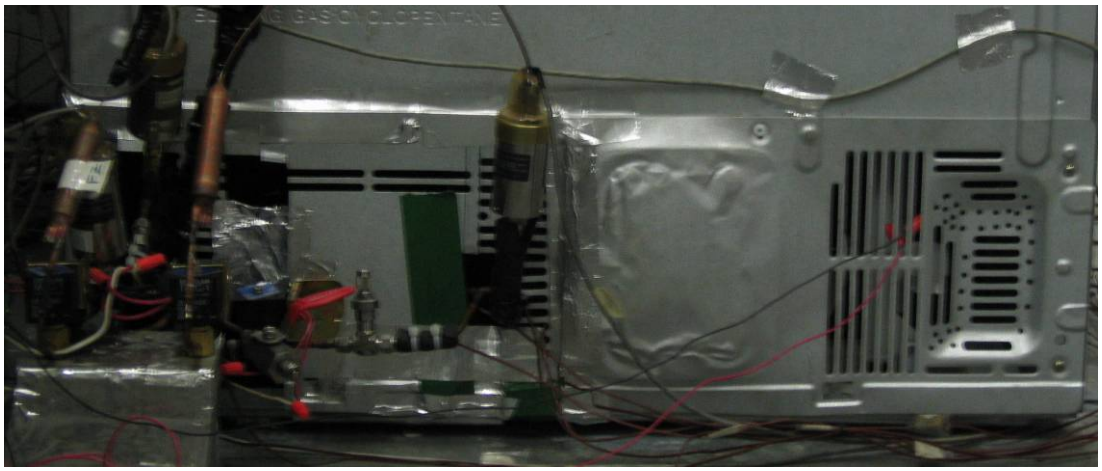

Figure 55 Compressor compartment

In the AED cycle, a hole was drilled in each of the side walls of the R and TC were inserted in the cabinets through these holes. After the TC were installed, these holes were filled with polyurethane foam. The F and R cabinets with TC holes are shown in Figure 56.

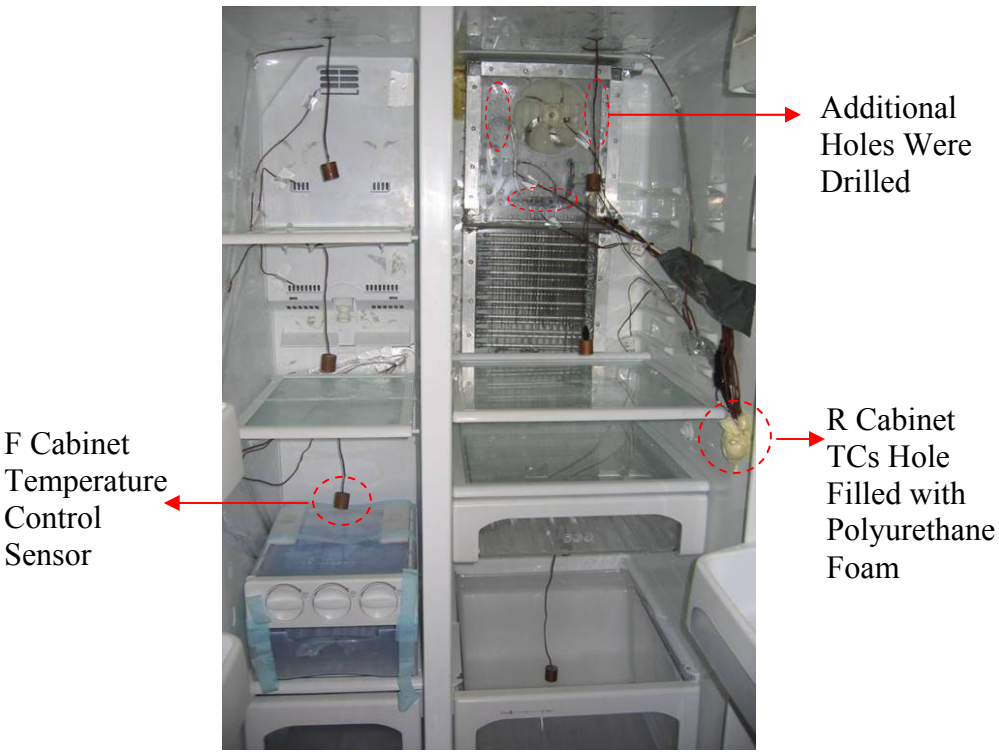

Figure 56 AED refrigerator cabinet inside with FC R evaporator

5.2.2 NC R Evaporator Test Setup

A tube-and-plate type NC evaporator was built for the R cabinet. The size of the evaporator was almost the largest possible size that could fit into the inner back side of the R cabinet. A 10 m long copper tube were used for the evaporator tube, as shown in Figure 43, and it was soldered to a 1 mm thick copper plate. The NC evaporator is shown in Figure 57.

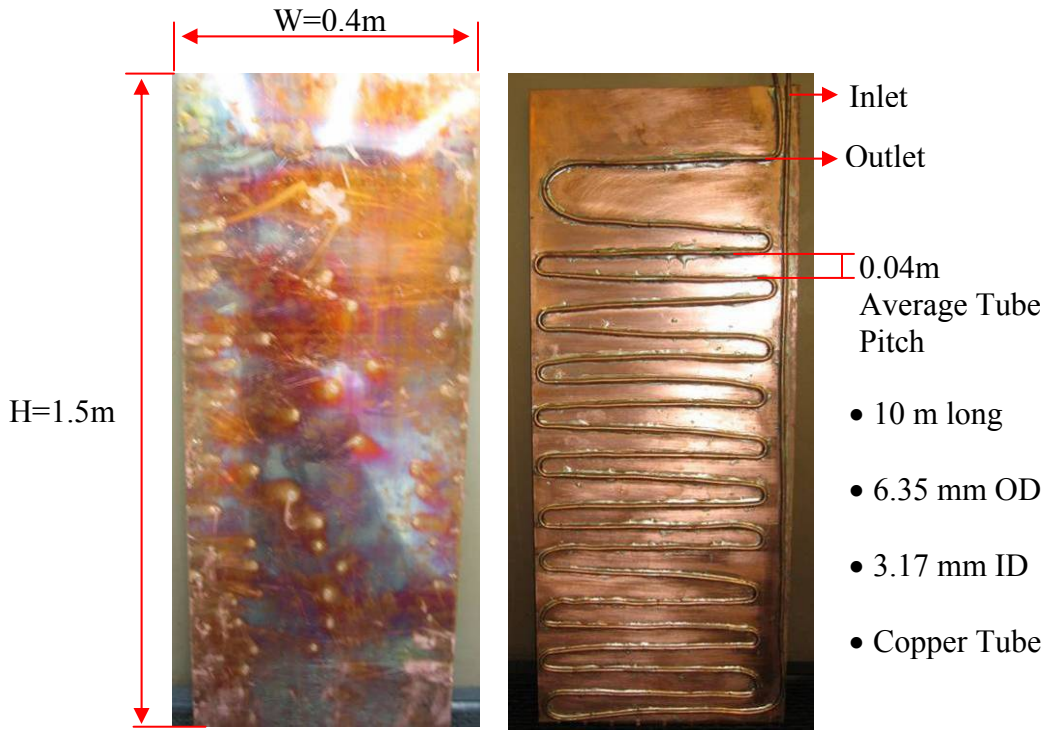

Figure 57 NC R evaporator

The R cabinet's back side plastic cover was cut off as same dimensions of new NCE. A new hole was drilled for the NC evaporator tubing and old holes were filled with polyurethane foam. Then the NC evaporator was attached to the cabinet. Finally, all edges of the evaporator were filled and sealed with silicon. The R cabinet, equipped with the NC evaporator, is shown in Figure 58.

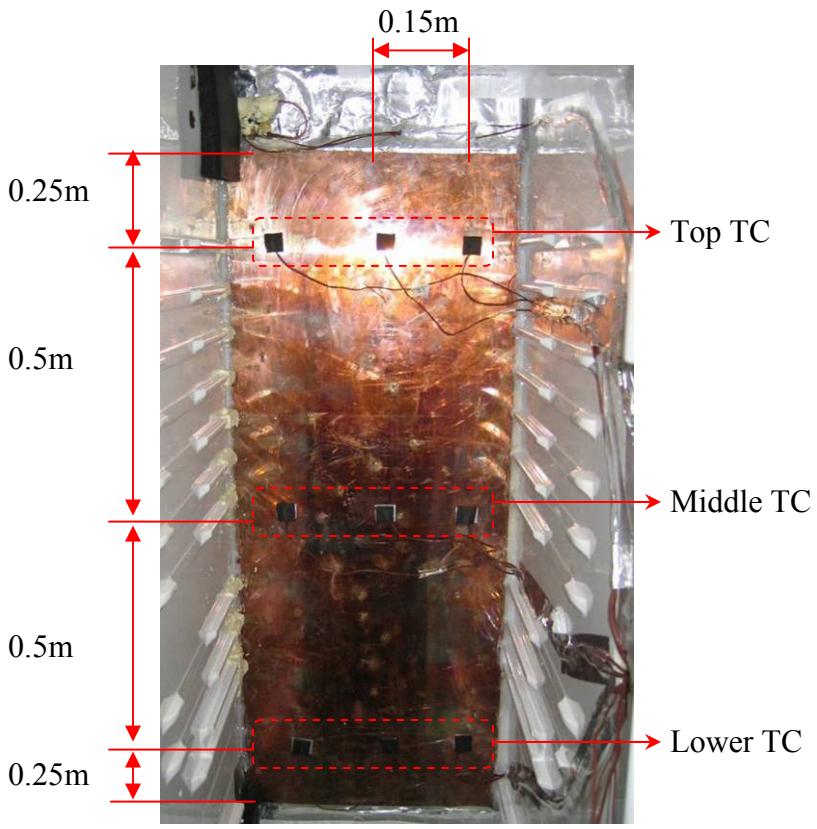

Figure 58 R Cabinet with NC evaporator

NC evaporator experiments included capillary tube optimization for the R cycle. Therefore, a new capillary tube connection was constructed for the NCE tests. Straight 1.6 mm (0.0625”) ID straight tube connections were used. Capillary tubes of different lengths were prepared in roll shape so that capillary tube length was easily adjusted for different tests. Moreover, the capillary roll was insulated with a 25.4 mm (1”) thick insulation sheet, as shown in Figure 59.

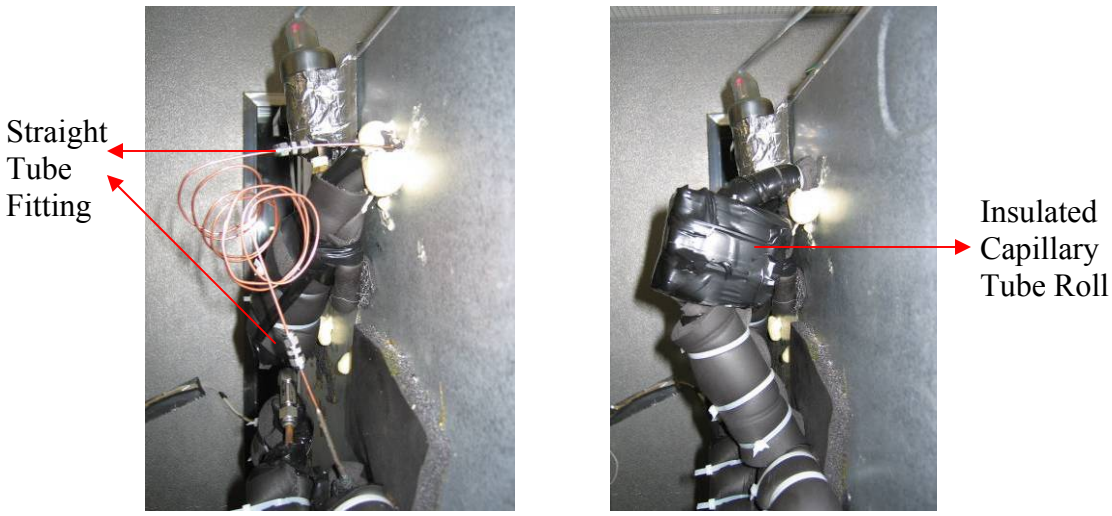

Figure 59 Capillary tube connection in NCE experiments

The schematic diagram of the AED cycle experimental setup is shown in Figure 60.

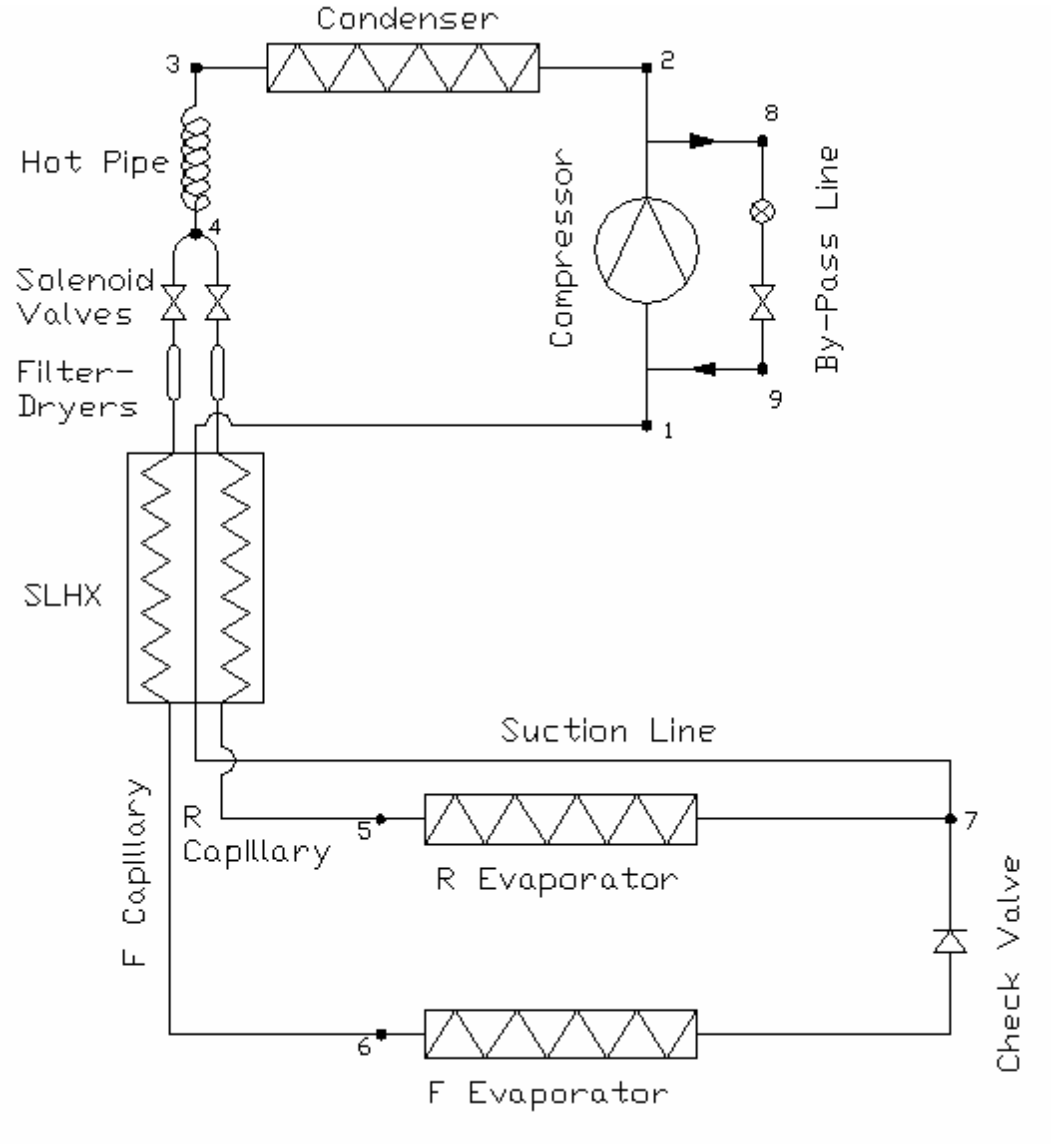

Figure 60 AED Cycle experimental setup

5.2.3 Bi-stable Solenoid Valve

Although normally closed one-way solenoid valves were used in the current study, using a bi-stable solenoid valve is recommended for the actual application of the AED cycle. First of all, bi-stable solenoid valves only consume energy while switching position. This means their energy consumption is virtually negligible. Secondly, bi-stable solenoid valves do not have a special off-time position, which means they keep their last

position until new voltage is supplied. Finally, bi-stable valves have the capability for more than 300,000 switching times, which is equivalent to more than a 25 year life cycle for a household R.

A commercially available bi-stable solenoid valve that is manufactured by Zhejiang Fenghua Sanshi Solenoid Valve Co.,Ltd. is shown in Figure 61.

Figure 61 Bi-stable solenoid valve

The specifications of this product are shown in Table 41.

Table 41 Specifications of the bi-stable solenoid valve

Rated peak pulse voltage	310V
Max pulse current	2.5A
Max operating pressure	2.5MPa
Max pulse width	0.155 Sec
Min pulse width	0.05 Sec
Max commutating frequency	20 times/min
Fluid permission temp	$-30^{o}C \sim +90^{o}C$
Internal leakage	< 2ml/min

Although solenoid valves were used instead of the bi-stable solenoid valve in the AED cycle experiments, the energy consumption of the solenoid valve was adjusted from that of the solenoid valve to that of the bi-stable valve.

5.2.4 Measurement and Data Acquisition

5.2.4.1 Measurement

In the AED cycle experiments, cycle pressures, temperatures, heat exchanger air side temperatures, cabinet air temperatures, compressor power, fan power and solenoid valve power were measured.

Refrigeration Cycle Pressure Measurement

As shown in Figure 62, pressures, important for analyzing refrigerant properties, were measured at five different locations. These locations include the compressor inlet (evaporator outlet), compressor outlet (condenser inlet), hot pipe outlet (capillary tube inlet), R evaporator inlet (R capillary outlet) and F evaporator inlet (F capillary outlet).

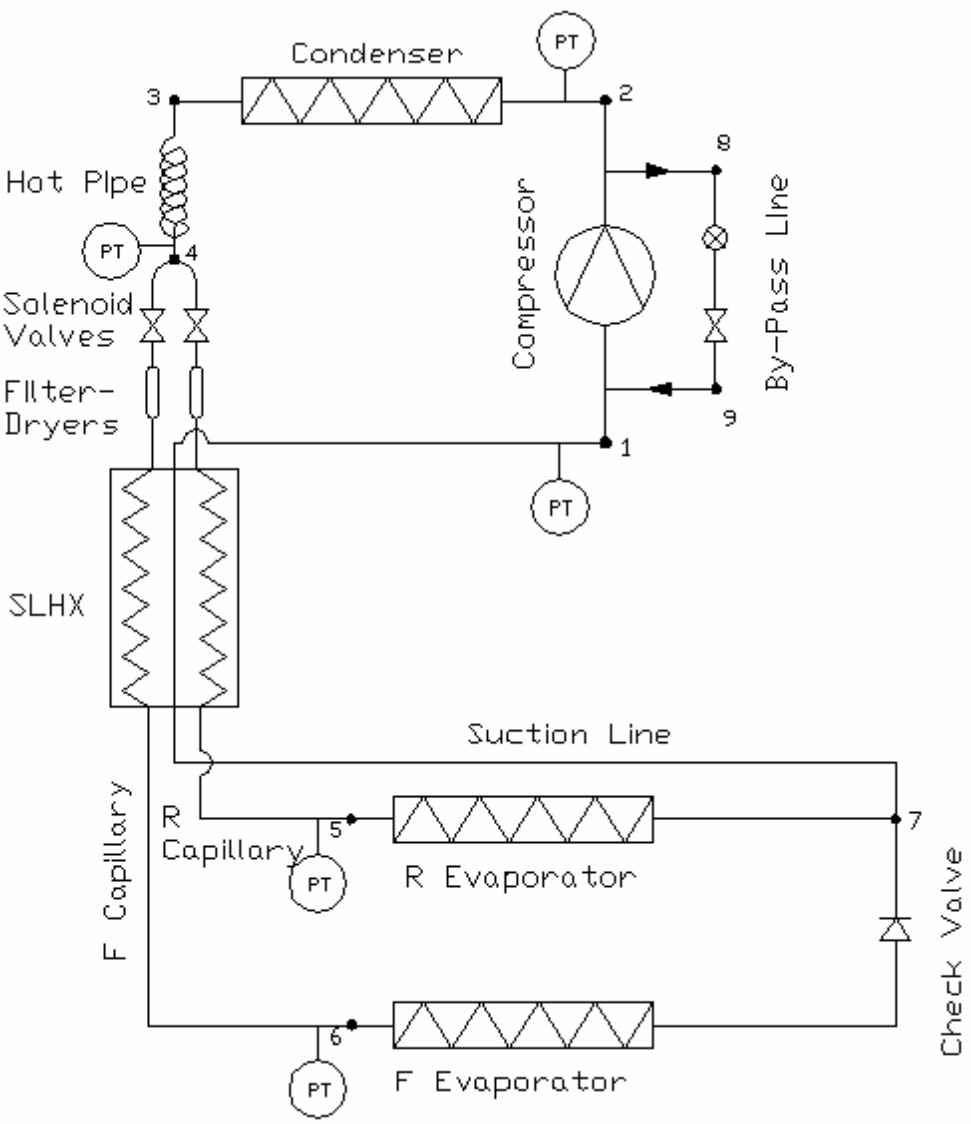

Figure 62 AED cycle experiments with pressure transducer locations

In AED cycle experiments, the same pressure transducers used in condenser Improvement experiments were used. Their specifications are shown in Table 3.

Refrigeration Cycle Temperature Measurement

As shown in Figure 63, temperatures, which are also important for analyzing refrigerant properties, were measured at 13 different locations. These locations include the compressor inlet, compressor dome, compressor outlet (condenser inlet), condenser outlet, hot pipe outlet (capillary tube inlet), R evaporator inlet (R capillary outlet), F

evaporator inlet (F capillary outlet), R evaporator outlet, F evaporator outlet, suction side SLHX outlet, by-pass line before expansion valve, and by-pass line after expansion valve.

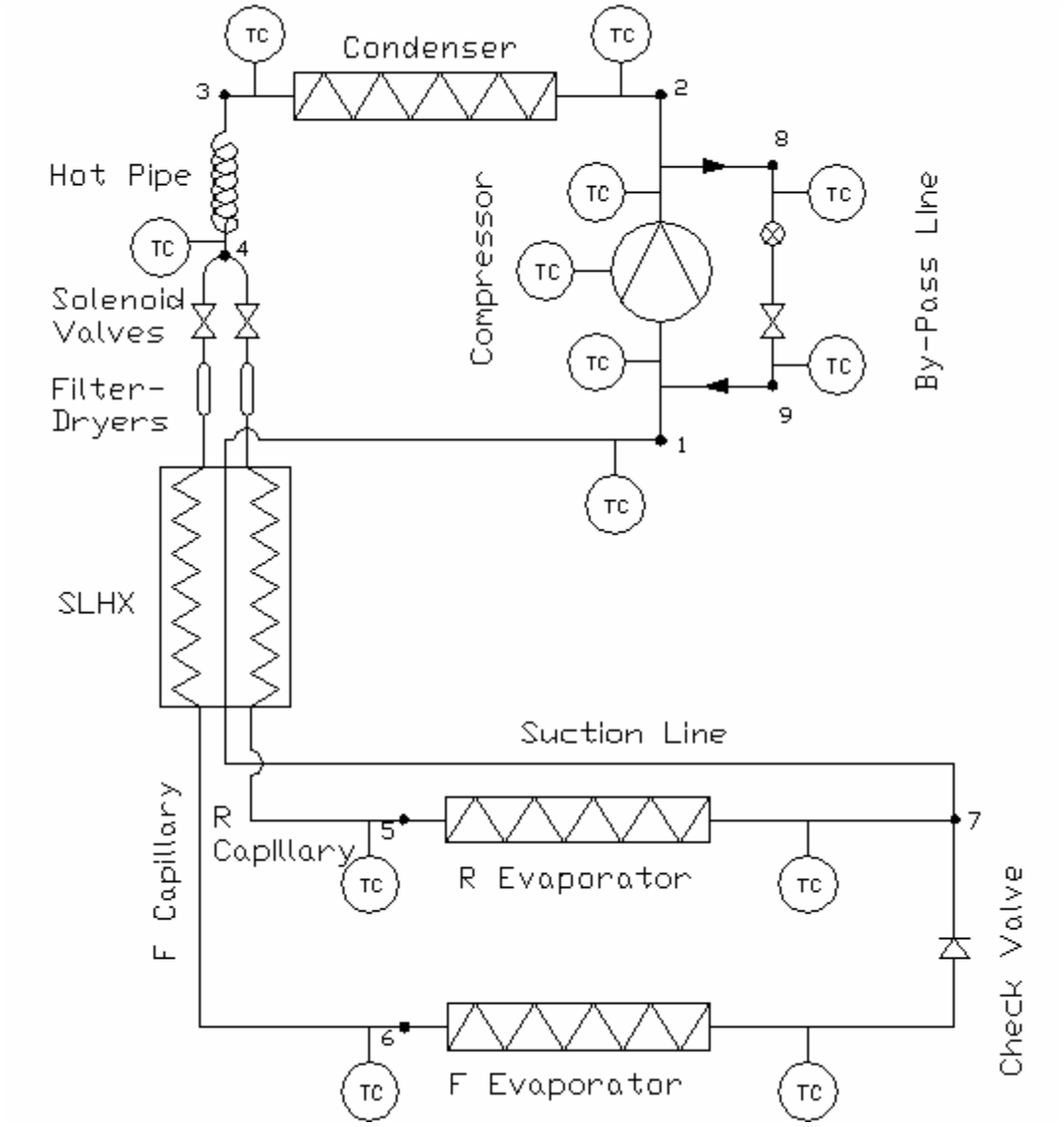

Figure 63 AED cycle experiments TCs locations

The TC that were used in the condenser Improvement experiments were also used for the AED cycle experiments. The TC specifications are in Table 4.

Similar to the condenser Improvement test, TC surfaces were covered with insulation to minimize the effect of the ambient conditions. Additionally, all cycle temperatures were measured on tube surface.

FC Evaporators Air Side Temperature Measurement

In the AED cycle experiment, the evaporator air side temperature measurement method is similar to that in the condenser Improvement experiments, as was explained in section 4.1.2.1. Figure 31 shows the F evaporator air side TC. In addition to the condenser Improvement experiments, the R evaporator air side temperatures were also measured in the AED cycle tests. The R evaporator air side TC are shown in Figure 48.

NC Evaporator Surface Temperature Measurement

In the NC R evaporator experiments, evaporator surface temperature was measured instead of evaporator air side temperatures from 9 different locations, as shown in Figure 58. TC were positioned 0.5 m horizontally away from each other and 0.15 m vertically away from each other. TC were attached to the evaporator surface using aluminum tape and insulation pieces were glued over the aluminum tape in order to prevent effects from the cabinet temperatures.

Cabinet Air Temperature Measurement

Similar to the condenser Improvement test, cylindrical copper masses of 2.54 cm in diameter and height which were soldered to the TC, were used to measure cabinet temperatures, as shown in Figure 64. Four copper cylinders were installed to the R compartment and three were installed to the F compartment.

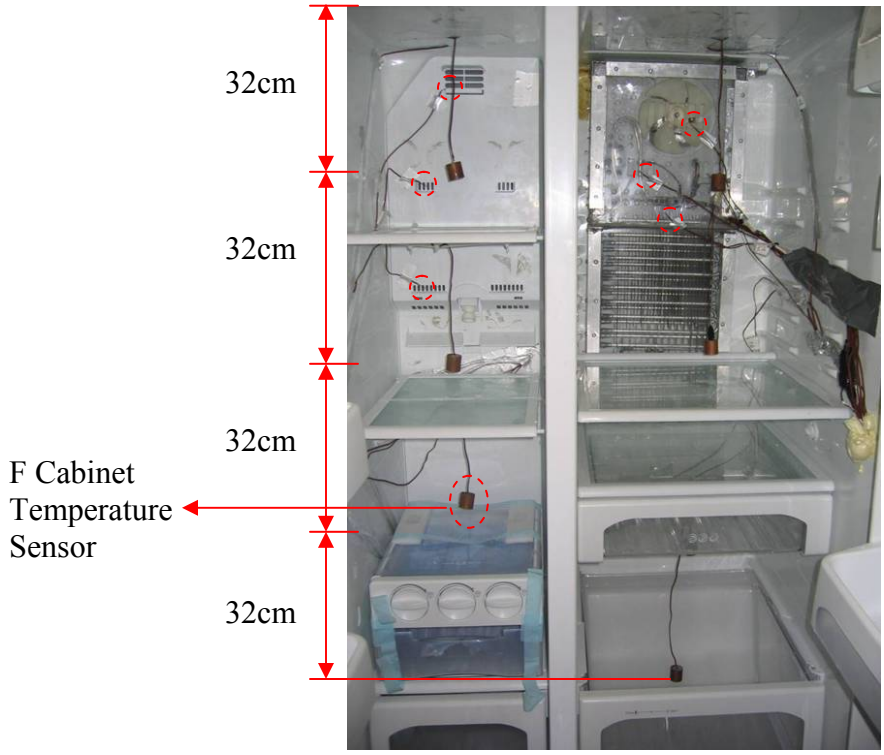

Figure 64 AED experiments cabinets' temperature measurement

Air inlet temperatures were also measured at three different locations for each cabinet, also shown in Figure 64.

Power Measurement

In the AED cycle energy consumption evaluation experiments, three watt meters were used. An AC voltage watt meter was used to measure the compressor's power consumption, an AC voltage watt meter was used to measure the power consumption of the solenoid valves, and a DC voltage watt meter was used to measure the total power consumption of the fan for the R and F evaporator and condenser. The Compressor's watt meter specifications are provided in Table 5. The specifications for the solenoid valves' watt meter are shown in Tables 42.

Table 42 Watt meter for Solenoid valves

Model Number	GW5 – 002X5-51	
Input	Volts AC	0 to 300 VAC
	Amps AC	0 to 5 amps
	Frequency Range	58 to 62 Hz
Output	Watts F.S.	1000 W
	Response time	400 msec
	Voltage DC	0 to 5 VDC
	Accuracy	0.2% Reading.
Manufacturer	Ohio Semitronics	

Watt meter specifications for the fans are shown in Table 43.

Table 43 Watt meter for fans

Model Number	PC8 – 003-08D	
Input	Volts DC	0 to 150 VDC
	Amps DC	0 to 5 amps
	Frequency Range	40 to 400 Hz
Output	Watts F.S.	750 W
	Response time	500 msec
	Voltage DC	0 to 10 VDC
	Accuracy	1% F.S.
Manufacturer	Ohio Semitronics	

Relative Humidity Measurement

In order to measure the cabinets' humidity ratio, two humidity sensors were used for each cabinet. Specifications for the humidity sensors are shown in Table 44.

Table 44 Specifications of humidity sensors

Model #	HMP233
Current Output	4 to 20 mA
Measurement Range	0 to 100% RH
Accuracy	±1% RH
Operating Temp	-40°C to +180°C
Power supply	24VDC
Manufacturar	Vaisala

Humidity sensors were installed into the cabinets next to the second from top copper cylinders as shown in Figure 65

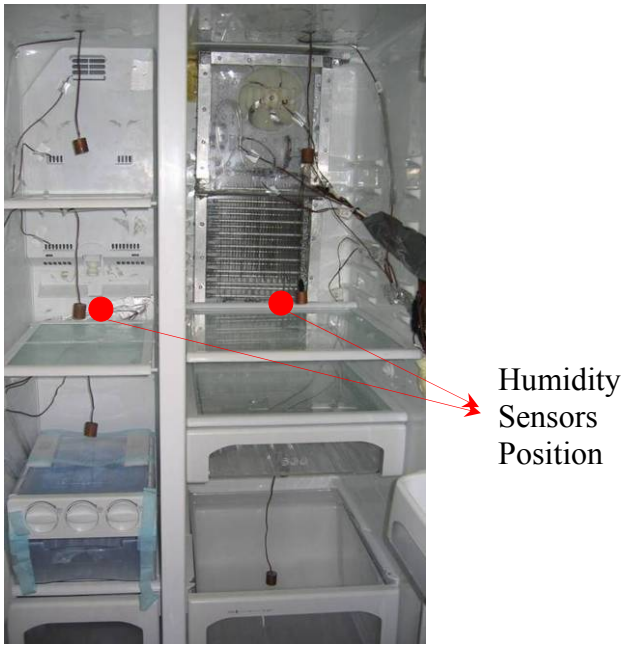

Figure 65 Humidity sensors position

5.2.4.2 Data Acquisition

System measurement devices such as TC, pressure transducers and watt meters, sent signals to a DAS, which has hardware and software components. A Hewlett Packard Data Acquisition Unit (HP 3497A) was used to collect the data and two DAS cards were used to accomplish different functions. The T-Couple Acquisition Card can measure

input signals from T-type thermocouples, and the Guarded Acquisition Card can measure voltage output from pressure transducers and watt meter.

All signals from the TC, pressure transducers, humidity sensors and watt meters were converted into physical properties such as temperature, pressure and power. While the experiments were running, data was displayed and stored in 13 seconds interval by a Q-Basic program.

5.3 AED Cycle Control Method and Algorithm

Since the AED cycle control algorithm is totally different than the conventional cycle control algorithm, new AED cycle components were controlled independently from the control of the base unit. The DAS and QBasic program controlled the system. Cabinet copper cylinders were used as control sensors of the system. For the R cabinet, the averaged readings of the four copper cylinders and for F cabinet $1/3^{th}$ of hight from bottom copper cylinder as shown in Figure 64 were used as control sensors.

When the system started, sensors sent signals to the DAS. Then the QBasic program analyzed the signals and compared them with the defined thermostat settings. Depending on the analysis, the program would run the required cycle components for continued operation.

The control algorithm was written to have minimum compressor on/off operation and to keep the R cabinet temperature every time between the thermostat settings. However, the F cabinet temperature can change in a wide range unless it is lower than -5^{o}C, which is still much lower than freezing point.

Seven solid state relays control the R evaporator fan on/off switch, the F evaporator fan on/off switch, condenser fan in two speed, the R on/off switch, the F on/off switch,

and the by-pass solenoid valves on/off switch. The control box of the AED cycle is shown in Figure 66.

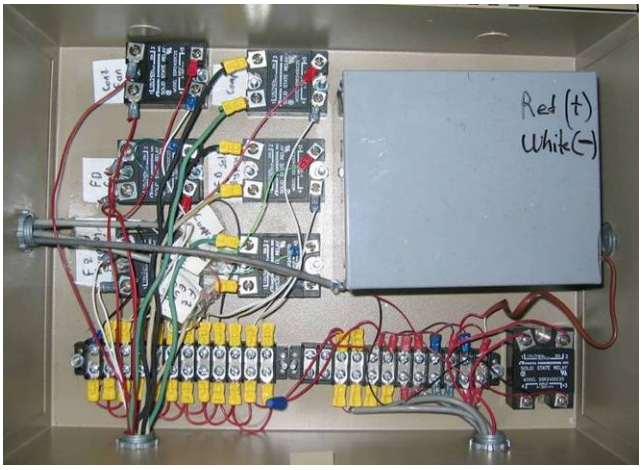

Figure 66 AED cycle control box

Pull Down Operation

For the pull down operation, the R cabinet temperature is first decreased to the lower thermostat setting and then the F cycle starts. If the R cabinet temperature reaches its upper thermostat setting before the F cabinet reaches its lower setting, the cycle switches to the refrigeration cycle.

Cyclic Operation

In cyclic operation, the R cycle starts first and decreases the R cabinet temperature to its lower setting point. As soon as the R cabinet reaches its lower setting point without any compressor on/off operation, F cycle starts. After the F cabinet reaches its lower set point, the off cycle starts and continues until the R cabinet temperature reaches its upper set point.

Safety Precautions

During testing, the following safety precautions were followed:

- If the suction pressure is lower than 50kPa and the discharge pressure is higher than 1600kPa, then all system components are shut off.
- At cycle start up, the solenoid valves are activated first, followed by the compressor.
- At cycle changing, the closed solenoid valve is opened first and then the open valve is closed.

5.3.1 Experimental Procedures

To verify the energy saving potential of a R equipped with an AED cycle and a capacity modulated compressor, many experiments were conducted with both the FC and NC evaporator for the R cabinet. Experiments were first conducted for the AED cycle with the FC evaporator for the R cabinet. During the experiments, many improvements were made on the cycle, cabinet and controls in order to find the most efficient system.

During the FC R evaporator tests, refrigerant charge amount, bypass opening, system control, thermostat settings, capillary tube length, condenser fan voltage and evaporators fan voltage were optimized and a total of 24 experiments were conducted. After achieving the most energy saving configuration, cabinet humidity ratios were measured.

After the FC R evaporator experiments, NC R evaporator tests were conducted with the most energy saving system configuration. In these experiments, refrigerant charge amount, by-pass valve opening, R capillary tube length and R cabinet thermostat settings were optimized and a total of 39 experiments were conducted. After reaching the minimum energy consuming configuration with the NC R evaporator, cabinet humidity ratios were measured.

5.3.1.1 Humidity Ratio Measurement Experimental Procedure

The experimental procedure was decided after investigating the base line test. The following procedure was used for 64 hour humidity ratio measurement tests:

- The ambient condition was set to 55% RH and 30^{o}C in the FCE experiment and 65% and 30^{o}C in the NCE experiment.
- After cabinet conditions were equalized to the ambient conditions with the doors open, the doors were closed and sealed.
- The AED started and after the F cabinet temperature (T_F) reached -5^{o}C, the cycle was turned off for 60 minutes.
- The system started again after the 60 minutes and ran continuously for 24 hours.
- After first 24 hours The first defrost cycle was done.
    - A TC which was attached to the last row of the F evaporator was used as the F evaporator defrost sensor. In the defrost cycle, the compressor, solenoid valves and evaporator and condenser fans were shut off. The heater started and ran continuously until the F evaporator defrost sensor temperature reached -5^{o}C. Then the heater turned off and the cycle restarted.
- One defrost cycle was completed every 10 hours .
- After the fifth defrost cycle, the humidity ratio measurement test was finished.

5.3.2 Experimental Data Analysis

After finishing the experiments, data stored by the DAS computer was converted into an excel file. Data was then copied to a template excel file, which was prepared beforehand and includes important cycle graphs displaying cabinet temperatures, pressures and power consumption.

The household R with an AED cycle has three operation modes: the R cycle, F cycle, and off cycle, which are shown in Figure 67.

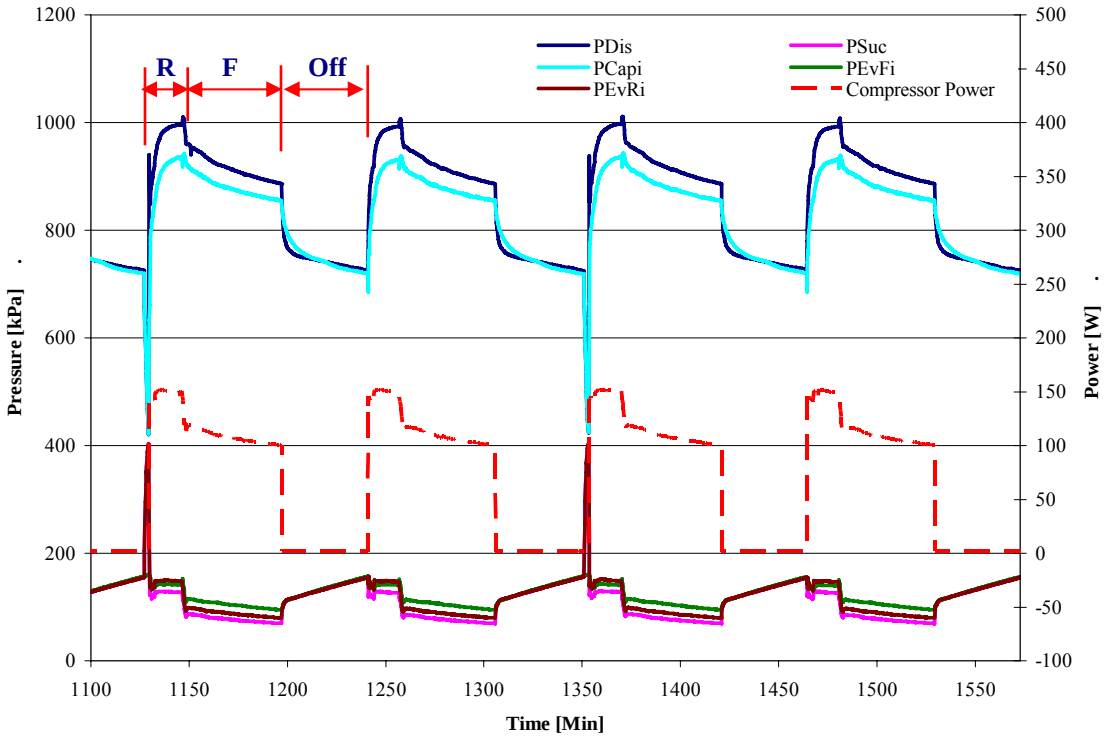

Figure 67 AED cycle pressures and power consumption

In an AED cycle same cycle didn't repeated continuously because due to the effect of the solenoid valves that were closed in the off cycle, compressor had start up problem occasionally which will be explained in detailed later. Therefore, the cycle that was repeated the most during the entire experiment was selected and analyzed. For each

test, the measured data were averaged for different cycle periods including the R, F and off cycle.

Since the R solenoid valve and by-pass solenoid valve were powered together, total solenoid valve power consumption in the R operation was around 12W. On the other hand, in the F operation, this value was around 6W. During the off period, the solenoid valve power consumption is obviously 0W. As a result, cycle periods were easily identified by examining the power consumption of the solenoid valves.

5.3.2.1 Calculations of the Cycle Properties

All calculations were done using an EES program similar to the condenser Improvement cycle calculations. EES provides an equation solving platform as well as many refrigerant properties.

5.4 AED Cycle Experimental Results

The AED cycle was optimized through 27 FC R evaporator tests. After optimizing, 39 NC R evaporator experiments were conducted using the new optimum system configuration. During the FC R evaporator experiments many challenges were encountered. Solutions were discovered for many of the challenges by considering the experimental results and desired outcomes.

5.4.1 FC R Evaporator Experimental Results

A total of 23 experiments were conducted with the FC evaporator for the R cabinet in order to evaluate the energy consumption of a household refrigerator with an AED cycle.

In this section, four important AED cycle test results are compared to each other and to the baseline test result. Compared test specifications are shown in Table 45.

Table 45 Specifications of compared tests

Test No.		Test 1	Test 2	Test 3	Test 4
Charge [g]		217	217	217	217
Bypass Opening		2 Turns	2 Turns	2 Turns	2 Turns
Control	R	T_{Mean}	T_{Mean}	T_{Mean}	T_{Mean}
	F	1/3th Copper Cylinder	1/3th Copper Cylinder	1/3th Copper Cylinder	1/3th Copper Cylinder
Thermostat Settings [^oC]	R	$[5.2>T_R>1.3]$	$[5.2>T_R>1.3]$	$[5.2>T_R>1.3]$	$[5.2>T_R>1.3]$
	F	$[-16>T_F>-20]$	$[-16> T_F >-20]$	$[-16> T_F >-20]$	$[-16> T_F >-20]$
L_{Cap} [m]	R	1.65	1.65	1.65	1.65
	F	2.5	2.5	2.5	2.5
Condenser Fan Voltage [V]	R	12.9	18.0	18.0	18.0
	F	12.9	18.0	18.0	18.0
Evap Fan Voltage [V]	R	12.9	12.9	12.9	12.9
	F	12.9	12.9	12.9	12.9

Calculated Values

Important properties of the AED cycle and CHLs were calculated and are shown in Tables 46 and 47.

Table 46 Comparison of cycle properties

	Cycle	Base Cycle	Test 1	Test 2	Test 3	Test 4
T_{Cond} [^oC]	R	39.6	40.5	38.2	37.9	37.9
	F	38.0	39.0	36.2	36.2	36.9
T_{Evap} [^oC]	R	-27.2	-19.5	-20.7	-21.2	-20.7
	F	-31.4	-30.3	-31.6	-31.8	-31.5
Superheat [^oC]	R	2.2	12.3	14.0	14.6	14.2
	F	1.6	6.3	8.1	8.1	7.3
Subcooling [^oC]	R	3.3	2.9	3.9	3.5	3.5
	F	2.7	1.9	2.4	2.4	2.4
MFR [g/s]	R	1.216	1.207	1.051	0.905	0.725
	F	0.814	0.876	0.831	0.825	0.839
X_{Evapi}	R	0.13	0.19	0.19	0.19	0.19
	F	0.13	0.18	0.17	0.17	0.17
Q_{Evap} [W]	R	227.9	215.3	189.9	163.6	131.1
	F	183.2	183.9	175.2	173.4	175.9

It is shown that T_{Cond} of Test 3 is around 2K lower than that of the baseline. Also T_{Evap} of Test 3 is 6K higher than that of the base F+R cycle and 0.4K lower than the base F cycle. Consequently, the AED cycle pressure ratio is smaller than that of the base cycle and accordingly, the cycle efficiency of the AED cycle is better than that of the base cycle. On the other hand, the base cycle evaporator inlet quality is lower than that of the AED cycles. It may also be matched for AED cycle by building a better SLHX and positioning it into the wall insulation for real applications.

Table 47 Comparison of cabinet heat loads

	Cabinet	Base Cycle	Test 1	Test 2	Test 3	Test 4
CHL [W]	R	28.0	34.4	27.9	23.1	18.9
	F	75.6	86.8	78.0	75.6	75.4

As explained before, higher condenser fan speed, additional insulation, and lower MFR cause less heat load to the cabinets. Although the F CHL is the same for AED cycle Test 3 and the base cycle, there is a 5W difference between the R CHL in the AED and base cycles.

Summary of FCE AED Cycle Test Results

Table 48 Summary of FCE AED cycle test results

Ref Model			AED With FCE							
			Test1		Test2		Test3		Test4	
T_{Amb} [^{o}C]			30.1		30		30		29.9	
T_{R} [^{o}C]			3.2		3.1		3.1		3.1	
T_{F} [^{o}C]			-17.0		-16.8		-16.9		-16.9	
T_{Evap} [^{o}C]	R	F	-19.5	-30.3	-20.7	-31.6	-21.2	-31.8	-20.7	-31.5
T_{Cond} [^{o}C]	R	F	40.5	39.0	38.2	36.2	37.9	36.2	37.9	36.9
Q_{Evap} [W]	R	F	215.3	183.9	189.9	175.2	163.6	173.4	131.1	175.9
W_{Comp} [W]	R	F	97.5	107.4	86.4	100.9	73.4	100.3	57.9	101.8
$Time_{On}$ [Min]	R	F	19.1	56.3	16.7	50.5	15.8	48.8	16.0	47.7
OTR [%]	R	F	16.0	47.2	14.7	44.6	14.1	43.6	14.4	42.9
W_{Total} [W]	R	F	104.9	115.8	94.8	110.2	81.8	109.6	66.3	111.1
W_{Total} OFF [W]			3.5		5.2		5.1		5.1	

5.4.2 FC R Evaporator Humidity Ratio Measurement Test Results

A humidity ratio measurement experiment was conducted to investigate how the humidity ratio level is controlled in the cabinets.

Humidity Ratios During Pull Down

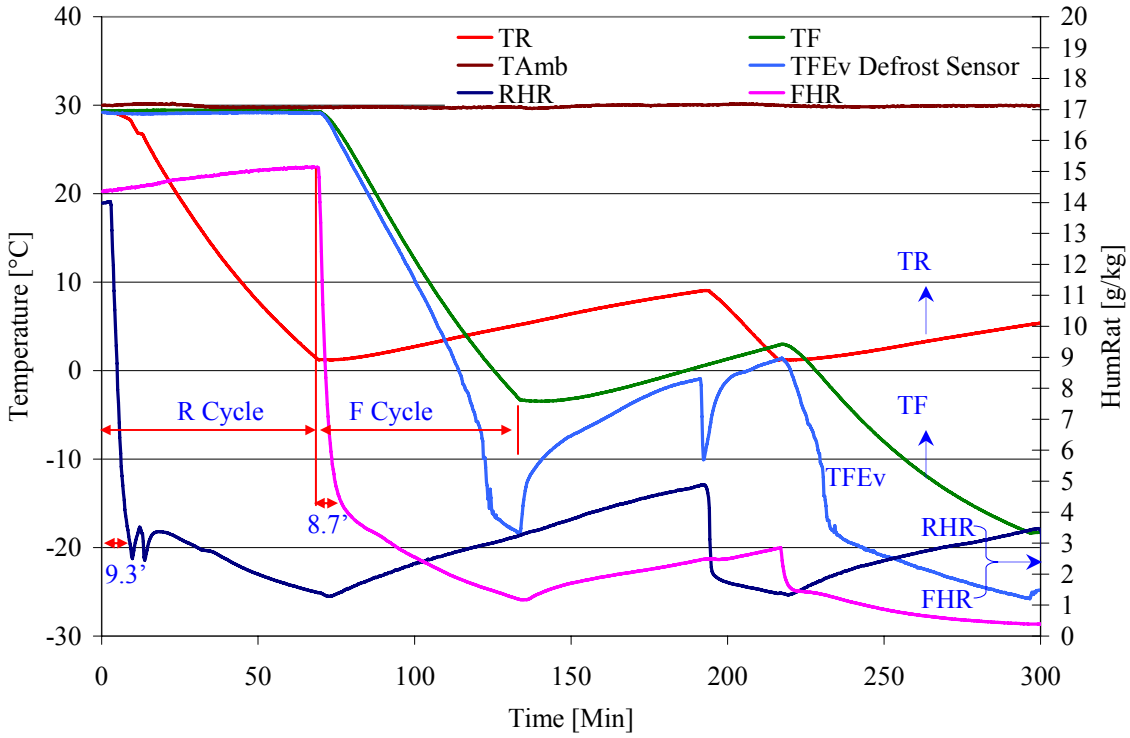

Figure 68 Humidity ratios during pull down operation

From Figure 68, it can be concluded that the moisture from the cabinet air condenses on the cold surface of the evaporator immediately after the evaporator fan starts to run. After most of the water vapor in the cabinet condenses, the humidity ratio changes according to the cabinet air temperature. The R cabinet HR reaches 3g/kg in 9.3 minutes and the F cabinet HR reaches 4g/kg in 8.7 minutes. In addition, it takes 66 minutes for the R cabinet temperature to reach 2°C from 30°C, and it takes 133 minutes for the F cabinet temperature to reach -3°C from 30°C. In other words, after the F cycle starts, it takes 67 minutes for the F cabinet temperature to reach -3°C.

Humidity Ratios During Cyclic Operation

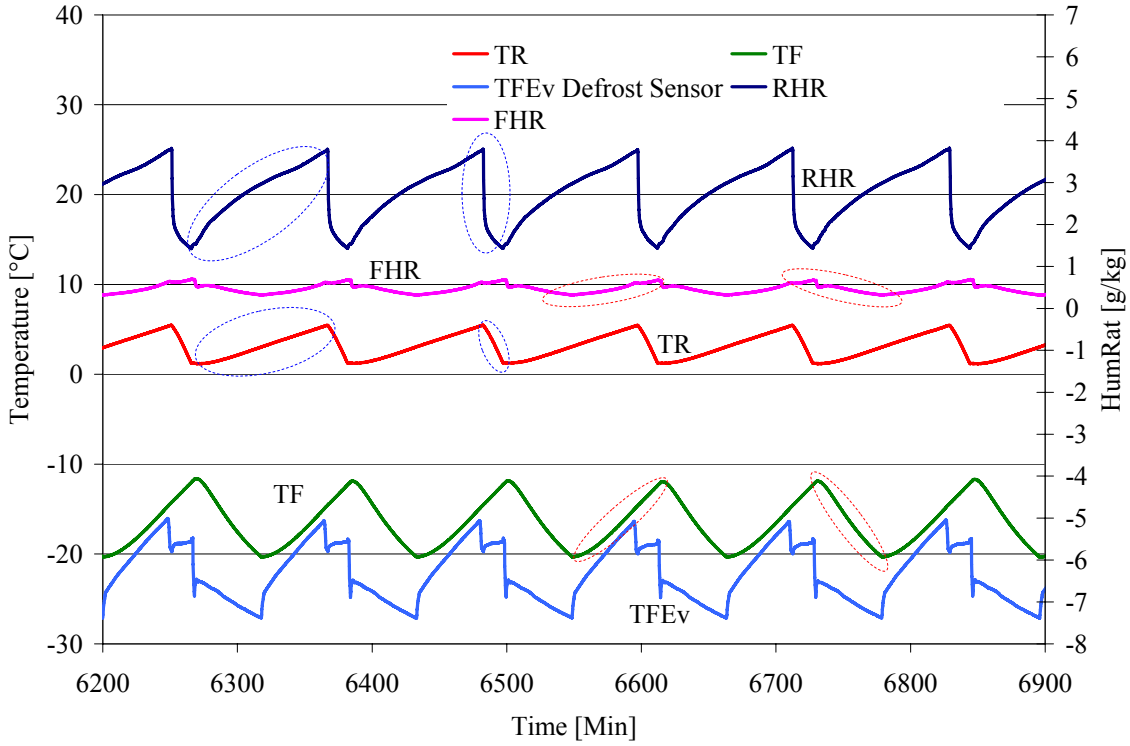

Figure 69 Humidity ratios during cyclic operation

1. R cabinet humidity ratio

The average R cabinet HR for one cycle is 2.5g/kg. During the on-time of the R cycle, water vapor in the air quickly condenses on the R evaporator surface, so the HR of R room quickly decreases. During the off-cycle, the R evaporator surface temperature increases above the freezing point and then the frost formed on the surface starts to melt and evaporate. In summary, the humidity ratio changes depending on the R cabinet temperature.

2. F cabinet humidity ratio

The averaged F cabinet HR for one cycle is 0.46g/kg. During the on-time of F cycle the water vapor in the air is condensed to the evaporator surface quickly, so the

humidity ratio of F room decreases. However due to lower humidity ratio this decrease is not as fast as R operation. During the off-cycle F evaporator surface temperature and cabinet temperature increases by 8 K and remain below freezing temperature. The humidity ratio changes due to this temperature changes

Humidity Ratios During Defrost Cycles

The defrost cycle procedure explained in section 5.4.11 was applied in these experiments. .

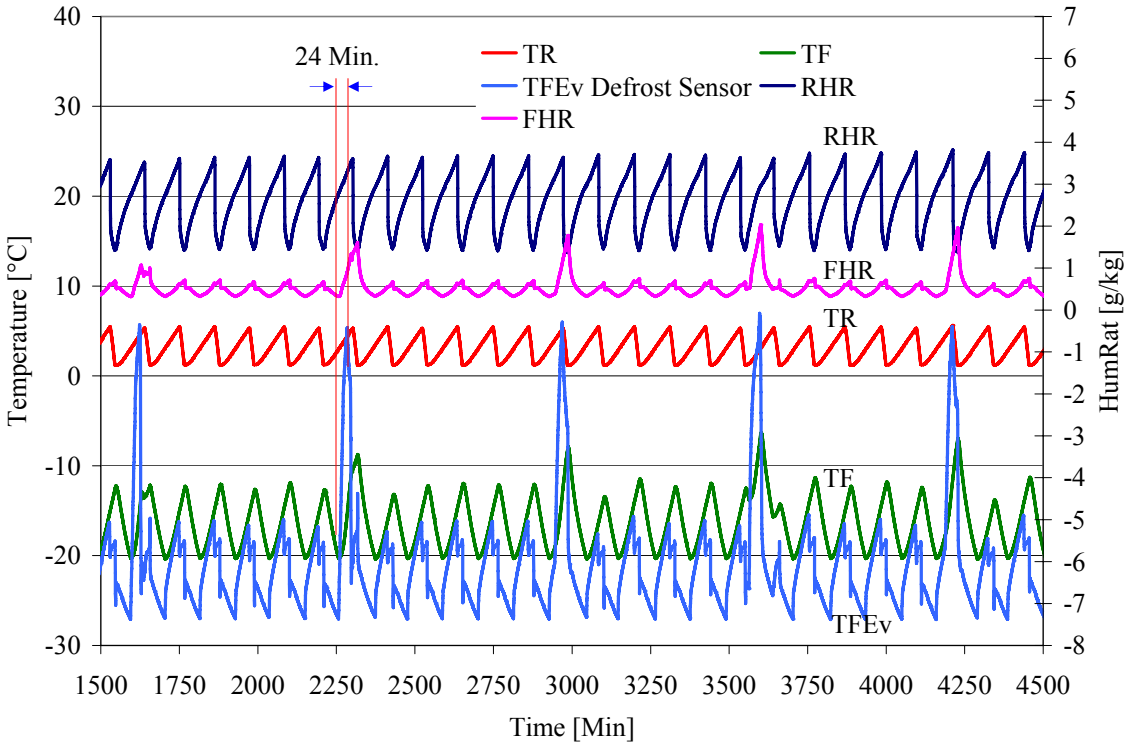

Figure 70 Humidity ratios during defrost cycles

In the defrost cycle, the F cabinet temperature increased to around -9°C. Also, the F HR increased to 2g/kg due to the cabinet air temperature increase and because of ice defrost occurring at the surface of the evaporator.

Results show that in the defrost cycle the AED R cabinet is not affected by the defrost heater. Since the R cycle can run individually during the defrost cycle it can continue running without being affected.

For the R cycle there is no need to run a defrost cycle because in the R off-cycle the evaporator surface temperature increases above the melting point and all frost on the evaporator surface melts. The R evaporator during the off-cycle is shown in Figure 71.

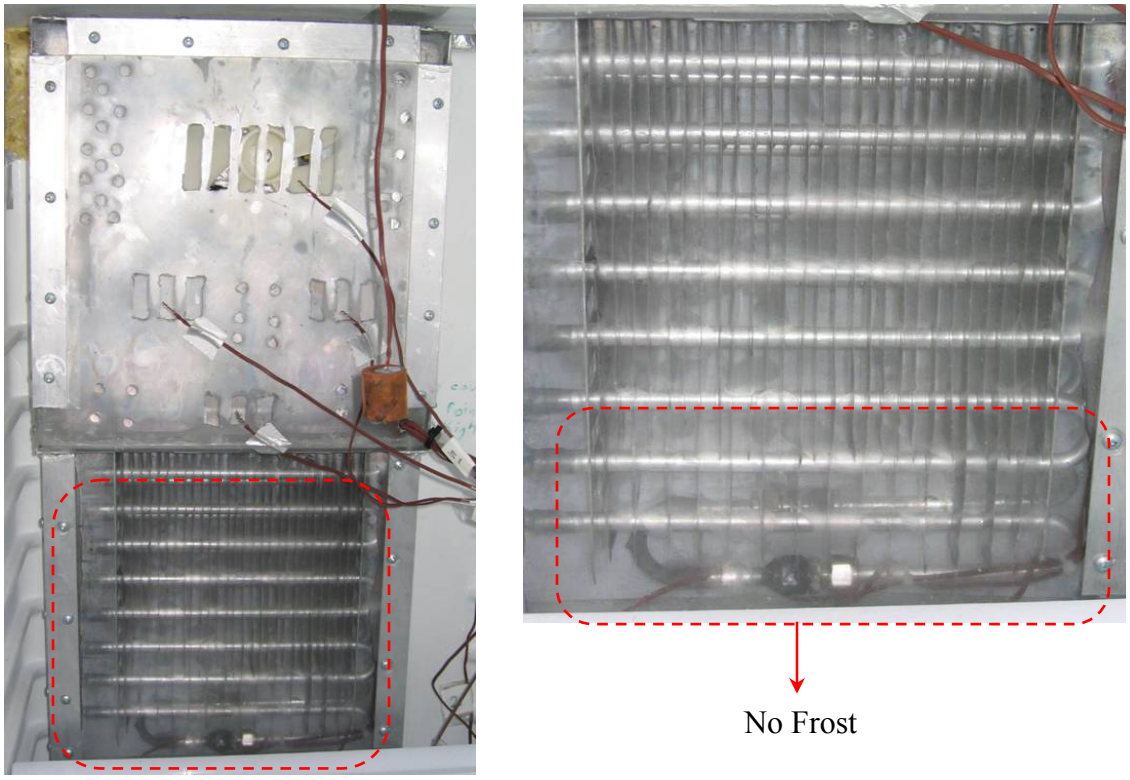

Figure 71 R evaporator condition during off-cycle

As can be seen in the figure, all of the frost was melted during the off-cycle.

Cycle properties for the HR experiment are shown in Table 49.

Table 49 Cycle properties for a HR experiment with FCE

Ref Model	AED with FCE	
	R	F
T_{Amb} [^{o}C]	30	
$T_{Cabinet}$ [^{o}C]	3.1	-16.8
T_{Evap} [^{o}C]	-21.1	-32
T_{Cond} [^{o}C]	37.6	36.2
Q_{Evap} [W]	196.4	173.8
W_{Comp} [W]	88.2	99.0
On Time [Min]	16.8	48.3
OTR [%]	15.2	43.6
W_{Total} On [W]	96.7	108.2
Wtotal OFF [W]	5.1	
HR On [g/kg]	2.1	0.4
HR Off [g/kg]	2.7	0.5

5.4.3 NC R Evaporator Experimental Results

38 experiments were conducted to optimize the AED cycle with a NC R evaporator.

NCE option did not work as well as FCE option, because the heat transfer from the R cabinet air to the NCE was not enough. In the beginning of the R cycle, before the evaporator mass temperature decreased close to the evaporating temperature, the refrigeration cycle worked well; but then, due to heat transfer limitation from the cabinet air to the evaporator, there was not enough evaporation in the NCE AED cycle. As a result, the refrigerant left the evaporator without being superheated. Consequently, the suction temperature decreased dramatically. In addition, because of the low SLHX efficiency, the evaporator inlet quality increased. All of these reasons caused a nearly doubled R and F cycle on-time with a shorter off-time.

The optimum NC R evaporator AED cycle is shown in Table 50.

Table 50 Optimum AED cycle with NCE

Test	NC AED	
Operation	R	F
Charge [g]	140	
Bypass Opening	1 Turns	
Control	T_{Mean}	1/3th Copper Cylinder
Thermostat Settings [^{o}C]	[4>T_R>2]	[-16>T_F>-20]
L_{Cap} [m]	3.4	2.5
Condenser Fan Voltage [VDC]	18.0	18.0
Evap Fan Voltage [VDC]	-	12.9

Pressures and Compressor Power

As explained before, compared to the FC AED cycle, the on-time was longer and the off-time was shorter in the NC design. The R cycle on-time especially was nearly doubled. Figure 72 shows the NCE test pressures and compressor power.

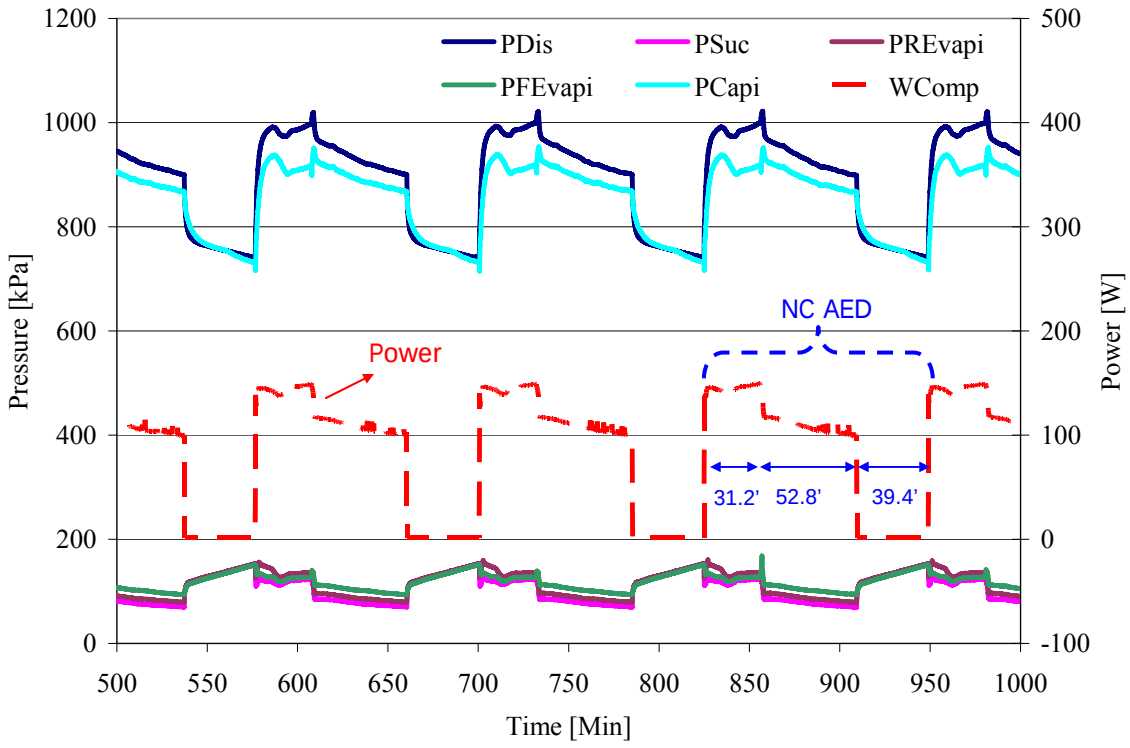

Figure 72 AED cycle pressures and W_{Comp} with the NC R evaporator

Evaporator Surface and Suction temperatures

For the plate-and-tube type NCE, the heat transfer from the cabinet air to the evaporator surface is directly related to the evaporator surface temperature and the NC heat transfer coefficient of the surface. Since the air-side NC heat transfer coefficient is a limiting factor, a lower evaporator temperature requires a higher heat transfer from cabinet air to the evaporator. In experimentation, therefore, it was attempted to decrease the NC R evaporator temperature. The minimum evaporator surface temperature achieved was -20°C and it was limited by the cycle.

In order to decrease the evaporating temperature, the capillary tube length was increased and the refrigerant charge was decreased. However, increasing the capillary tube more than 3.4 m did not produce any change. Therefore, it was concluded that a capillary tube length of 3.4 m is the optimum size for the NC AED cycle. Decreasing the

charge resulted in a decreased evaporating temperature and R cycle compressor power. Decreasing the charge lower than 140g, however, resulted in a decreased F cycle efficiency. Therefore, the optimum charge of refrigerant was 140g.

R evaporator surface temperature, suction temperature, cabinet temperatures and compressor power for a 3.4m capillary tube length and 140g refrigerant charge are shown in Figure 73.

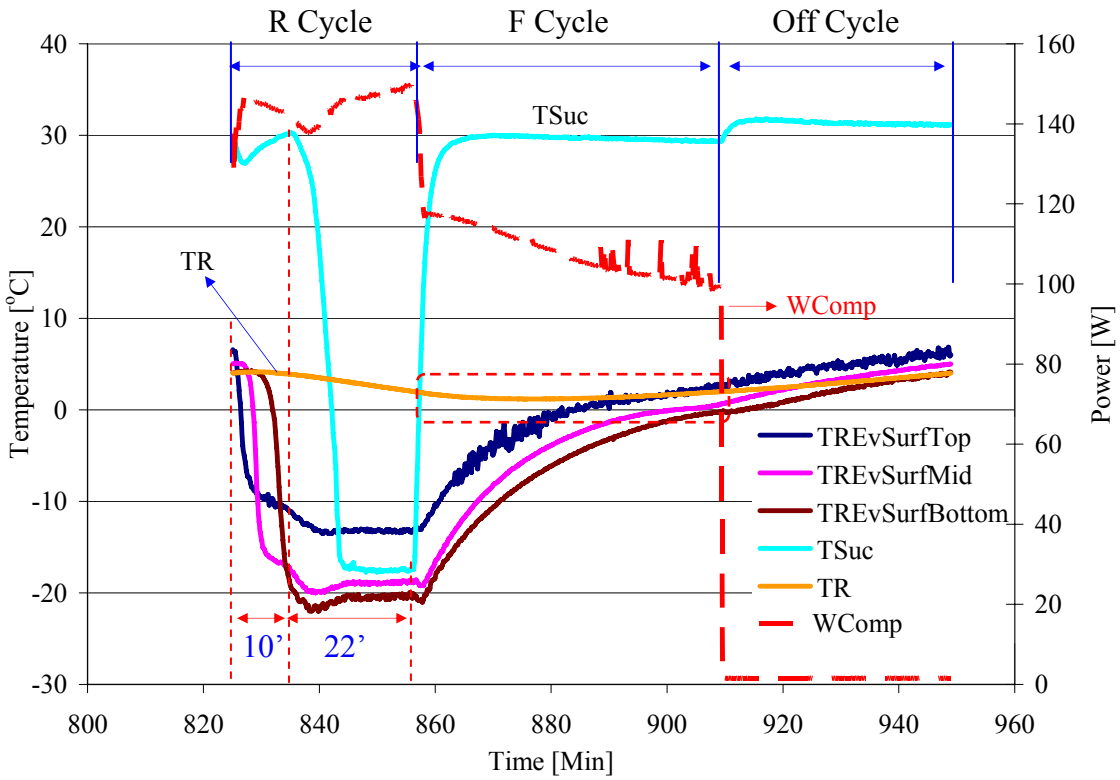

Figure 73 NCE surface temperatures

It should be noted that the R cycle power consumption that is shown in the graph is the measured power value and not the prorated R cycle power consumption.

During the first 10 minutes of the R cycle, the evaporator's surface temperature is decreased. Because of the limited air-side heat transfer from the cabinet air to the evaporator surface, as explained earlier, the suction temperature then decreases to -17.5^{o}C. In this period, the R cabinet temperature continues to decrease for the next 22 minutes. Right after the F cycle starts, T_{Suc} increases again.

It is obvious that if the evaporator surface temperature is decreased, then R cycle on-time is shortened. However, with the current evaporator this could not be achieved.

The NC R evaporator top-surface temperature is 5.5K higher than the mid-surface temperature and 6.7K higher than the bottom-surface temperature. As shown in Figure 57, these differences exist because the top part of the evaporator has fewer rows, so the area is not as efficient in heat transfer as the middle and bottom areas are.

As shown in Figure 73, the R cabinet temperature keeps decreasing after the R cycle ends because the NCE holds its temperature longer by its thermal capacity associated with its mass. Because of this effect, the R cycle thermostat settings were changed from [1.3^{o}C<T_R<5.2^{o}C] to [2^{o}C<T_R<4^{o}C].When T_R reaches 2^{o}C, the R cycle stops but the R cabinet temperature keeps decreasing to around 1.3^{o}C. It eventually steadies back to 2^{o}C after approximately 53 minutes. When the R cycle starts again, the evaporator surface temperature is higher than the R ambient temperature.

Calculated Values

Important properties of the NC AED cycle and CHLs were calculated and are shown in Tables 51 and 52.

Table 51 NCE AED cycle properties

	NCE		FCE	
	R	F	R	F
T_{Cond} [^oC]	38.5	36.7	37.9	36.2
T_{Evap} [^oC]	-22.4	-31.6	-21.2	-31.8
Superheat [K]	6.0	8.5	14.6	8.1
Subcooling [K]	3.5	2.4	3.5	2.4
MFR [g/s]	0.773	0.831	0.905	0.825
X_{Evapi}	0.26	0.17	0.19	0.17
Q_{Evap} [W]	124.1	175.2	163.6	173.4

Table 52 NCE AED cycle cabinet heat loads

	Cabinet	NCE	FCE
CHL [W]	R	31.3	23.1
	F	75.0	75.6

The results show that the AED cycle with a NC R evaporator has a higher condensing temperature and a lower evaporating temperature than the cycle with the FCE. It should be noted that the R cycle superheating is 2K after the first 10 minutes of the R cycle. However, when it is averaged for all on-time then it seems high enough. In addition, because of low superheating, the evaporator inlet quality is higher than that of the FCE. From the calculated results, it is concluded that high evaporator inlet quality and low superheating result in low evaporator capacity.

Table 53 Summary of NCE AED cycle test results

Ref Model			AED with NCE		AED with FCE	
T_{Amb} [^oC]			30.0		30	
T_R [^oC]			2.4		3.1	
T_F [^oC]			-16.2		-16.9	
T_{Evap} [^oC]	R	F	-22.4	-31.6	-21.2	-31.8
T_{Cond} [^oC]	R	F	38.5	36.7	37.9	36.2
Q_{Evap} [W]	R	F	124.1	175.2	163.6	173.4
W_{Comp} [W]	R	F	63.3	100.9	73.4	100.3
On Time [Min]	R	F	31.2	52.9	15.8	48.8
OTR [%]	R	F	25.3	42.8	14.1	43.6
W_{Total} On [W]	R	F	69.1	110.1	81.8	109.6
W_{Total} OFF [W]			5.3		5.1	

5.4.4 NC R Evaporator Humidity Ratio Measurement Test Results

A HR measurement experiment was conducted to evaluate the HR levels in the cabinets with the NCE used in the R cabinet. The best AED cycle with a NCE configuration was used for the HR test.

Humidity Ratios During Pull Down

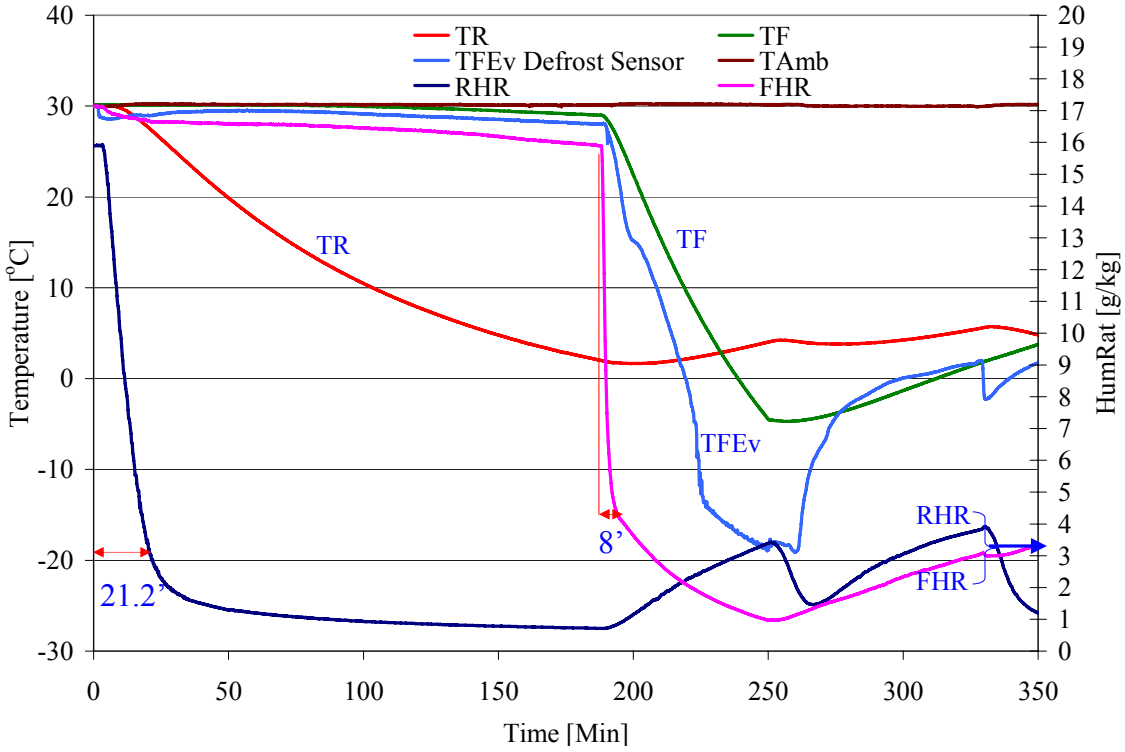

Figure 74 Humidity ratios during pull down with NCE for R cabinet

NC evaporator HR variation during pull down is similar to the FC evaporator case. The R cabinet HR reaches 3g/kg in 21.2 minutes and the F cabinet HR reaches 4g/kg in 8 minutes. In addition, it takes 187 minutes, which is 121 minutes longer than the time for the FCE cycle, to reach 2°C from 30°C, and it takes 246 minutes in total for the F cabinet temperature to reach -3°C from 30°C. In other words, after the F cycle starts, it takes 59 minutes for the F cabinet temperature to reach -3°C.

It can be concluded that pull down time is a big drawback for NCE cycles.

Humidity Ratios During Cyclic Operation

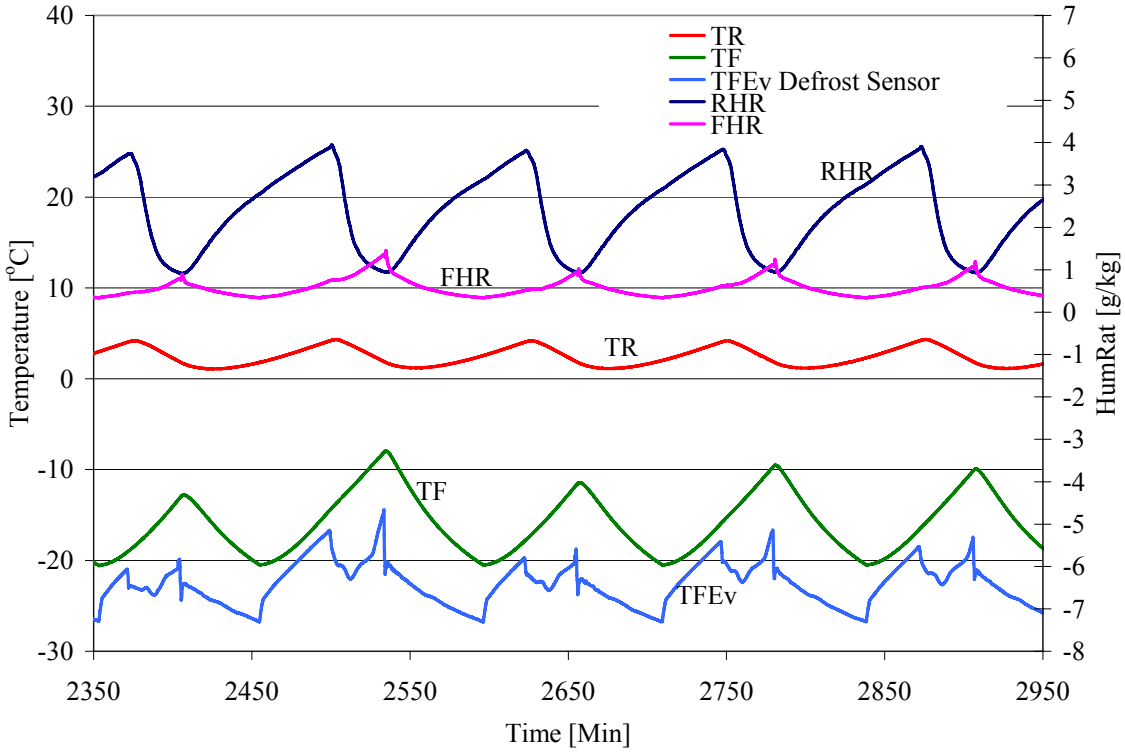

Figure 75 Humidity ratios during cyclic operation with NCE

R cabinet humidity ratio;

The average R cabinet HR for one cycle is 2.4g/kg. Compared to the FCE cabinet, the NCE cabinet has nearly the same HR for one cycle. It should be noted, however, that in the NCE test, the R cabinet temperature was approximately 0.7°C lower than the cabinet temperature in the FCE test. This means that the NCE can keep a HR higher than the FCE in the same cabinet condition. During the on-time of the R cycle, the water vapor in the air quickly condenses on the NC R evaporator surface, so the HR of the R room quickly decreases. During the off-cycle, the R evaporator surface temperature increases above the freezing point and then the frost condensates on the surface and starts to melt and evaporate.

F cabinet humidity ratio;

The average F cabinet HR for one cycle is 0.6g/kg, which is nearly the same as that with the FCE. During the on-time of the F cycle, the water vapor in the air quickly condenses on the evaporator surface, so the HR of the F room decreases. Due to a lower HR of the cabinet air, however, this decrease is not as fast it is in the R operation. During the off-cycle, the F evaporator surface temperature and cabinet temperature increase by 8K. The HR changes due to this temperature changes.

Humidity Ratios During Defrost Cycles

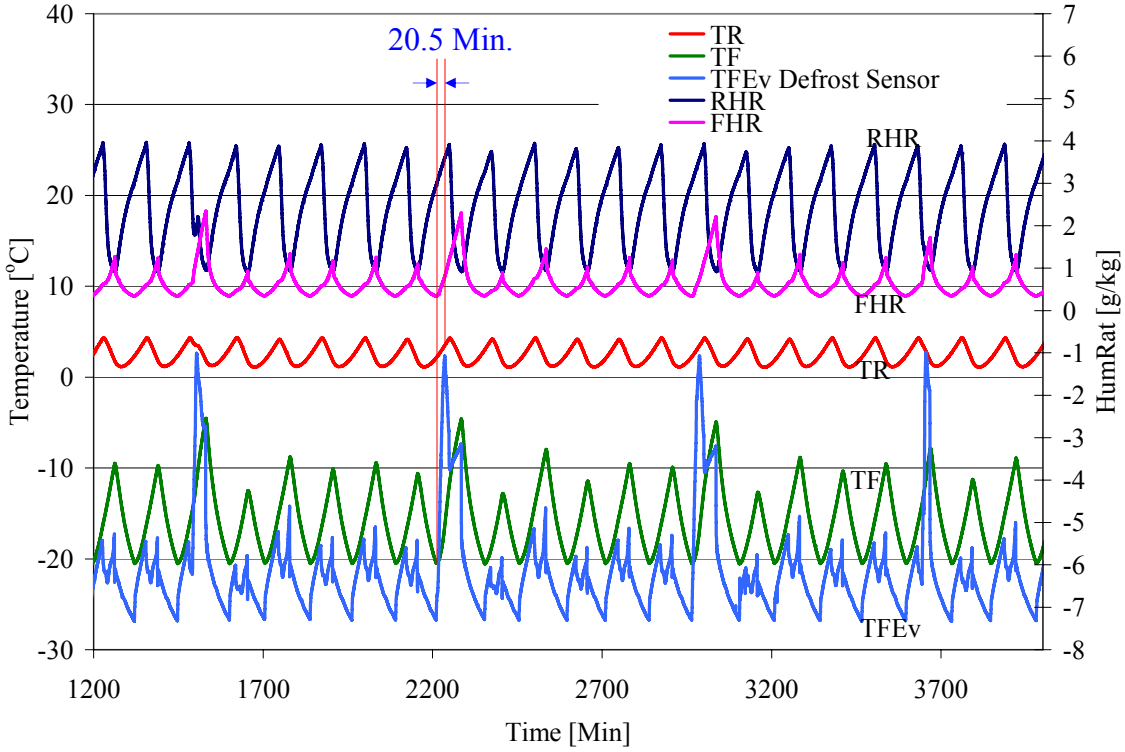

Figure 76 Defrost cycles with NCE

During the defrost cycle, the F cabinet temperature increased to approximately -7°C. The F HR also increased to 2g/kg, similar to the FCE test, due to a cabinet air temperature increase and the melting of the ice from the evaporator surface. The defrost cycle ended when the F evaporator defrost sensor temperature reached 2°C.

Table 54 One cycle properties of HR experiment with NCE

Ref Model	AED with NCE		AED with FCE	
	R	F	R	F
T_{Amb} [^{o}C]	30.0		30.0	
$T_{Cabinet}$ [^{o}C]	2.4	-15.7	3.1	-16.8
T_{Evap} [oC]	-23.0	-31.7	-21.1	-32
T_{Cond} [oC]	38.4	36.6	37.6	36.2
Q_{Evap} [W]	89.1	169.1	196.4	173.8
W_{Comp} [W]	46.6	100.7	88.2	99.0
On Time [Min]	31.8	59.8	16.8	48.3
OTR [%]	26.1	49.0	15.2	43.6
W_{Total} On [W]	53.3	118.1	96.7	108.2
Wtotal OFF [W]	5.2		5.1	
HR On [g/kg]	2.1	0.6	2.1	0.4
HR Off [g/kg]	2.5	0.7	2.7	0.5

5.4.5 AED Cycle Defrost Energy Consumption Calculations

There is another energy savings potential for AED defrost cycles that was not included in the current energy consumption calculations. Since AED cycle F and R cabinets are totally separated from each other, the defrost cycles of the cabinets must also be separated. This means that the frost build up on the F evaporator only comes from moisture in the F cabinet.

AED cycle HR experimental results show that there is no need to run a defrost cycle for the R evaporator because during the off-cycle, the R evaporator's surface temperature increases above the freezing point. Figure 71 shows the FC R evaporator during the off-cycle. It shows that there is no frost on the evaporator at all. As the result, a defrost cycle only needed the for the F evaporator in an AED cycle household R.

In daily life, the R cabinet is accessed more often than the F cabinet. The F cabinet is opened much less compared to the R cabinet. Accordingly, a Korean refrigerator industry's door opening standard [9] describes that the R door is opened every 12 minutes for 10 seconds and the F door is opened for every 40 minutes for 10 seconds. This is equivalent to 120 door openings for the R cabinet and 36 door openings for the F cabinet per day. In addition to the opening frequency, the standard specifies that the room temperature should be 30 ^{o}C with 75% RH. Moreover, the standard assumes that the complete air volume change happens at each door opening.

For the given ambient conditions, ambient humidity ratio (AHR) was calculated as 20.3 g water vapor / kg dry air.

The moisture amount ($W_{Moisture}$) that enters the cabinets per day is calculated using Eq.69.

$$W_{Moisture} = \rho_{Air} \cdot V_{Cabinet} \cdot AHR \cdot (\#DoorOpening) \text{ [g Water vapor/Day]} \quad (69)$$

As given in section 4.1.1, the R cabinet volume (V_R) is 0.426m^3 and the F cabinet volume (V_F) is 0.25m^3. In addition, ρ_{Air} is found to be 1.126kg/m^3 for the given ambient condition. Using these values, the daily moisture provided to the cabinet is calculated as following:

$W_{MoistureR}$ = 1168.5 g Water vapor/Day

$W_{MoistureF}$ = 205.7 g Water vapor/Day

In a conventional unit, 1374.2 g of water vapor can be transformed into frost at the F evaporator surface. On the other hand, in an AED cycle refrigerator, only 205.7 g of water vapor can turned into frost per day. Consequently, the AED cycle R can remove 6.5 times less frost than the conventional R.

As the result, the AED cycle refrigerator requires a defrost cycle 6.5 times shorter than that needed for the conventional unit. This means that the AED defrost cycle consumes 6.5 times less energy compared to the conventional defrost cycle.

Average power consumption for one defrost cycle in a conventional refrigerator is 241W and one defrost cycle is 13.7 minutes which consumes 55Wh/Defrost. In addition, the base-line experiment of the conventional unit shows that a conventional unit makes one defrost cycle in every 10 hours, totaling 2 defrost cycles per day. Therefore, the conventional unit consumes 110Wh/Day just for the defrost cycles The same estimate for the AED cycle refrigerator is 17Wh/Day.

5.5 Conclusions

- Simulation results show that AED cycles equipped with capacity modulated compressors can theoretically save 20% of energy as compared to the base cycle. With appropriate components, the AED cycle can save practically 10% of energy as compared to the base cycle.
- The NCE option has some drawbacks when it comes to application. The main drawback of the NCE is that the natural convection heat transfer from cabinet air to the cold surface of the evaporator is not high enough. Therefore, the cycle efficiency decreases and R cycle on-time increases dramatically, which also increases F cycle on-time.
- Average temperature of F and R compartments during the cyclic operations are 3.1^{o}C and -16.9^{o}C, respectively with FCE and 2.4^{o}C and -16.2^{o}C, respectively with NCE.

- Average humidity ratios of F and R compartments during the cyclic operations are 0.5 g/kg of dry air and 2.5 g/kg of dry air, respectively with FCE and 0.6g/kg of dry air and 2.4g/kg of dry air, respectively with NCE. Therefore, the humidity ratio of R compartment is maintained in 4-5 times higher level than that of F compartment for AED cycle and R and F compartments for base cycle.
- Since R cabinet temperature with NCE is 0.7K lower than FCE R cabinet temperature, it can be concluded that NCE has potential to keep the cabinet humidity level higher than FCE can do.
- Since R cabinet air temperature is higher than freezing point, frost formed at the R evaporator surface is defrosted naturally during off-cycle.

6 Recommendations and Future Work

- At least, at suction and discharge line in-stream TCs should be installed.
- Instead of using compressor performance map to estimate the cycle MFR, a mass flow meter which has a small measurement range should be used.
- A charge optimization should be done for a new AED cycle starting from 50g lower to 50g higher than base unit's optimized charge within 10g intervals to determine an optimum charge for both cycles. The optimum charge should be decided based on the whole system energy consumption.
- For a conventional refrigerator it is recommended to use the counter-flow condenser with insulation above the condenser and run condenser fan voltage higher than the current voltage.

7 References

[1] Binneberg, P., Kraus, E., Quack H., Reduction in Power Consumption of Household Refrigerators by Using Variable Speed Compressors, Purdue International Refrigeration Conference, R17-4, 2002.

[2] Lee J., Cho K. Y., Lee K. T., Daewoo Electronics Company, Ltd., Korea; A New Control System of a Household Refrigerator-Freezer, Purdue International Refrigeration Conference, R-5, 1994.

[3] Park J. K., Park, S. T., Kwak, T. H., Im K. S., LG Electronics, Korea; Dual-Controlled Indirect Cooling Refrigerator/Freezer Using Two Capillary Tubes and an Air Flow Switching System, Purdue International Refrigeration Conference, R-12, 1998.

[4] Lorenz, A., Meutzner, K., On Application of Non-azeotropic Two Component Refrigerants in Domestic Refrigerators and Home Freezers, XIV International Congress of Refrigeration, Moscow, 1975.

[5] Lavanis, M., Haider, I., Radermacher, R., Experimental Investigation of an Alternating Evaporator Duty Refrigerator/Freezer, ASHRAE Transactions 1998, Vol. 104, P. 2.

[6] US Patent, 2002, US Patent No., 6,370,895, Sakuma et al., Refrigerator with Two Evaporators and Variable Speed Compressor.

[7] ASHRAE Handbook, 1997.

[8] Kline, S.J., McClintock F.A., Describing Uncertainties in Single-Sample Experiments, Mech. Eng., P.3, 1953.

[9] Bejan A., Vargas J. V. C., Lim J. S., When to Defrost a Refrigerator, and When to Remove the Scale From the Heat Exchanger of a Power Plant, Journal of Heat and Mass Transfer, Vol:37, Iss:3, Pg:523-532, 1994.

[10] Setra Systems, Inc., http://www.setra.com/tra/pro/p_hv_280.htm, 2005

[11] Omega Engineering, Inc., http://www.omega.com/ppt/pptsc.asp? -ref=GG_T_TC_WIRE&Nav=temh06

[12] Ohio Semotronics, Inc., http://www.ohiosemitronics.com/pdf/PC5-RevA.pdf

[13] Zhejiang Fenghua Sanshi Solenoid Valve Co.,Ltd., http://www.china-sanshi.com/enprosoall.asp?fl=Bistable-Pulse-Valve-For-Refrigerator&sele=26&text=26, 2006.